MERGING TERRADYNAMICS AND MUSCULOTENDON NEUROMECHANICS: TOWARDS WEARABLE ROBOTS FOR AUGMENTED HUMAN LOCOMOTION ON NON-UNIFORM SURFACES

A Dissertation
Presented to
The Academic Faculty

by

Jonathan R. Gosyne

In Partial Fulfillment
of the Requirements for the Degree
Doctor of Philosophy in the
George W. Woodruff School of Mechanical Engineering

Georgia Institute of Technology
December 2022

MERGING TERRADYNAMICS AND MUSCULOTENDON NEUROMECHANICS: TOWARDS WEARABLE ROBOTS FOR AUGMENTED HUMAN LOCOMOTION ON NON-UNIFORM SURFACES

Approved by:

Dr. Gregory Sawicki, Advisor
School of Mechanical Engineering and School of Biological Sciences
Georgia Institute of Technology

Dr. Frank Hammond III
School of Mechanical Engineering and School of Biomedical Engineering
Georgia Institute of Technology

Dr. Craig McGowan
Keck School of Medicine
University of Southern California

Dr. Ye Zhao
School of Mechanical Engineering
Georgia Institute of Technology

Dr. Young-Hui Chang
School of Biological Sciences
Georgia Institute of Technology

Date Approved: 12/12/2022

People are more important than things*. They can be phenomenal mentors, friends, and change your life forever**. They can be cruel, selfish and they can let you down.*
Regardless- Love them anyway. *- Reverend Naipaul Ricky Gosyne*

To the love of my life, Victoria. My calm in the storm. My home.

ACKNOWLEDGEMENTS

When I first started at Georgia Tech, I had no idea that a few years studying abroad in Atlanta would turn in to a decade-long journey of a lifetime. I can definitively say that there is absolutely no way that I could have even come close to completing this Chapter of my life on my own- any degree I hold was earned largely by the giants on whose shoulders I stood, who gave me the opportunity to go that last mile out of the hundred.

I like to extend my heartfelt thanks to Drs. Craig McGowan, Young-Hui Chang, Ye Zhao and Frank Hammond III for their time spend on the dissertation committee, and their constant stream of guidance through collaborations, special projects, classroom instruction and feedback. I would like to thank my advisor, Dr Greg Sawicki, for his constant stream of advice, guidance, and mentorship- upon joining his lab, he completely redefined in my mind what an advisor looks like. Greg has truly gone above and beyond for myself and my family in so many ways, sometimes in ways he may not have even realized- it's just who he is. I'll never forget the efforts he made both inside and outside of lab, and I look forward to a long and rich relationship with him, his family and all the PoWeR lab family in the years to come.

I have found that Georgia Tech, and especially the PoWeR Lab, is nothing short of a magnet for incredible people and would like to extend my gratitude to each and every member over the years for their support throughout the entirety of this process. I'm proud of the fact that I can call many of these folks not just my co-workers or colleagues, but truly my friends. From early morning collections and late night conference patio beers with Owen and Ben, modelling and simulation as well as hop city-Dark Horse adventures with

Laksh, to eating some of the best food I've ever eaten from Pawel and Jordyn, to trying to steal Ruby from Lindsey and Darrian during one of their legendary house parties. To Ian and Kenny from the Master's days, Stacey, Prerna and the entire LEAD team, and to Owen, Max S, Emily, Kristen, Lindsey, Ben, Amro, Jenny, Jordyn, Luis, Melody, Pawel, Max A, Felicia and Thendral- you all have been absolutely amazing, and I can't imagine this journey without any of you. Special thanks go to my project team of undergraduate, and now even Master's students, Qingyi, Claudia and Nil. These young men and women stuck with me through it all, through the late nights and early mornings, through recruitment, data collection, processing- the entire design and testing process. I am so grateful for the impact they have had on my life, and I look forward to continuing to be part of their journey as they become leaders in their field.

I would like to thank my parents, Ricky and Denise and my brother, Josiah, for being a never-ending source of support. I certainly have not had the most linear path to completing this program, and they were there at every single step of the way. They have always been there to help lift me out of the lows and celebrate the highs. They've done the unimaginable, working their way up from absolutely nothing, so that I would not have to start from zero. I will never understand the kind of sacrifice that this took and continues to take; know I can never thank you enough.

To my found family: my in-laws and my closest friends- thank you. Thank you for taking me in when I moved to a new country with nothing but two suitcases worth of clothes to my name. Thank you for welcoming me to your dinner tables for Thanksgivings and Christmases, for celebrating and crying with me and never making me feel alone. To Fritz, Sharlene and all the Johs, thank you for welcoming this islander and supporting my

academic journey with overwhelming love and support, To Kuttler, Tyler, Samuel, Key and all the others- Thank you all for being my brothers. Thank you for being there to help me think, for bringing me food and the never-ending supply of doctor jokes.

To those who could not be here- Thank you. I think about you every day. To Grandpa Ralph giving me Legos and science books, to Jacqueline and Pinky helping me buy textbooks and computers when I could not afford to; to Dolly dancing up and down and Grandpa Ganness hugging me with me when they heard I got into Georgia Tech. To Jeff, who helped stoke my fire for teaching, and helped me to see the awe-inspiring significance of mentoring the next generation of engineers. To everyone else looking down, you are the giants on whose shoulders I stand.

To Victoria- I could write volumes and volumes, dissertations and dissertations worth of words and never fully express how much you have helped me in this journey. Thank you for walking with me step-by-step from day one till the end. Thank you for never wavering in your support and encouragement and love; for always being there, come hell or high water. Thank you, my love. This one is for you.

TABLE OF CONTENTS

LIST OF TABLES

LIST OF FIGURES

LIST OF SYMBOLS AND ABBREVIATIONS

Act	Muscle Activation
A_{exo}	Exo Skeleton Area
A_{stim}	Stimulation
CE	Contractile Element
CSA_{sol}	Soleus Cross Sectional Area
EMA	Effective Mechanical Advantage
F_{ank}	Ankle Force
F_{CE}	Contractile Element Force
F_{exo}	Exoskeleton Force
F_{GRF}	Ground Reaction Force
F_{hip}	Hip Force
F_{knee}	Knee Force
FL	Force-Length Relationship
FL_{active}	Active Muscle Force-Length Relationship
$FL_{passive}$	Passive Muscle Force-Length Relationship
F_{max}	Maximum Muscle Force
F_{MTU}	Muscle-Tendon Unit Force
F_{sol}	Soleus Force
F_{system}	System Force
FV	Force-Velocity Relationship
g	Acceleration due to gravity
K_{exo}	Exoskeleton Stiffness
k_T or k_{SEE}	Tendon stiffness

l_{CE}	Contractile Element Length
L_{exo}	Exoskeleton Length
l_{MTU}	Muscle Tendon Unit Length
l_o	Resting Contractile Element Length
m	Subject mass
M_{ank}	Ankle Moment
M_{exo}	Exoskeleton Morphology
M_{hip}	Hip Moment
M_{knee}	Knee Moment
MTU	Muscle Tendon Unit
P_{ground}	Ground Power
P_{mech}	Mechanical Power
P_{met}	Metabolic Power
P_{MTU}	Muscle Tendon Unit Power
r_{AT}	Ankle Moment Arm
SEE	Series Elastic Element
SLS	Standard Linear Sinkage
T_{stim}	Stimulation Time
v_{CE}	Contractile Element Velocity
v_{max}	Maximum Contractile Element Velocity
v_{MTU}	Muscle Tendon Unit Velocity
W_{exo}	Exoskeleton Width
x_{sink}	Surface Sinkage
β	Volumetric Surface Damping
θ_{ank}	Ankle Angle

θ_{hip}	Hip Angle
θ_{knee}	Knee Angle
θ_p	Pennation Angle
κ	Volumetric Surface Stiffness
τ_{act}	Muscle activation time constant
τ_{deact}	Muscle deactivation Time constant

SUMMARY

The field of wearable robotics is advancing quickly, however, most devices still struggle in environments with complex terrain. Perhaps, poor field performance of wearable devices stems from mechatronic design that does not consider the non-linear physics of interaction between the human-machine system and the environment. Now is the time to combine knowledge from studies of locomotion on granular substrates, and insights from wearable devices designed to interact with the physiological properties of underlying musculoskeletal structures. For example, the mechanisms underpinning the increased cost of moving in sand may be attributed to sinkage into the granular substrate, or inability to tune limb compliance in a dissipative environment. Thus, this research effort focuses on understanding these complex neuromechanical relationships, toward the end goal of engineering a wearable device that adopts a bio-inspired approach in to achieve augmented human locomotion over complex, dissipative terrain. To this end, my project seeks to (i.) robustly model nominal and augmented human locomotion over a variety of dissipative terrains (e.g., concrete, sand, snow, mud), (ii) empirically and experimentally characterizing the complex interaction dynamics and Neuromechanics of human locomotion over dissipative terrain (e.g., sand); (iii.) use these findings as a foundation for development of a bio-inspired wearable robotic device that enables its user to reduce effort to traverse complex dissipative terrain- one that will serve to provide a far more robust, adaptive platform for real-world locomotion on terrain with changing surface properties than currently available wearable devices. Through the characterization of human-terrain interactions in this study, we look toward creating more informed devices and solutions for novel wearable robotics paradigms in recreation, agriculture, defense, and beyond.

CHAPTER 1. INTRODUCTION

1.1 A Brief Introduction to the Study Series

Locomotion on sand is energetically costly and requires a higher metabolic cost than that over hard, structured environments. Previous work attributes this to two main factors: sinkage into the sand itself, and the structural properties of the human leg [1-5]. Sinkage into the sand is conventionally represented as a function of kinematic properties such as depth, contact area, intrusion force, and intrusion velocity, as well as material properties such as density or grain size. Additionally, the added metabolic cost of walking on sand has been attributed to the need for additional net power to overcome force dissipation and sinkage of the medium, as well as the occurrence of extra tendon stretching during sinkage, thereby causing contraction of muscles; this contraction causes higher levels of stimulations and reduced force production capacity.

However, many of these factors have not yet been well examined [5]. Lejeune et al found that on dissipative substrates, the amount of metabolic power required exceeded the mechanical work required for locomotion across a variety of speeds and hypothesized that this was due to inefficiencies in the muscle tendon units (Figure 1). Mortiz, and Farley, as well as Birch et al [6-8], found specifically that in terms of injection of additional mechanical work, the ankle was the key contributor (Figure 2), but still did not examine the muscle level dynamics around this joint.

While wearable devices and their effect on energetics and muscle dynamics has been studied for years, their context has largely been the same: hard ground and lab use.

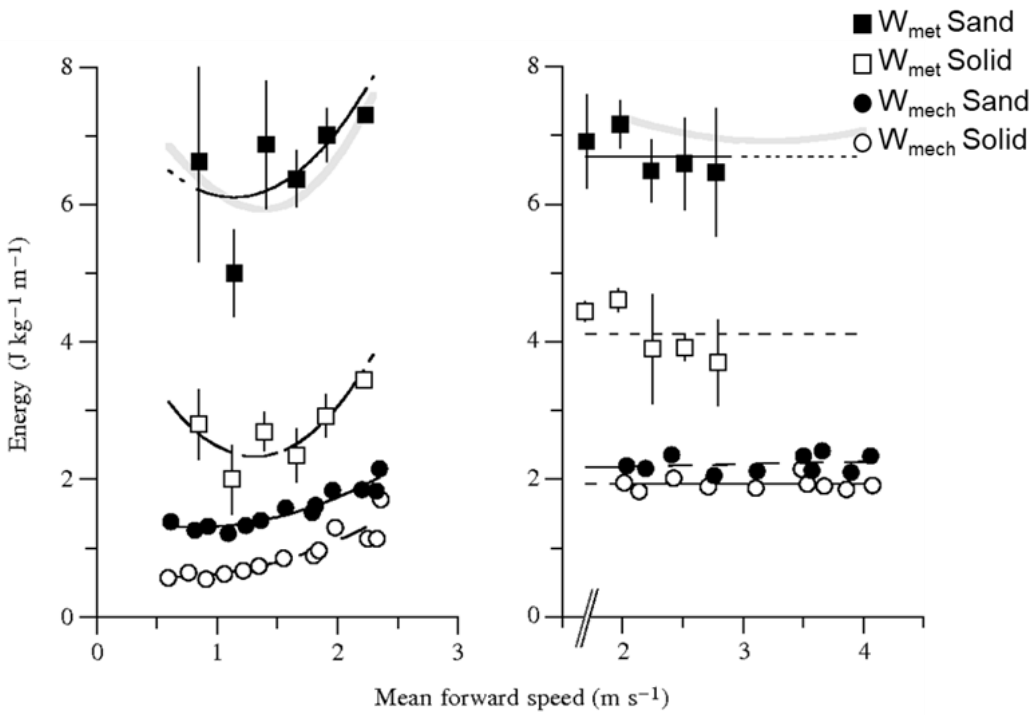

Figure 1. Findings of Lejeune et al when comparing mechanical work done during dissipative terrain locomotion to that of the metabolic power.

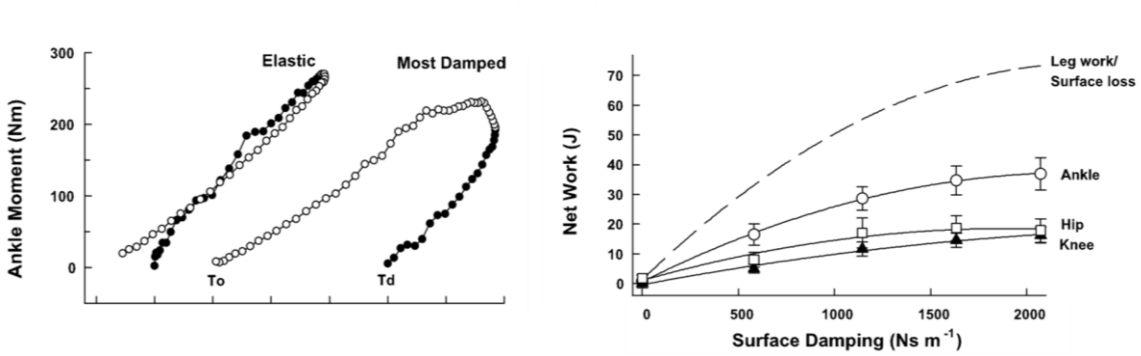

Figure 2 Moritz and Farley's examination of the leg joints, highlighting that the ankle is the main contributor to the injection of additional mechanical work.

Typically, these devices are unstable, energetically taxing, or even unusable once they are taken out on to real world, dissipative terrain. Perhaps, poor field performance of current wearable devices then stems from mechatronic design that does not consider the non-linear physics of interaction between the human-machine system and the environment. Now is

the time to combine knowledge from studies of locomotion on granular substrates, and insights from wearable devices designed to interact with the physiological properties of underlying musculoskeletal structures. Thus, this research effort focuses on engineering a wearable device that adopts a bio-inspired approach in order to achieve augmented human locomotion over complex media. Towards this goal, this project seeks to (i.) robustly model nominal and augmented human locomotion over a variety of terrains, (ii) empirically characterize the complex interaction, dynamics, and biomechanics of human locomotion over dissipative media and (iii.) use our findings as a foundation for development of a bio-inspired wearable robotic device that enables its user to effortlessly traverse complex terrain. Our novel device will serve to provide a far more robust, adaptive platform for real-world' locomotion on changing terrain than currently available wearable devices.

1.2 Study Goals.

More specifically, the work performed on this project is expected to produce (1) greater understanding of kinematic, kinetic and energetic profiles of human locomotion over metabolically taxing terrain such as and, snow or mud and (2) allow for the rapid prototyping of a plug and play control scheme for an ankle exoskeleton that draws inspiration from this characterization. The prototype will leverage neuromuscular input from the user, as well as input from the foot-media boundary interaction to then improve the efficiency of the wearer on complex media. The goals of this study are further explored below.

1.2.1 Study Goal 1: Characterize the multi-scale Neuromechanics of humans during locomotion on dissipative substrates – from whole-body energetics to individual muscle dynamics.

The mechanics and energetics of bipedal locomotion has been widely studied in both animals (both human and non-human) and robots. However, due to methodological challenges, little work has been done to yield a mechanistic understanding of lower-limb joint and muscle-level Neuromechanics of human locomotion over complex terrain. In this study, we develop a simple modelling and simulation framework to examine the metabolic energy cost of hopping in sand to drive testable hypotheses regarding changes in joint and muscle dynamics during human hopping on dissipative granular material (i.e., sand). This allows us to analyze, both in silico and in vivo, how the complex physics of foot-ground interaction drive multiscale compensatory mechanisms that manifest as increased metabolic cost during human locomotion in dissipative environments. We hypothesized that that ultimately, the increased metabolic cost of dissipative terrain locomotion is due to altered muscle dynamics including elevated contraction velocity and short muscle operating lengths – both known factors underlying poor economy of force production. Through the use of indirect calorimetry along with high-speed motion capture, instrumented foot soles, B-mode ultrasound, and surface electromyography we linked changes in lower-limb joint and muscle-tendon dynamics during human hopping in a novel' sandbox' under controlled conditions (e.g., hop height and frequency) to observed increases in metabolic rate. We will then used this novel data to inform development of the wearable foot-ankle device at the foundation of Specific Aim 2.

1.2.2 Study Goal 2: Optimize structural properties of a wearable foot-ankle device for augmenting locomotion performance in dissipative terrain.

This aim sought to develop a novel approach for the design of wearable assistive device using bottom-up, bio-inspired design based on novel understanding of the mechanisms driving increased metabolic effort to move in complex, dissipative terrain (see Aim 1). Using our modelling and simulation framework, we explored the space of foot-ankle devices comprised of viable combinations of increased foot contact area + supplemental elastic ankle joint stiffness in silico, searching for combinations that can minimize the metabolic energy cost of fixed energy hopping in sand. Then we constructed a prototype capable of applying the 'best' morphologies and tested them on mechanically matched human locomotor tasks. We hypothesized that a device with the optimal combination of foot-contact area + supplemental ankle stiffness can mitigate the metabolic penalty of human hopping in dissipative terrain.

1.3 Impact, Significance and Contributions to the Field

This project is expected to produce a greater understanding of kinematic, kinetic and energetic profiles of human locomotion over metabolically taxing terrain such as sand, snow or mud and allow for the leveraging of these findings to prescribe the design of a bio-inspired foot-ankle exoskeleton that can reduce the metabolic burden of the user on complex, dissipative terrain.

1.3.1 Significance

1.3.1.1 Development of a modelling and simulation framework of human interaction with complex media- taking conventional hill type models off-road:

Bipedal gait has been widely studied, both in the context of biomechanics and robotics, but little work has been done to yield a general formula for locomotion over complex media[2, 3, 7-22]. This work develops a generalized modelling and simulation framework to examine the metabolic energy cost of hopping in any dissipative terrain, with and without a novel, unpowered exoskeletal device. These findings open up the possibility for and inform the direction of further *in-vivo* investigation in Chapters 3, 4 and the Appendices, where we verify and test both unassisted and assisted hopping tasks experimentally.

1.3.1.2 Rethinking Instrumentation from the ground up- A first full, directly measured inverse kinematic analysis of human locomotion on complex media.

To date, there has been no human study that allows for direct inverse kinematics from human locomotion studies. Lejeune et. al used buried force plates and relied on the whole-body mechanical vs metabolic cost comparison [2]. While these analyses are well documented for hard ground studies, there has not been a reliable way to obtain the center of pressure and ground reaction force vector [18, 23-25]. Through the use of an insole on the subject to provide center of pressure, and muscle level force readings, we can reliably interpolate the real time ground reaction force vector on dissipative substrates. This unique

sensor fusion approach lays the foundation for sensing on non-uniform terrain, and allows us to now test the implementation of our devices without being confined to the laboratory setting.

1.3.1.3 Muscle level mechanics of walking in dissipative terrain- A first look at the muscle level:

Human locomotion on deformable media has been studied for decades, but little has been done to understand the underlying causes associated with the increased cost of transport in humans [2, 3, 5, 26-31]. Lejeune, Willems and Heglund assessed the locomotion mechanics and overall metabolic effects of movement on sand, and found mechanical work and energy expenditure requirements of up to 1.15 and 1.6 times higher respectively for walking and bounding gaits on sand when compared to hard ground trials [2]. They highlight that energy expenditure is not linearly scalable to actual mechanical work, especially over dissipative terrain. On the other hand, there have been many studies [32, 33] that explain increased metabolic cost over hard ground as factors stemming from neuromuscular effects. For example, Minetti and Alexander relate added metabolic cost during walking to a combination of muscle activation, as well as some function of muscle force-velocity [19]. As such, this project investigates the yet unexplored intersection of the above factors.

1.3.1.4 Terrain-tunable deign- prescribing more robust and effective design and control techniques for wearable robotic devices operating in complex media:

After the initial experimental analysis in Chapters 2 and 3 yield a more complete understanding of the human neuromuscular response to the complex non-linear behavior of changing substrates, we will then leverage this information to make more informed design and control schemes for devices that are better suited to "real-world" use. To do this, we seek to design and build an exoskeleton device, informed by the results of Chapter 2. This type of ground-up development is necessary, since current wearable device design and fabrication follows traditional techniques for rigid body robotics or medical devices [10, 34-37]. In the last few years, there have been significant advances in terms of designs that optimize energetics on hard surfaces, however, little has been done to change the approach of this to specialize the design for use on complex substrates. The culmination of this project will be to discover fundamental muscle level principles and establish a methodology that can be used to design devices at the human-machine-environment interface for human performance optimization, with respect to physical and metabolic function.

1.3.2 Contributions and Innovation

1.3.2.1 Development of a modelling and simulation framework of human interaction with complex media:

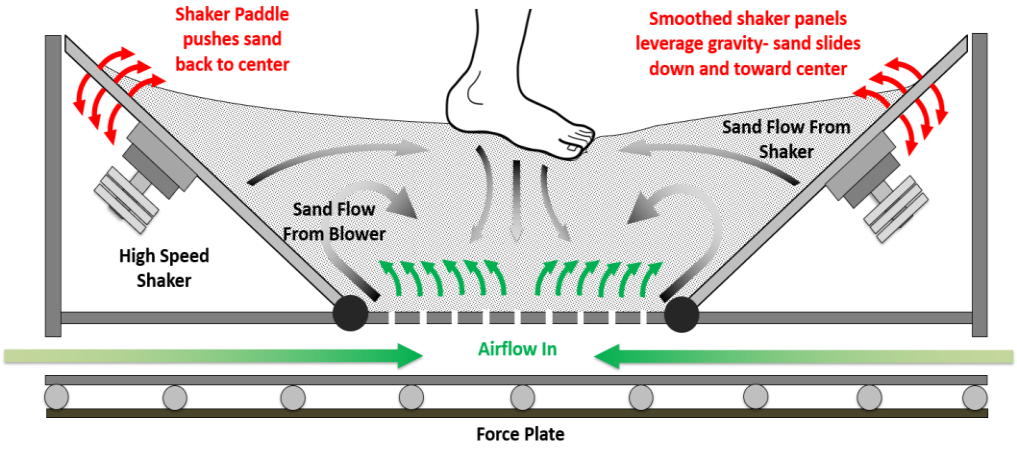

Figure 3 Schematic demonstrating the setup for sand leveling and data collection for Chapters 2 and 3. Shakers leverage gravity to help the sand flow back to the center of the box, while a fluidization apparatus can be used as well for leveling the pit as well when necessary.

Preliminary modelling of a foot-ankle exoskeleton that combines added contact area between foot and ground with modified stiffness around the ankle joint represents the first look at the muscle level mechanics of human locomotion on dissipative substrates Additional experimental continuation of this study in Chapters 2 and 3 yield the data for us to perform, the first comprehensive neuromechanical analysis of the human neuromuscular response to the complex non-linear behavior of changing substrates. This information is leveraged to make more informed optimal control schemes and devices that are better suited to "real-world" use in Appendix A.

1.3.2.2 Examining human locomotion in sand- pushing the boundaries of instrumentation:

In order to effectively analyze the complex interactions and compensatory mechanisms that come into play during complex biological control [5, 8], as well as the

metabolic costs associated with human hopping locomotion under differing conditions in complex matter, specialized equipment must be used. We use a custom-built terrain platform and sensing setup, that fuses sensing from onboard force measurement (insoles), force platforms, and direct force measurement from muscles using acoustics that can finally allow us to conduct inverse dynamic studies over dissipative media, and is the first setup that allows for robust analysis of dissipative terrain in a controlled laboratory setting.

1.3.2.3 Using widely studied design and control techniques to identify a prescriptive, universal design and control scheme locomotion in changing terrain:

Many control and design schemes implemented on wearable systems today have the same primary underpinnings of more traditional devices developed in decades past [9, 10, 35]. As such, although many modern devices are significantly more functional and technologically complex than their earlier counterparts, their effective context of use (locomotion on flat, even terrain) has remained largely the same. By studying human locomotion in dissipative substrates, we then prescribe bioinspired design and control schemes based on our understanding of these complex surface interactions. While this study largely examines the effect of an in-parallel exoskeleton, this prescriptive scheme can be translated to prosthetics, and legged robotics, as well as a number of use cases across a variety of industries

1.4 Study Structure

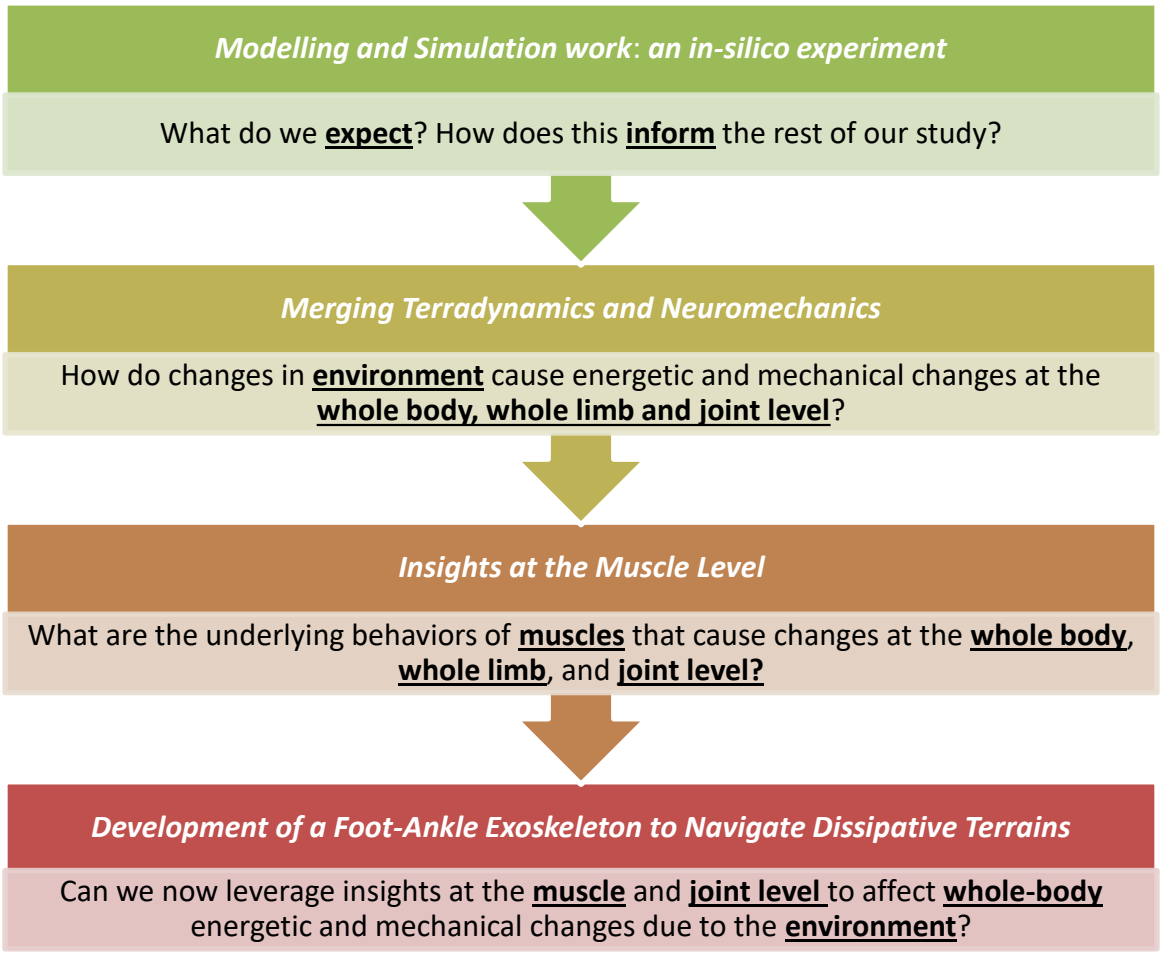

Figure 4 Workflow and arrangement of the chapters in this dissertation manuscript

The arrangement of this study presents a series of journal and conference papers that step through a series of studies that all contribute to addressing the study goals (Figure 4). Each chapter contains a contained introduction to the question, literature review and background, methodology, results and discussion. Ultimately, the sum total of these studies seek to answer the questions: (i) why, at the muscle level, is dissipative terrain locomotion so costly? And (ii) can we design a wearable device to mitigate these effects? These questions will be explored at length in the chapters to follow.

CHAPTER 2. IN-SILICO ANALYSIS OF DISSIPATIVE TERRAIN LOCOMOTION AT THE NEUROMUSCULAR LEVEL TO OPTIMIZE CONTACT AREA AND JOINT STIFFNESS OF A PASSIVE FOOT-ANKLE EXOSKELETON.

Designing wearable devices for use on deformable terrain is an ongoing engineering challenge. This is particularly apparent when we examine locomotion on dissipative surfaces such as sand or snow. These surfaces have complex, variable dynamics which lead to increased fatigue and metabolic cost during locomotion. To begin to investigate this, we developed a modelling and simulation framework to examine the mechanics and energetics associated with hopping to a fixed height in a variety of dissipative terrain conditions. After narrowing our focus to one dissipative substrate by using one set of ground stiffness and damping parameters, we then conducted a metabolic cost study with and without a novel, unpowered exoskeleton device. Our model couples a simple human neuromechanical adaption of the ankle joint to a passive elastic exoskeleton with variable stiffness and contact area. To achieve this, we used the Hill-Type muscle model to represent the human triceps surae- Achilles tendon muscle tendon unit (MTU), allowing for a lumped model of a single contractile element (CE) and series elastic element (SEE). Using a nominal gravitational load, the model was subjected to cyclic stimulation at a set frequency to simulate the effect of hopping to a specified height from rest; this was done both with and without exoskeleton assistance. We investigated the effect that both exoskeleton morphology, (W_{exo}, L_{exo} and k_{exo}) and muscle activation (A_{stim}) have on combined MTU and Exo, MTU and CE/SEE mechanics and energetics. Using our modelling framework, we found a set of intermediate values of [W_{exo}, L_{exo}, Ratio k_{exo}/k_t] that allowed the system to hop to the same height at a comparable metabolic cost as if the system were operating unassisted on hard ground. Thus, we conclude that our model that

combines added contact area between foot and ground with modified stiffness around the ankle joint allows for the elimination of the penalty associated with energy dissipation during locomotion on granular substrates. This informs our design of future physical studies and opens up the possibility for a new class of wearable devices that can mitigate the metabolic penalty of moving in complex, dissipative terrain.

2.1 Introduction

The field of wearable robotics is advancing quickly, however, most devices still struggle in environments with complex terrain[9-11, 38, 39]. A key contributor to this is that wearable device design and fabrication still follows traditional techniques for rigid body robotics or medical device design. Furthermore, and in line with the focus of this study, poor performance of wearable devices can be linked to mechatronic design that does not consider the non-linear physics of interaction between the human-machine system and the environment. For example, the mechanisms underpinning the increased cost of moving in sand may be attributed to sinkage into the granular substrate, or inability to tune limb compliance in a dissipative environment. As such, while there have been significant advances in the area of optimizing locomotion energetics on hard surfaces, little has yet been done to change the design of these for specialization on complex substrates.

While unassisted human locomotion on deformable media has been studied for decades[2, 40], little has been done to understand the underlying causes associated with the increased cost of transport in humans. Lejeune, Willems and Heglund assessed the locomotion mechanics and overall metabolic effects[2] of movement on sand, and found mechanical work and energy expenditure requirements of up to 1.15 and 1.6 times higher respectively for walking and bounding gaits on sand when compared to hard ground trials. They highlight that energy expenditure is not linearly scalable to actual mechanical work, especially over dissipative terrain. On the other hand, there have been many studies that

explain increased metabolic cost over hard ground as factors stemming from neuromuscular effects. For example, Minetti and Alexander [19] relate added metabolic cost during walking to a combination of muscle activation, as well as some function of muscle force-velocity. The opportunity to investigate the intersection of these two has yet to be explored.

Terradynamics and ground interactions themselves are incredibly complex, non-linear phenomena [31, 38, 41, 42] that require knowledge and characterization of the given ground substrate. Li, Zhang and Goldman [43] highlight methodologies that allow for prediction of legged locomotor behaviour on dry, loosely packed granular substrates using the Resistive Force Theory (RFT). However, a simplified, lumped-parameter Standard Linear Solid model [15, 19, 41, 42, 44] has been used for simplified computational cases[41], particularly when estimating environments with varying levels of saturation, such as soils and clays[42, 44]. This typically consists of layers of area-dependent, experimentally determined, unidirectional stiffness and damping elements, that illustrate layer-by-layer sinkage into a particular substrate. Indeed, this lends itself to integration into real time modelling and simulation studies where the primary focus is the neuromuscular effects of the locomotor.

When considering that human locomotion is typically in the form of a ‘bouncing gait’ [2, 32], the rationale for modelling the leg as an inverted spring-mass pendulum can be seen. As such, in-parallel, passive spring exoskeleton devices have the potential to easily integrate into existing hard ground locomotion models [35, 36]. It has been shown that various spring compliances and combinations can indeed produce significant changes at the muscle level [35, 36]. To this effect, many studies have shown that passive elastic exoskeleton devices, when used in parallel, can reduce the metabolic cost associated with bouncing gait[32, 37, 45]. Robertson, Farris and Sawicki illustrated through a modelling study that for a lumped Hill-Type muscle model, there was an optimal in-parallel

exoskeleton stiffness associated with this minimum $\bar{P}_{met}$ as related to amount of $\bar{P}_{mech}$ performed by the system[36].

However, augmenting locomotion on dissipative terrain presents a unique set of compounding challenges. It has been shown that much of the increase in energy cost can be attributed to ground energy dissipation, primarily during sinkage into the ground [2]. The simplest way to address this issue is through the reduction of plantar pressure through surface area augmentation at the ground surface, leading to less sinkage and dissipation before compaction [5, 9]. However, this typically decreases the mechanical advantage of the triceps surae–Achilles tendon unit, also leading to potential increases in energy costs [35-37].

It has been clearly shown that both dissipative terrain and passive-elastic parallel exoskeletons are able to significantly impact net human metabolic cost during bouncing gaits. Thus, we present a simplified model of a tricep surae-Achilles tendon system in parallel with a variable stiffness exoskeleton and variable area plantar surface that adopts a bio-inspired approach in order to achieve augmented human locomotion over complex media. Based on previous findings from modelling and human studies, we predicted that our model would (1) show increased muscle activation and less optimal velocity characteristics versus hard ground when hopping on a dissipative surface, (2) conversely show decreasing muscle activation and more optimal force-velocity operating points at optimal parameters of M_{exo} on soft ground and (3) by virtue of the Standard Linear Solid pressure dependent model used in the ground modelling, showcase a length dependent minima when assessing the impact of contact profile and stiffness on $\bar{P}_{met}$ Finally, we predicted that (4) our model would show that it is possible to mitigate the added metabolic cost of locomotion on dissipative media through equivalent $\bar{P}_{met}$ values at a specific morphology.

2.2 Methods

2.2.1 Modelling of Dissipative Terrain

The sandy surface in our model was modelled as a lumped system using the Standard Linear Solid (SLS) Representation for unidirectional sinkage into soils *[1, 15, 16, 41-44, 46, 47]*. Over the last few decades, the non-linear behaviour of soils has been captured and applied to simulations through various means such as Resistive Force Theory (RFT) *[10, 22, 34, 43, 48]* and Experimental fit [48]. We chose to employ a simplified Maxwell representation to provide a simplified, unidirectional, lumped-parameter system that was tuneable based on literature and experiments [1-4, 28, 31, 42, 44, 46, 49].

$$x_{sink} = \frac{F_{grf}}{\kappa A_{exo}}\left(1 - e^{-(\kappa/\beta)t}\right)$$

This convention was particularly useful when estimating environments with varying levels of stiffness and damping, such as soils and clays [42]. Implementation of this SLS model typically consists of pressure dependent sinkage of sheets of unidirectional stiffness and damping elements that estimate layer-by-layer sinkage into a particular substrate.

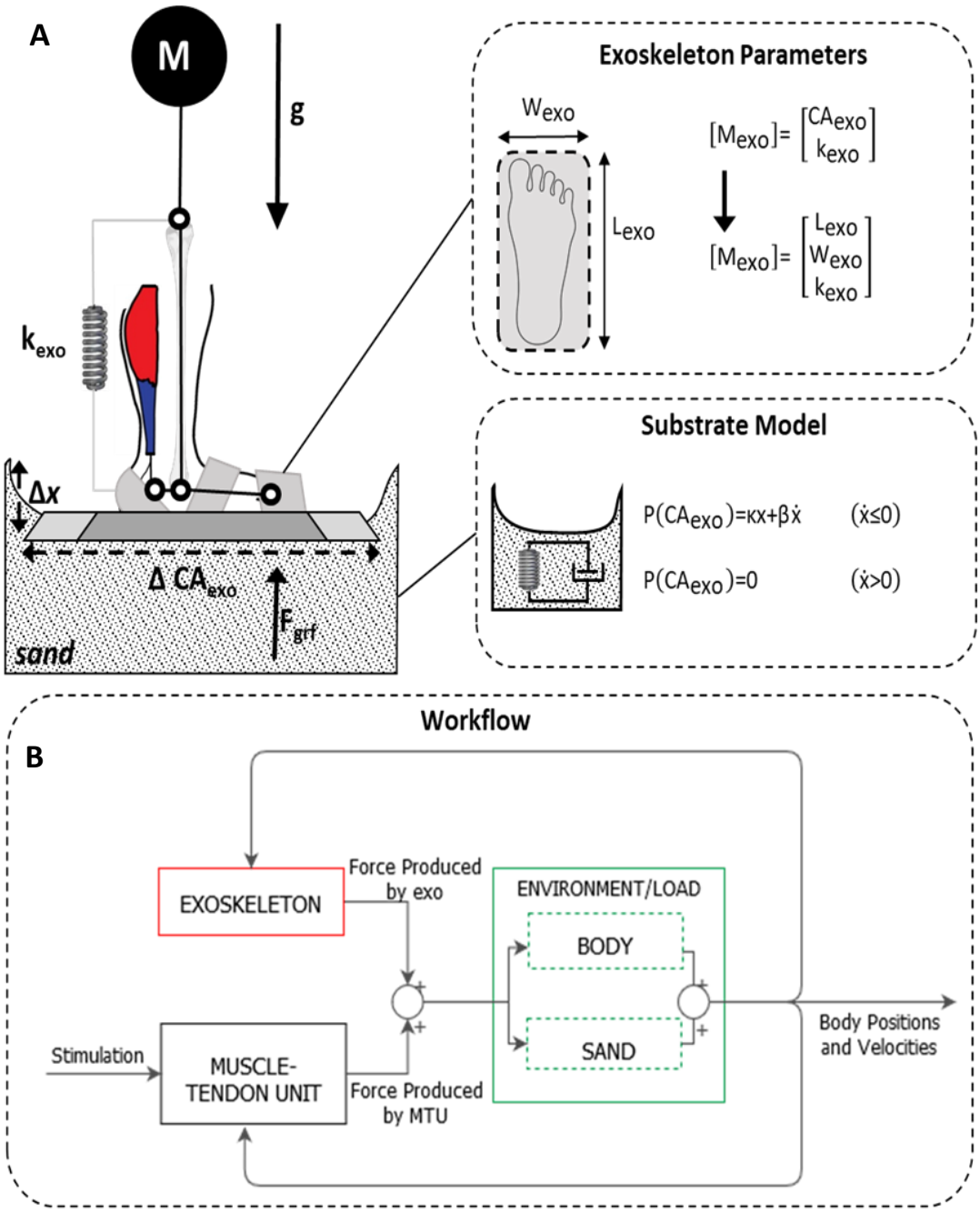

Figure 5 - Emulated (A) exoskeleton assisted human hopping, showing exoskeleton parameters, as well as the piecewise ground power space model for stiffness and damping combinations. (B) indicates the model workflow, showing the interaction of the MTU-exoskeleton system in (left) with the environment (right) to produce model output data.

2.2.2 Modelling Ankle Mechanics during bouncing gait

Since the Standard Linear Solid (SLS) model is most easily evaluated in a single direction [16, 41], and since we sought to emulate a bouncing gait [5, 32, 37], a hopping model was chosen for this set of experiments. As shown in Robertson *et al[36].*, hopping using the Hill-Type MTU model can be effectively used in passive elastic exoskeleton studies. This lumped MTU model is well suited to investigate the effects of mechanical augmentation on the full mechanics and energetics of the biological system using in-parallel elastic elements and moment arm modification. Another key strength of using hopping in this modelling framework is the ability to compare model predictions against parallel in-person mechanic and energetic hopping studies, as well as a plethora of past studies involving passive elastic assistance [35, 36] and substrate-dependent bouncing gait [1-4, 28, 31]

2.2.3 Modelling of Lumped Muscle Tendon Unit and Environment

Much like in our previous studies[36]., our muscle-tendon unit (MTU) was modelled based on a Hill-type CE governed by non-linear force-length *(F-L)* and force-velocity activation dynamics (*F-V*). It should be noted that the CE was able to generate both passive and active force due to the presence of a parallel-elastic element within the CE itself. The MTU and exoskeleton were both attached at a single point using the same fixed mechanical advantage for each gait cycle, and each cycle was performed under constant gravity. Additional details concerning parameters and rationale are discussed further in Robertson *et al[36]*. and in Appendix B.

2.2.4 Model Assumptions and simplifications

Much like in Robertson *et al[36].*, many key simplifications and assumptions were made in order to allow for computational realization of this model. As seen in our previous work[36]., both the gastrocnemius and the soleus muscles of the lower leg were combined into a single lumped muscle system[36]. This was combined with a single in-series elastic element representing the Achilles tendon (Figure 5). Secondly, while the model accounted for variation in mechanical advantage based on exoskeleton foot size, a fixed [47]value was used for each specific set of simulations and hopping trials. This does not account for variable biological gearing which alters the mechanical advantage of the tricep-surae-Achilles tendon system during each gait cycle[36]. Additionally, it was assumed that ground contact consisted of only one layer of substrate, unlike many cases in the SLS model where multiple in-series layers are used [42, 44]This serves to simplify the simulation complexity and speed, while still providing an accurate estimate of dissipative behaviour. Additional rationale and justification of model parameters can be found in Robertson *et al[36]*. and Farris *et al [35]*

2.2.5 Modelling the foot-ankle exoskeleton

To augment our Hill-Type muscle model of human hopping with a passive elastic device, we modelled three main parameters within our exoskeleton: Foot width (W_{exo}), Foot Length (L_{exo}), and Added parallel stiffness (Ratio k_{exo}/k_t). This made up our exoskeleton morphology vector (M_{exo}) that spanned the design space of our modelled device.

$$M_{exo} = \begin{bmatrix} W_{exo} \\ L_{exo} \\ k_{exo}/k_t \end{bmatrix}$$

The profile of the foot was estimated as a rectangle, with independently tuneable foot lengths (L_{exo}) and foot widths (W_{exo}). EMA was modelled to be dependent on L_{exo} and was approximated using the derived relationship:

$$EMA_{est} = 0.33 \frac{\left(L_{nominal} - \left(L_{nominal}/4\right)\right)}{\left(L_{exo} - \left(L_{nominal}/4\right)\right)}$$

Where $L_{nominal}$ for this study was 250mm, the chosen nominal length of an adult human foot. Similar to previous work in Robertson *et al[36]*, our modelled exoskeleton included a parallel-elastic element in the form of a linear spring in parallel with our biological MTU system. The resting length of the MTU corresponded to the slack length of the exoskeleton ($l_{o(MTU)} = l_{o(exo)} = l_o$ = 0.4m). As shown in literature, this was done to allow for scaled exoskeleton assistance during CE activation. Further details and parameters concerning the parallel elastic element are outlined in Robertson *et al[36]*.

2.2.6 Modelling Experiment Procedure

This modelling study was conducted in two main sections. Firstly, the model was stimulated at a frequency (ω_{stim}) of 2.5Hz, and held to a constant hop height (h) of 10mm. The size of the foot and mechanical advantage applied were held constant and

approximated that of a nominal human foot (W_{exo}= 150mm, L_{exo}=250mm), and exoskeleton assistance was held at 0 to simulate no assistance (k_{exo}/k_t=0). The viscoelastic stiffness κ was then varied from 10 Pa/mm (high sinkage) to 100 Pa/mm (almost no sinkage, pseudo-hard ground) in 5Pa/mm. Similarly, the viscoelastic damping was also varied from 0.02 Pa s/mm (almost no damping, pseudo-hard ground) to 0.05 Pa s/mm (highly damped). Much like in previous studies [36] stimulation was provided to the CE by a square wave pulse with a duty factor of 10%, chosen based on first order biological muscle activation dynamics. Simulations were run for 20s to allow for the system to become stable and achieve steady state hopping dynamics. The final 2 hopping cycles (t = [19.2 20]) were then used for analysis.

After this, a set of ground parameters that approximated human trials [5] [κ=40, β=0.045], was selected for use in the exoskeleton portion of the modelling study. Because of the inverse relationship between area and energy dissipation due to sinkage, and because W_{exo} has no effect on EMA in our model, we chose to set W_{exo} at a constant value of 250mm. This value was chosen based on the approximate maximum width before causing gait obstructions during nominal human walking [32]. The exoskeleton length (L_{exo}) was then varied from 175 mm to 450 mm in 25mm increments. Exoskeleton stiffness was varied from 0 kNm^{-1} to 180 kNm^{-1} (biological tendon) in 9 kNm^{-1} (5% k_{SEE}) increments, allowing for stiffnesses between 0% and 100% biological SEE. Similar to the first section of the modelling study above, stimulation was provided to the CE by a square wave pulse with a duty factor of 10%. Simulations were again run for 20 s to allow for the system to become stable and achieve steady state hopping dynamics. The final 2 hopping cycles (t = [19.2 20]) were then used for analysis.

2.2.7 Modelling Parameters

As seen in previous bouncing gait modelling and simulation studies[35, 36], the key criteria for successful trials are 1) the model successfully achieves a flight phase and 2) the model successfully stays within parameters that are both achievable and not injurious when juxtaposed to comparable human studies. As such, much like in Robertson *et al[36]*, we determined a hop to be successful when 1) The system as outlined in Figure 5 went slack, with the only force acting on the system being the weight due to gravity ($F_{net} = mg$), when 2) the normalized peak CE strain (ε) remained lower than 0.3 [35, 36] and finally 3) when the steady state hopping analysed was cyclic. Further information on computation of these parameters can be found in Robertson *et al.*

For successful trials, an analysis of the system mechanics and energetics was performed using a "ground up" approach. Beginning with the ground, the power ($\overline{P^+}_{ground}$) was found using the relationship:

$$\overline{P^+}_{ground} = \int_{t=0}^{T_{stim}} \left[F_{grf}(t) \times |x_{sink}(t)|\right] dt$$

Where $|x_{sink}(t)|$ represents the absolute value of sinkage into the ground. This allowed for the determination of the work dissipated, (or developed ground power) of each cycle.Similarly, average biological system powers were calculated over each cycle for the entire system, as well as the powers for each individual component (MTU and EXO, CE, SEE, Exo) as follows:

$$\bar{P}_{net} = \frac{1}{T_{stim}} \times \int_{t=0}^{T_{stim}} P_{mech}(t)\, dt$$

Where we use the relationship:

$$P_{mech}(t) = F_{system} \times v_{system}$$

This allows for the calculation of net powers per cycle, $\bar{P}_{net}$, indicating the biological work dissipated over each cycle.

Forces and activations were also explored in our analysis, particularly peak system forces (F_{peak}) and activations (α_{peak}) during a cycle. As seen in previous studies[35, 36], examination of this at the level of each of the system components allows for the observations of how load is shared during peak force production for a given ground condition and M_{exo}. Much like in Robertson *et al*, reported values in this study include both active and passive CE force contributions.

Investigation of the mitigation of metabolic cost was a key point of this study, and as such, we examined system energetics in our model through the use of an averaged metabolic rate ($\bar{P}_{met}$). As seen in Minetti *et al[19]*, this allows use to have a standardized value at each dynamic muscle state based on CE Force (F_{CE}), CE velocity (v_{CE}), and CE activation (α_{CE}). This equation over a cycle can be represented as:

$$\bar{P}_{met} = \frac{1}{T_{stim}} \times F_{max} \times v_{max} \times \int_{t=0}^{T_{stim}} \left[\alpha_{CE}(t) \times p_{met}\left(\frac{v_{CE}(t)}{v_{max}}\right)\right] dt$$

Where $p_{met}\left(\frac{v_{CE}(t)}{v_{max}}\right)$ is the time-dependent dimensionless metabolic cost factor *[19]*. Further details concerning the parameters, equations, constants and model structure can be found in Appendix B.

2.3 Results

2.3.1 Ground Powers

Ground power ($(P^{+})^{-}_{ground}$) was found to vary with ground stiffness (κ) and damping (β). We found an increase in $(P^{+})^{-}_{ground}$ as stiffness decreased, attributed to the non-compliance (unidirectionality) of the ground surface (Figure 6). Similarly, $(P^{+})^{-}_{ground}$ was found to increase as damping increased. Due to the use of the SLS Maxwell model, these variations were not independent. No flight was observed for κ-β combinations with low (<10) values of κ, as well as high (>0.035) values of β.

Based on previous literature, various points were selected within the ground space, and assigned names based on behavioural similarity to various terrain, including "hard ground", "dirt", "compacted sand" and "loose sand". [6, 9, 24, 28-35]. Ground power time series and work loops for these selected points are shown in Figure 6.

2.3.2 CE Powers

Analogous to $(P^{+})^{-}$ground relationships, MTU powers increased as the ground became more dissipative (increasing κ and β), with maximal average power being observed for a "loose sand" condition, (κ ≈ 20 and β ≈ 0.45). We found an increase in power dissipation from $P^{-}_{(MTU)} \approx 0$W to $P^{-}_{(MTU)} \approx 8$W. This can be seen in Figure 6, Figure 7, Figure 8and Figure 9, which show the power dissipation calculated at the ground, MTU, CE and foot level.

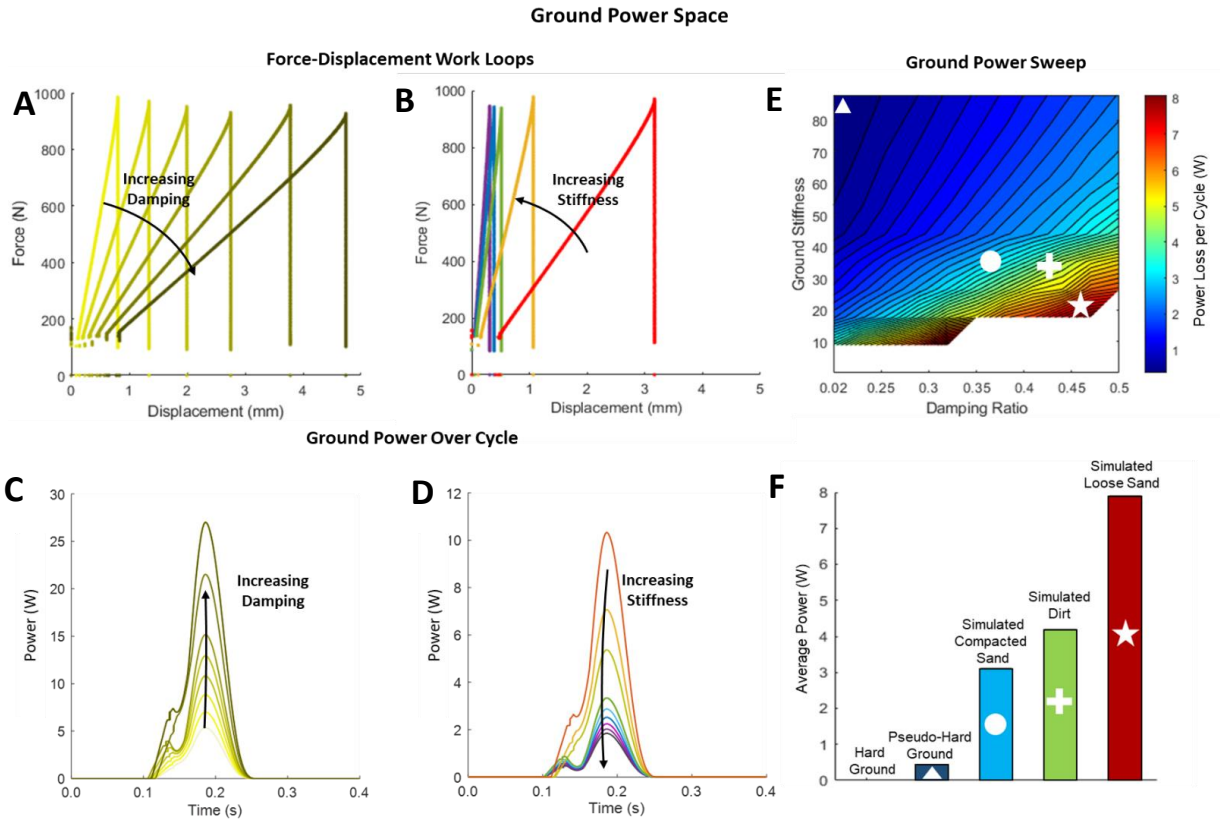

Figure 6 - (A) and (B) show the effect of increasing damping and stiffness respectively on the total work performed by the muscle on the ground, or by the ground through deformation, with (C) and (D) showing this with respect to time. Since our sinkage is unidirectional, this acts as a "ratchet", and does not allow for conservation of energy as seen in a nominal bidirectionally compliant surface. (E) and (F) shows the power loss space for the ground, with the equal and opposite being applicable to the MTU system.

2.3.3 Forces and Activations

As seen in Figure 8 (A), activations for the loose sand conditions showed an 11% increase from the nominal hard ground case, with CE activation (A_{CE}) increasing from a 0.54 to 0.6. As seen in Figure 8(A) F_{MTU} also saw a 9.1% increase in this interval. In general, both activations and F_{MTU} of the unassisted conditions increased as the terrain became more dissipative, while F_{GRF} remained consistent, indicating comparable hop heights

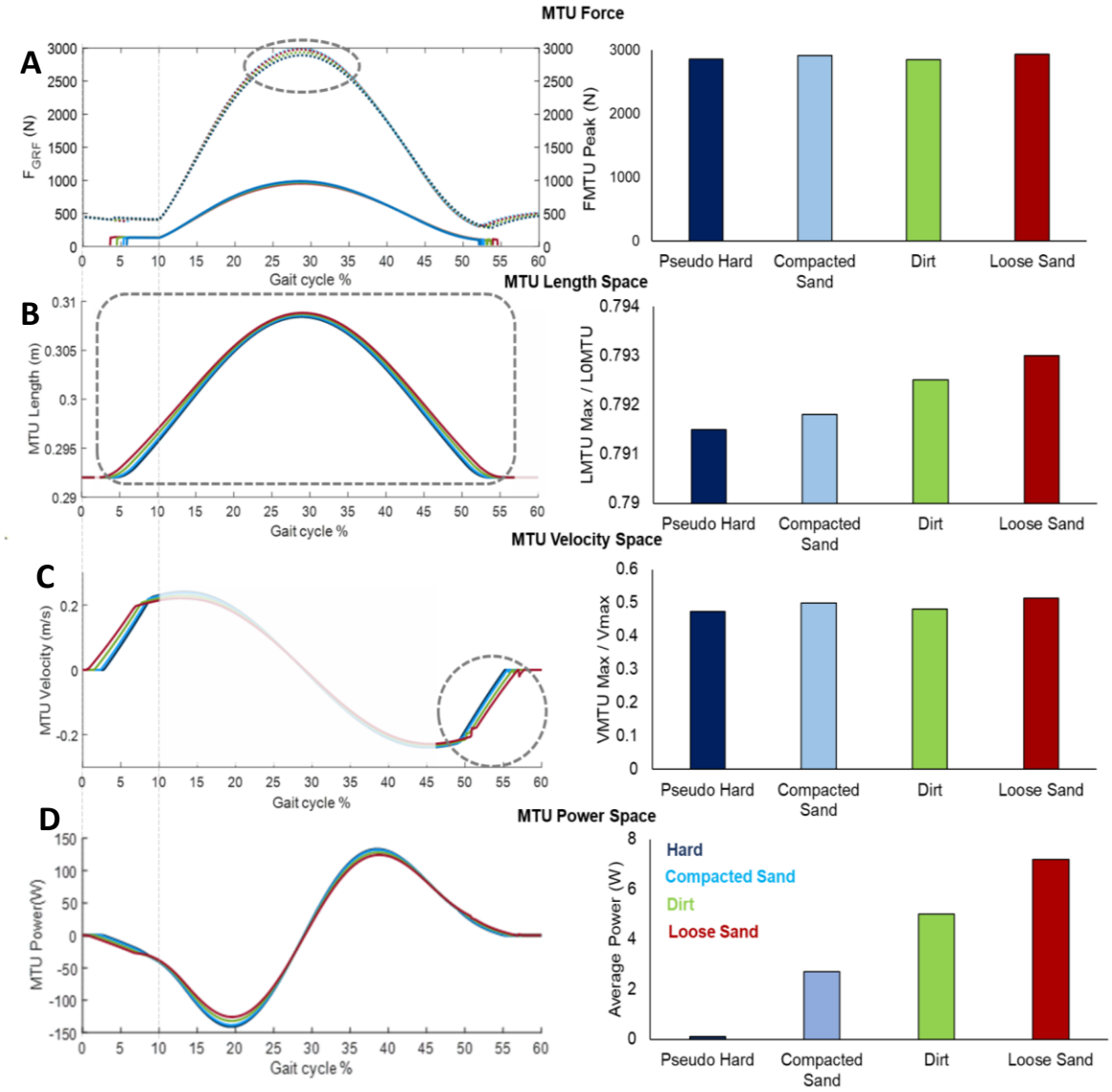

Figure 7 - (A) Forces for the unassisted MTU system (left) as well as peak Force values at different ground conditions. (B) MTU Length during stance on selected terrain (left). In general, we see a small increase in average, maximum and minimum operating length as dissipation of the ground surface increases. (C) MTU velocity during stance (left) as well as minimum, average and peak CE velocity achieved as a function of v_{max} (right), (D) CE power space over stance (left), as well as average power (right). In general, we note the trend of average power becoming increasingly positive from 0 as the ground becomes more dissipative.

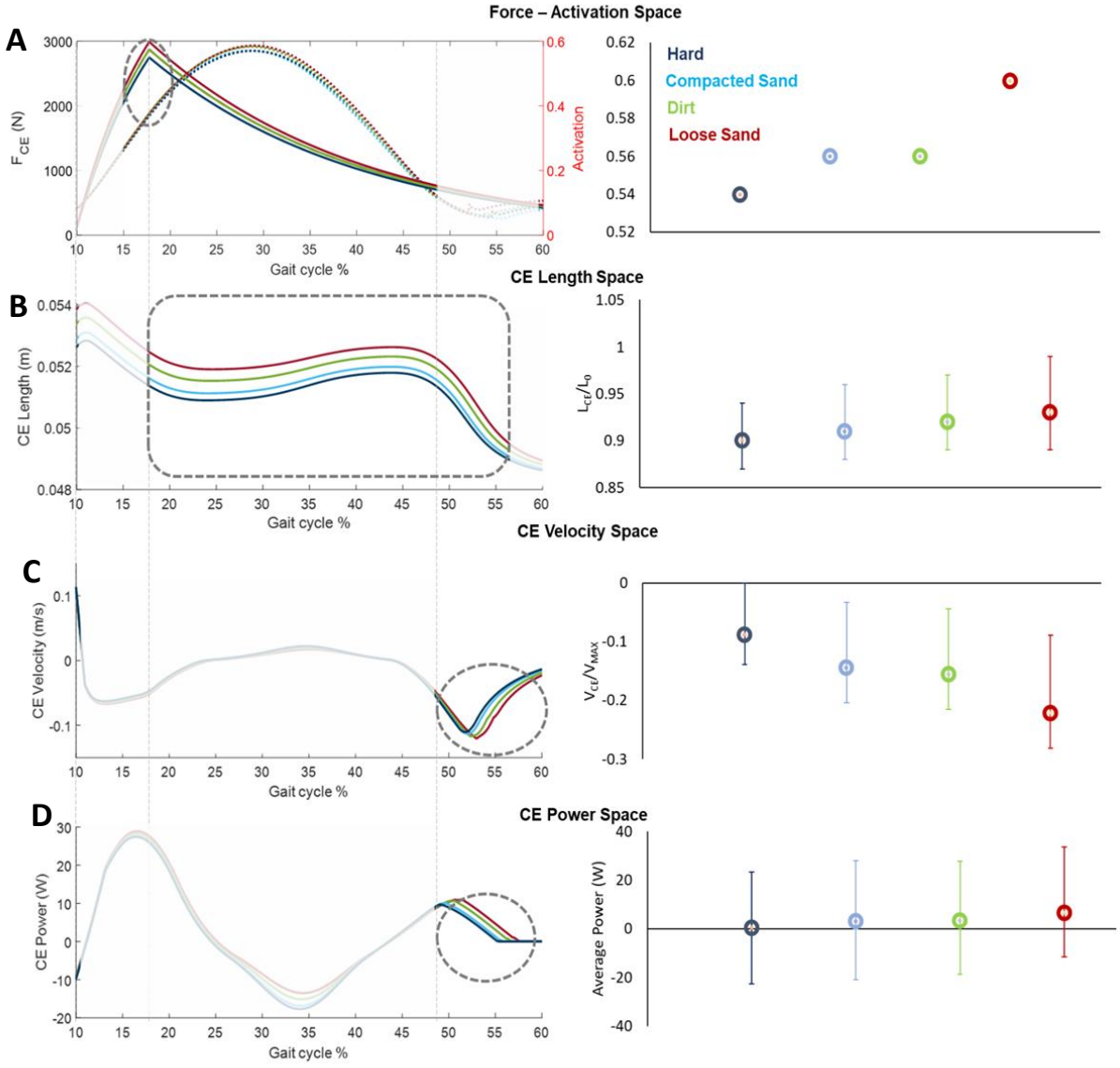

Figure 8 - (A) CE Forces and activations for the unassisted MTU system (left) as well as peak CE activation values at different ground conditions. (B) CE Length during stance on selected terrain (left). In general, we see a small increase in average, maximum and minimum operating length as dissipation of the ground surface increases. (C) CE velocity during stance (left) as well as minimum, average and peak CE velocity achieved as a function of v_{max} (right), (D) CE power space over stance (left), as well as net work (right). In general, we note the trend of net work becoming increasingly positive from 0 as the ground becomes more dissipative.

2.3.4 Energetics and Metabolic Rate of Unassisted System

Values for metabolic rate (P_{met}) of the unassisted system (Figure 9) scaled almost directly with A_{CE} (Figure 8(A), with A_{CE} values increasing as the media become more dissipative, with an increase from 1.51W/kg to 1.87W/kg, indicating an increase of ~23% across conditions. In addition to an increase in activations, as dissipation in the given media increased, there was an increase in shortening velocities represented by $\frac{v_{CE}}{v_{max}}$ (Figure 8(C)) , allowing for more costly force production[2, 35, 36, 38, 50], however, this was offset by the CE operating lengths ($\frac{L_{CE}}{L_0}$) (Figure 8(B)) operating at a slightly increased length, leading to less costly force production[2, 35, 36, 38, 50].

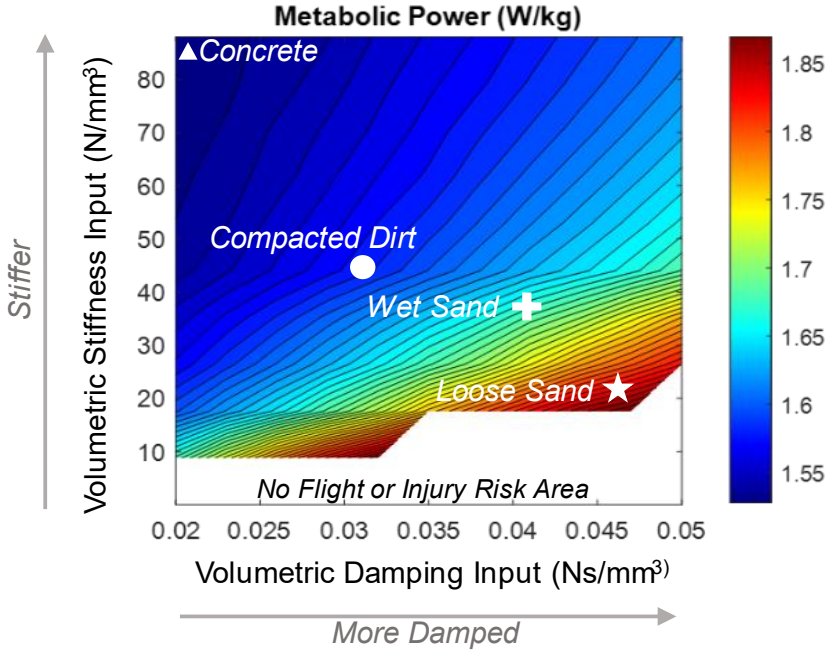

Figure 9 - Net metabolic power of the unassisted system in the ground space, with corresponding shape annotations indicating different corresponding ground conditions on the contour.

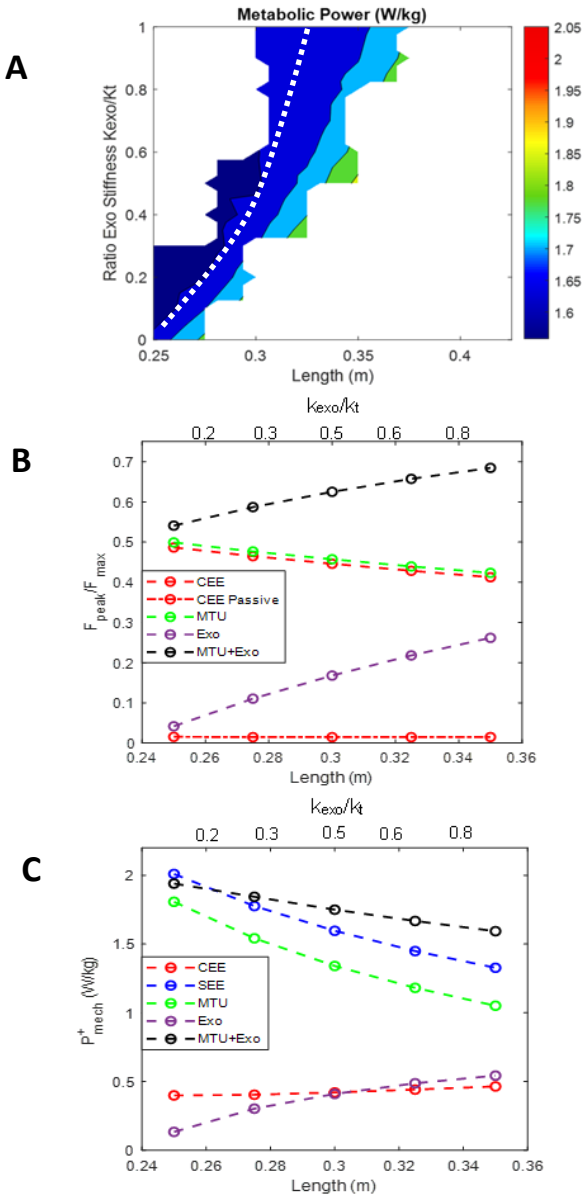

Figure 10- (A) Average metabolic rate for the various combinations of the exoskeleton used for augmentation of the loose sand condition identified in Figure 9 above. With X highlighting the chosen parameters. And - - showing a constant Pmet (W was held at 0.25m) (B) MTU + Exo peak force and system component contributions for points indicated by white dots in (A). Biological components are unloaded as Exo contributions rise in conjunction with increased passive contributions from CE. (C) Average positive power output from MTU + Exo and its components for the same points as in (B). System level power decreases and MTU/SEE power output decreases, while CE positive power remains nearly constant.

2.3.5 Exoskeleton Contribution

2.3.5.1 Force and Power Sharing

Selected points of constant P_{met} can be seen on Figure 10(A). with force and power sharing relationship highlighted in Figure 10(B) and Figure 10(C). Figure 10(B)) shows traded energy cycled in biological tendon for energy cycled in the modelled exoskeleton, thereby reducing F_{MTU} in the biological MTU for the loose sand condition. While CE force decreased, Force from the increased in order to overcome the additional moment arm as the EMA of the system decreased with increasing length of the foot.

Despite increased $F_{MTU} + F_{exo}$ these was actually a decrease in total power ($P_{MTU + Exo}$) due to the reduced sinkage and dissipation into the media for increasing values of contact areas as L_{exo} increased. While Exo power increased with increasing values of kexo/kt, and MTU power decreased for the same points, it was found that CE power actually increased for high values (>0.32 of L_{exo})

2.3.5.2 Energetics and Metabolic Rate Reduction

Values for metabolic rate (P_{met}) of the augmented system once again (Figure 10) scaled almost directly with A_{CE} (Figure 8(A), with A_{CE} values decreasing at the chosen parameters from, 1.87W/kg unassisted to 1.57W/kg, indicating a decrease of ~16% from the loose ground condition, with the final morphology given as:

$$M_{exo} = \begin{bmatrix} 0.25 \\ 0.3125 \\ 0.5 \end{bmatrix}$$

This indicates a total increase of ~1.3% over the Pmet requirement for unassisted hard ground hopping as seen in Figure 9.

In addition to a decrease in activations, there was an additional increase in v_{CE}/v_{max} (Figure 11(C)), allowing for less costly force production. We also found a relatively smaller increase in, CE operating lengths (L_{CE}/L_0) (Figure 11(B)) .

2.3.6 Comparison to literature and Experimental Data

An increase in P_{met} of approximately 23% was found between the unassisted hard ground and loose sand conditions. This is lower than both the increase of approximately 50.1% from preliminary in vivo experimentation at 2.5Hz*[5]*, and the initial findings of Lejeune et al, who reported approximate energy expenditure increases of 60% for running on a sand track*[2]*. In these studies, participants were allowed to hop to a preferred height*[5]*, or run at a preferred pace. Qualitative assessment of these subjects indicated the need for additional hop height, and thus additional CE activation to appropriately propel the subject above the area of compression in the substrate and avoid collection of particles on the dorsal region of the foot. This increased height and activation gives insight into the offset between experimental and modelled values of ΔP_{met}.

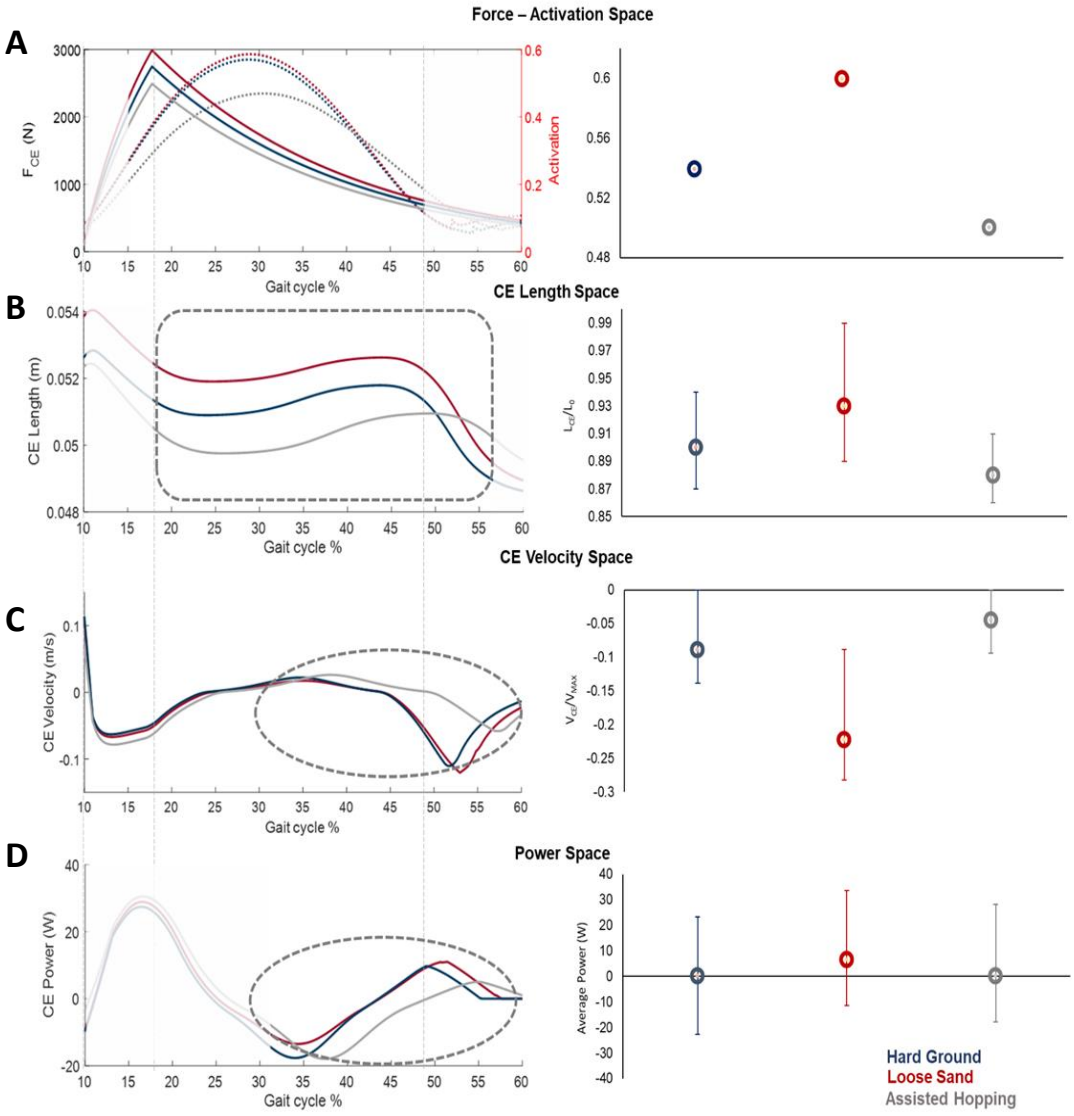

Figure 11 - (A) CE Forces and activations for the unassisted MTU system and MTU + Exo for the chosen Mexo at the loose sand conditions. (B) CE Length during stance on the selected terrain. In general, we see a decrease in average, maximum and minimum operating length when the system is augmented with the exoskeleton. (C) CE velocity during stance (left) as well as minimum, average and peak CE velocity achieved as a function of vmax (right), (D) CE power space over stance (left), as well as average power over cycle (right). In general, we note the trend of average power decreasing to near 0 when the system is augmented.

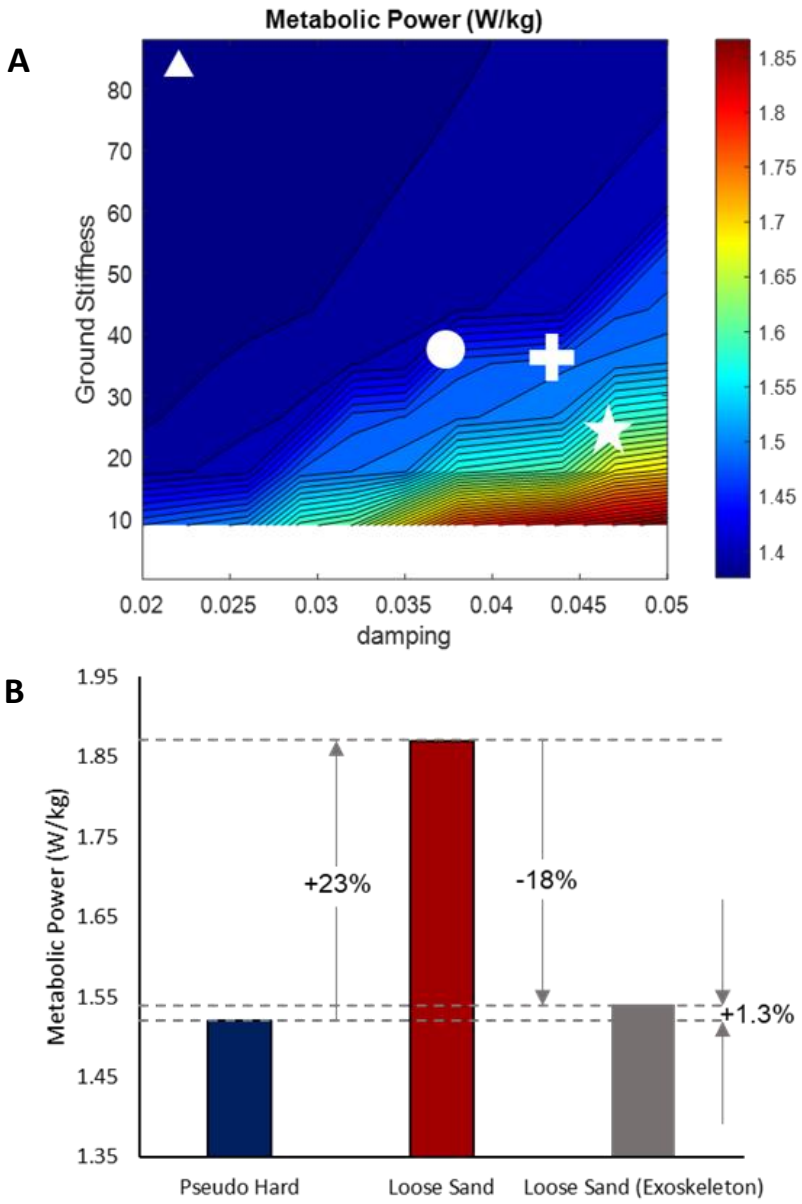

Figure 12 – (A) Net metabolic power of the assisted system at the specified Mexo in the ground space, with corresponding shape annotations indicating different corresponding ground conditions on the contour. (B) Comparison of Metabolic costs across unassisted and assisted conditions

2.4 Discussion

The purpose of this study was to comparatively investigate the mechanics and energetics of human hopping to a fixed height from rest, with conditions of hard ground, dissipative terrain, and an augmented system with a foot-ankle exoskeleton over dissipative terrain. This was performed as a first step in a comprehensive modelling, simulation, and real-world series of experiments, with the intention of further expanding the limited scope of knowledge and literature pertaining to muscle-level human locomotion on dissipative terrain[1-4, 7, 8, 26-31, 49]. Based on the results of our model, we were able to identify trends and insights into the unassisted hopping on dissipative terrain, as well as design considerations, benefits and drawbacks associated with the use of our proposed device.

2.4.1 Activation and Velocity Dynamics of the Unassisted System

Previous experimental studies demonstrated an increased metabolic cost when running and walking over dissipative terrain for a series of comparable conditions **[2]**. As such, we hypothesised that our model would show increased muscle activation and less optimal velocity characteristics versus hard ground when hopping on a dissipative surface. These activation and velocity changes were hypothesised because of their direct correlation to Pmet in our model, due to the use of the metabolic cost estimation presented by Minetti et ***al[19]***, as well as previous literature showing this to be the case for 1 DOF Hill-Type hopping model scenarios with increasing P_{met} among different parameters for comparable mechanical tasks **[35, 36]**. To this end, we found that our model's activation and velocity behaviours agreed with this hypothesis. As seen in Figure 8(A), activation increased 13%

from ~0.54 to ~0.61 when comparing hard ground to the loose sand condition. Additionally, maximum push off velocity (Figure 8(C)) was found to increase from (-)0.11m/s to (–)0.14m/s (27%), providing a less energetically favourable condition for force production**[2, 35, 36, 38, 50]**. Upon confirmation of this hypothesis, further investigation was also carried out through the examination of the length of the CE, due to implicit effects on P_{met} in the metabolic model used. Unlike the velocity characteristics found in our model, we found that the CE average operating lengths across conditions increased up to 10% per cycle from hard ground to dissipative terrain. This value is associated with slightly less costly force production **[2, 35, 36, 38, 50]**, leading us to further predict that to some degree, a more costly CE force-velocity was offset by the less costly force-length dynamics in the modelling system. This is inconsistent with previous experimental literature **[35, 36, 38]**, as well as initial human trials that analyse muscle level dynamics for increasing P_{met}. As such, we believe that this response was due to modelling and optimization limitations. We predict that for the *in-vivo* experimental realization of this study, we will experience even higher P_{met} values due to less favourable CE operating lengths as activations and velocities increase, in line with literature and pilot data. This can in turn further inform the refinement of the modelling and simulation framework to provide a more robust platform for future studies.

2.4.2 Activation and Velocity Dynamics of the Assisted System

Our second hypothesis predicted that, much like previous models that included a passive elastic exoskeleton in parallel with the Hill-type muscle model, [32, 35, 38], we

would find decreasing muscle activation and more optimal force-velocity operating points at optimal parameters of M_{exo} on soft ground. Much like our first hypothesis, these activation and velocity changes were also hypothesised because of their dependence on the metabolic model presented by Minetti et *al[19]*, as well as results from previous work presented by Robertson *et al*. Like our unassisted hopping condition, our model findings fully supported this hypothesis. As seen in Figure 12(A), activation decreased 15% from ~0.61 to ~0.52 when the unassisted loose sand condition is compared to trials using our optimal set of parameters as found in Figure 10A. Maximum push off velocity (Figure 11(C)) was again found to decrease from -0.14.m/s to -0.06m/s, providing once more a more energetically favourable condition for force production[2, 35, 36, 38, 50]. Because of the unexpected force-length relationship in our first hypothesis, we also examined the CE length changes for the augmented system (Figure 11C). Even though the force-velocity operating point was found to be more favourable, we found that the CE lengths once again decreased by an average of 3% per cycle between the unassisted and assisted conditions. While this decrease is associated with more costly force production[2, 35, 36, 38, 50], the amount of CE length reduction was not sufficient to allow the system from having a significant net reduction in $\bar{P}$met.

2.4.3 Analysis of Exoskeleton Morphology

Thirdly, we hypothesised, by virtue of the Standard Linear Solid pressure dependent model used in the ground modelling, that our $\bar{P}$met results would showcase a length dependent minima when assessing the impact of contact profile and stiffness. This

hypothesis was confirmed (figure 10(A)). For increasing values of Lexo, and constant maximal values of Wexo, we found a decrease in $\bar{P}_{met}$, until a minima dependent on k_{exo}, with moderate values of Lexo and kexo giving the lowest value for $\bar{P}_{met}$ in the metabolic space. This is due to the reduced ground force at a given activation and level of CE force reduction as Lexo increases, since our model scaled EMA with foot size. Because of the independence of EMA and contact width, our W_{exo} was maximized at 0.25m, representing the maximum nominal width for current devices such as snow and sand shoes, that allows for minimum interference between legs during gait cycles **[10, 18, 22, 51-53]**. Based on these trade-offs of EMA and reduced sinkage/dissipation, we predict that further attention to exoskeleton design that leverages the 3-dimensional behaviour packing of granular substrates **[34]** can further reduce $\bar{\boldsymbol{P}}_{met}$ by allowing further lowering of CE forces and P_{mech} than seen in figure 10 (B, C). This layer of simulation would add significant complexity and computation time to the modelling framework since it would require deeper substrate modelling than the SLS model and higher degrees of freedom in the coronal plane. As such, this morphology optimization will be further explored experimentally in our future work, and is discussed further below

2.4.4 Combined System Energetics

Finally, as a culminatory hypothesis, we predicted that our model would show that it is possible to mitigate the added metabolic cost of locomotion on dissipative media through equivalent $\bar{\boldsymbol{P}}_{met}$ values at a specific morphology. As seen in figure 7, at the loose sand condition, $\bar{\boldsymbol{P}}_{met}$ was found to be 1.57 W/kg, a 1.3% overall increase over the hard

ground condition for Mexo = [0.25, 0.3125, 0.5]. As shown in previous studies[35, 36], in-parallel passive elastic elements showcase a maximum reduction in CE power and at $\overline{\boldsymbol{P}}_{met}$ at moderate values of kexo before a subsequent increase and no flight condition. This is seen in our contour in figure 10(A). Similarly, since dissipation is linked inversely to contact area, we expect that the minimum value of Pmet for **Wexo** is found at the maximal allowable width. Minimum values of $\overline{\boldsymbol{P}}_{met}$ with respect to Lexo were expected at a local minima of length due to its EMA correlation and sinkage dependent effects (figure 10 A). Based on these findings, and the muscle level insight from the hypotheses above, we have confirmed this hypothesis.

Similar to the hard ground study in Robertson et al [36] and there was an ideal compliance of the in-parallel elastic element that produced a metabolic minima (figure 10A) However, because of the introduction of a morphology to reduce power transfer to the environment, we see a reduction in overall P_{mech} along equivalent metabolic cost values as Lexo and kexo increase (Figure 10B). We see that L_{exo} has a more drastic effect on P_{met} values (Figure 10A), and as such we believe the foot morphology to be the most significant optimization factor when reducing P_{met} *in-vivo*.

2.5 Conclusions, Future Directions and Implications

2.5.1 Conclusions and Implications

Bipedal gait has been widely studied, both in the context of biomechanics and robotics, but little work has been done to yield a general formula for locomotion over

complex media. We have presented a preliminary modelling and simulation framework to examine the metabolic energy cost of hopping in sand, with and without a novel, unpowered exoskeletal device. These findings now open up the possibility for a new class of wearable devices that can mitigate the metabolic penalty of moving in complex, dissipative terrain.

An implication of this model, much like in *Roberson et* al, was that it is in fact possible to use the augmented device to achieve improved metabolic performance at a specified mechanical task, not just at the selected ground surface, but across all examined terrains, including hard ground (figure 9(A)). We expect that foot geometry that increases EMA in order to reduce sinkage becomes less necessary as the surface becomes less dissipative, however, even with a lower mechanical advantage, the CE was able to operate at a lower metabolic rate on hard ground due to in-parallel passive assistance from the exoskeleton. In conclusion, our model predicts that added contact area between foot and ground with modified stiffness around the ankle joint allows for the elimination of the penalty associated with energy dissipation during locomotion on granular substrates.

2.5.2 Experimental Realization

Looking to the future, experimental continuation of this study can first yield a more complete understanding of the human neuromuscular response to the complex non-linear behaviour of changing substrates, and then leverage this information to make more informed optimal control schemes and devices that are better suited to “real-world” use. To do this, we are currently in the process of designing and building this exoskeleton device, informed by the results of this study. This type of ground-up development is

necessary since current wearable device design and fabrication follows traditional techniques for rigid body robotics or medical devices. Over the last few years there have been significant advances in terms of designs that optimize energetics on hard surfaces, however, little has been done to change the approach of this to specialize the design for use on complex substrates. Thus, a key long-term goal of this study is to discover fundamental principles and establish a methodology that can be used to design devices at the human-machine-environment interface for human performance optimization, with respect to physical and metabolic function. This opens up the paradigm for tuneable, passive, terrain-specific augmentative devices that allow their users to go further than ever before.

2.5.3 Associated Publications

This work will be submitted to the Journal of Bioinspiration and Biomimetics following final editing and revision.

CHAPTER 3. LINKING THE NEUROMECHANICS AND TERRADYNAMICS OF LOCOMOTION ON SAND

Human locomotion over dissipative terrain carries a significant metabolic penalty when compared to similar gait over hard ground. Recent studies have begun to quantify this penalty, finding metabolic rate to be greater than expected based on the mechanical work estimated at the whole-body level. To that end, joint-level studies have highlighted differences in contributions from the ankle, knee and hip, but the link between these two is not well established. Motivated by previous work *in-silico*, we determined that for a mechanically matched hopping task *in-vivo*, locomotion in sand indeed warranted a higher metabolic cost than that of hard ground, stemming primarily from more work being done at the ankle ($p \leq 0.05$), and determined that the metabolic cost increase exceeded the anticipated value, based on combined leg work ($p \leq 0.05$), using an expected efficiency of positive mechanical work of 0.25. This study presents the first analysis of human locomotion on dissipative terrain that links the whole-body metabolic effects to the joint level and ground level terrain level mechanics and sets the stage for further exploration into muscle level neuromechanical changes to determine the underlying effects of these inefficiencies.

3.1 Introduction

The mechanics and energetics of human locomotion on deformable media have been studied for decades, with works examining the metabolic expenditure and joint level effects across various forms of locomotion. While these works have linked whole body mechanics to energetics, little has been done to understand the underlying causes associated with the increased cost of transport in humans at the joint, muscle and ground surface level [2, 3, 5, 26-31].

To date, much of this has been attributed to the limitations of instrumentation and sensing, however, there are indeed a few key pieces of work that begin to paint a picture of what some of these causes may be. Lejeune, Willems and Heglund examined the locomotion mechanics and overall metabolic effects of movement on sand and found mechanical work and energy expenditure requirements of up to 1.15 and 1.6 times higher respectively for walking and bounding gaits on sand when compared to hard ground trials [2]. They highlight that energy expenditure is not linearly scalable to actual mechanical work, especially over dissipative terrain, with potential causation at the muscle level, as well as discrepancies due to assumptions concerning instrumentation, since Lejeune et. al used buried force plates for their whole-body mechanical vs metabolic cost comparison [2].

Even still, to date there have been no human studies that allows for direct inverse dynamics from human locomotion over these substrates that directly link these mechanics to muscular function. While these analyses are well documented for hard ground studies, there has not been a reliable way to obtain the center of pressure and ground reaction force

vector [18, 23-25], and as such, for in-vivo locomotion on damped substrates, there has yet to be a direct measure of joint level effects on substrates such as sand, snow or mud.

Perhaps the best approximation of this damped terrain locomotion can be found throughout a series of experiments conducted by Moritz and Farley that began to explore the joint level effects of locomotion on damped terrain. Through the use of a custom built platform, they explored the effect at the joint level of bouncing gait locomotion through hopping on a damped surface [7, 8]. Through this analysis, they concluded that as the surface became more damped and the leg increasingly became more like an actuator, and less of a spring, as modeled by the conventional spring-loaded pendulum model of bipedal bouncing gait. Additionally, they found that the ankle was the primary joint that accounted for the additional work needed to overcome dissipation. Birch et al [6] had similar findings, where they concluded that the extra injection of work was most important at the ankle and foot surface in order to overcome the effects of damping on a similar apparatus. These works however, do not link the whole body energetics, or the muscle level mechanics to these observed mechanical differences. This study begins to bridge this gap

More recently, Kowalsky et al [40] continued investigating this link between energetics and mechanics, and further suggested that some of the additional cost of transport of locomoting in these dissipative terrains stemmed from differences in gait parameters, such as stride length and clearance. As such, in this study, we find it important to provide subjects with mechanically identical tasks on both hard ground and dissipative terrain in order to begin to examine the key differences between individual joint contribution and their relation to the whole-body energetics, while accounting for these

changes. Additionally, when considering that humans exhibit a “bouncing gait” [2, 32] the rationale for using hopping as the form of investigated locomotion can be seen [35, 36]

When considering the link between mechanics and energetics, there have been multiple studies that establish this link for a variety of hard ground locomotor tasks, both at the joint and muscle mechanics levels. At the whole body level, hard ground studies have shown that mechanical requirement of bounding gait is well explained by the energetic cost of muscle work [54], with the ankle being the primary mover for hard ground hopping [5, 35-37, 55, 56]. This actual muscular work has been further been reported to be related to both the amount of active muscle, as well as the rate of use [57].To further investigate this, Beck et al [55] directly measured this active muscle volume variation (as a function of muscular force-length and force-velocity), for the soleus as a measure of activation rate and time (in the form of duty cycle), with metabolic rate being found to relate to both factors. At the observable joint level, changes in muscle-tendon unit length can be seen as they relate to the ankle joint angle, and, given comparable forces to allow for matched heights, soleus velocity can be related to the power of around the ankle joint. While these studies provide insight into the basic neuromuscular causes of changes in ground locomotion, linking these to the joint and muscle mechanics of dissipative terrain locomotion has yet to be explored, and is a key objective of this study.

Thus, as seen above, while there have been many studies that begin to establish the link between the mechanics and energetics of hard ground locomotion [2, 6, 7, 32, 40], as well as whole body energetic and analyses dissipative terrain locomotion, little has been done to begin to relate these energetic effects at the whole body level to that of joint level mechanics with implications at the muscle level. Our study presents a first step toward

linking energetics to joint level mechanics, using a customized in-lab apparatus to perform the first comprehensive analysis of the joint-level inverse dynamic relationships for human locomotion on sand. The goal of this study was to understand why, at the joint level, it is more metabolically costly to locomote on sand, when compared to a comparable locomotor task on hard ground, in order to further inform the direction of future, muscle level studies. To this end, based on previous findings from modelling and human walking studies, we hypothesized that participants would (1) show an increase in metabolic cost when performing a mechanically comparable task on sand versus hard ground, (2) Show increasing powers at the ankle, knee and hip joints, with the ankle joint being the primary contributor (3) Show more plantarflexion at the ankle, indicating shorter soleus operating lengths, and (4) show that the increase in mechanical changes are not sufficient to account for metabolic rate differences. These results serve to further the scope of knowledge of bipedal locomotion in dissipate substrates and can further inform future studies at the muscle level, as well as the design of wearable devices that allows users to go further and farther than ever before.

3.2 Methods

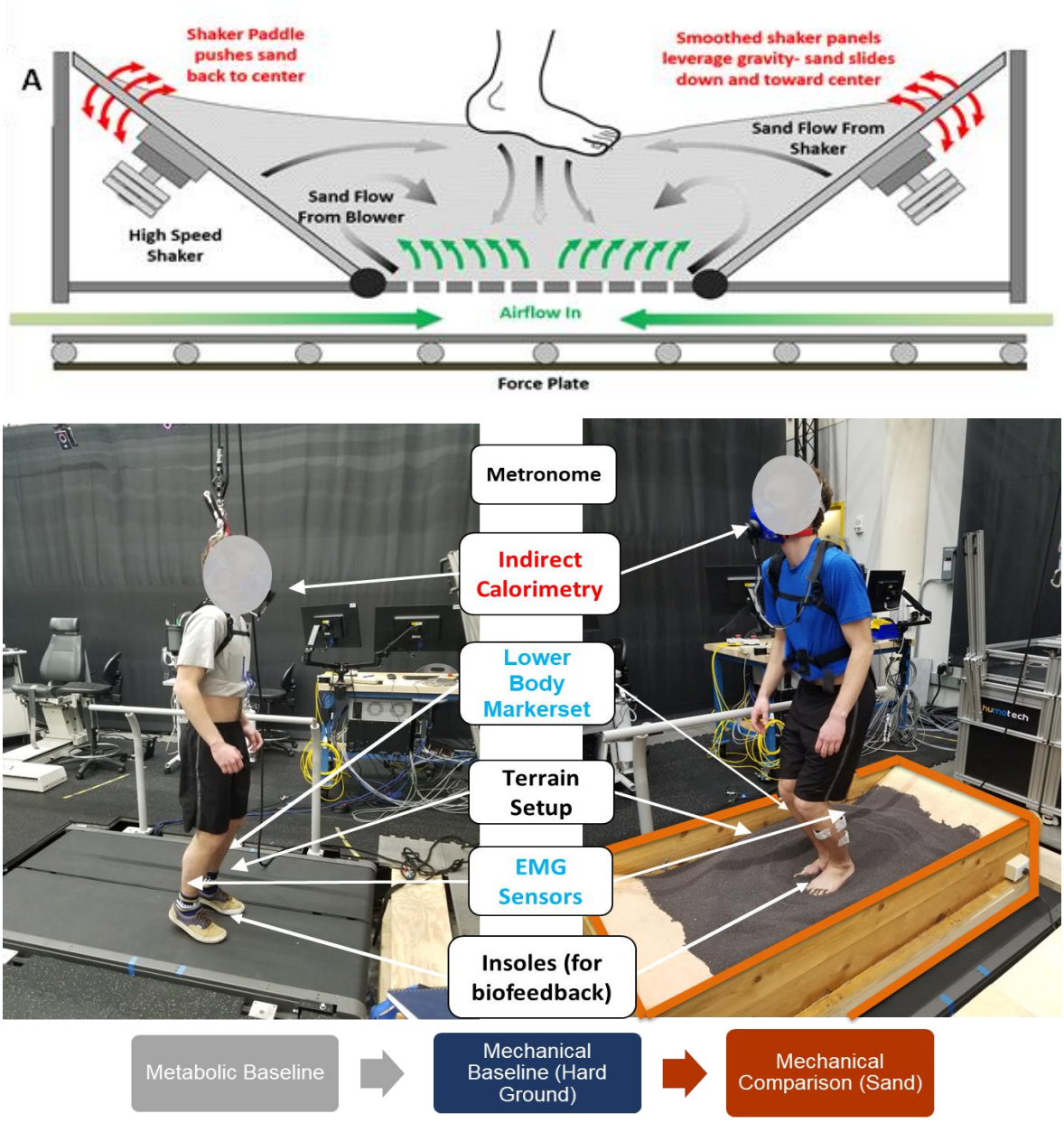

Figure 13 - The experimental setup for the hard ground and sand hopping studies over the course of this series of studies. A custom sandpit setup was built (A) that allowed for sand leveling and prevented "bottoming out" during data collection (B) through the use of shakers and blowers if necessary

In order to begin to examine the connection between the whole body energetics and joint level effects of locomotion on sand, we performed hopping trials over a series of

frequencies and heights, with a focus on mechanically matched conditions across subjects. eight of the ten volunteers who enrolled in our study completed the protocol in its entirety (average ± standard deviation; age: 23.63 ± 2.67 years; height: 1.78 ± 0.05 m; mass: 81.5 ± 10.1 kg; resting metabolic rate 1.48 ± 0.14 W/kg). The two volunteers were excluded from the analysis were removed due to the inability to maintain a Respiratory Exchange Ratio (RER) < 1 for more than 50% of the trials . All participants reported themselves to be free of cardiovascular and metabolic disorders. Prior to starting study, informed consent was obtained in accordance with the Georgia Tech Institutional Review Board.

3.2.1 Metabolic Trials

For metabolic measurement sessions, participants were asked to fast overnight, and upon arriving in the morning, they were asked to stand still and upright with their hands at their sides. In this standing position, participants performed a 10-minute resting trial while breathing in-and-out of a mask that connected to an indirect calorimetry system (COSMED K5, COSMED Srl, Italy).

For sessions 1 and 2, participants were asked to don a pair of force sensing insoles (novel, Germany), and reflective makers were placed at the left and right posterior superior iliac spine to provide height biofeedback to serve as a secondary biofeedback measure and validation through motion capture (Vicon, Oxford, UK). Subjects were then asked to 6 x 5-minute hopping trials each on hard ground and soft ground for a total of 12 trials over two sessions. Trials were performed at 2.5Hz with to specified height, at 2.2Hz, 2.5Hz, 2.8Hz and 3.2Hz to the subject's preferred height, and finally at the subject's preferred

frequency and to a set height. Frequency and terrain conditions were randomized, and height and frequency control were performed using real-time biofeedback and a metronome respectively. Hard ground hopping and Sand hopping were performed on different days in random order to mitigate the effects of subject fatigue, with a corresponding resting trial for each day. During each hopping trial, metabolic expenditure was measured through the same means as the resting trial, but all other measures (force data and motion capture) were measured during a third, muscle mechanics focused session.

3.2.2 Mechanics Trials

During the third session, participants were once again asked to don a pair of force sensing insoles (novel, Germany). And were prepared for collection by administering a full lower body Vicon plug-in gait marker set. Subjects were then asked to complete 6 x 2-minute hopping trials each on hard ground and soft ground for a total of 12 trials. Trials were once again performed at 2.5Hz with to specified height, at 2.2Hz, 2.5Hz, 2.8Hz and 3.2Hz to the subject's preferred height, and finally at the subject's preferred frequency and to a set height. Frequency and terrain conditions were randomized, and height and frequency control were performed using real-time biofeedback and a metronome respectively. During these trials, force and motion data were captured.

3.2.3 Outcome Measures and Data Analysis

For the 5-minute metabolic trials, we recorded the rates of oxygen uptake and carbon dioxide production (V02 and VC02) over the last minute of each trial, from which we were able to calculate the normalized metabolic power (W/kg). To obtain the metabolic cost of each trial, we subtracted the normalized resting condition (W/kg). We removed two of one hundred and eight metabolic data points from our analyses because the corresponding respiratory exchange ratio reflected a respiratory quotient value that fell outside of the range that indicated nominal and/or carbohydrate oxidation (0.7-1.0)

Using a custom MATLAB script (MathWorks Inc., Natick, MA, USA we synced force data from the force plates and insoles. Further details on this process can be found in Appendix C. Ankle, Knee and Hip torques and powers were then computed using a Vicon plug-in gait pipeline. We averaged ankle torque from 5 consecutive hopping cycles and assumed that the[26] Achilles tendon moment arm lengths and ground reaction center of pressures were constant over the course of the trials.

Values and results presented in this paper are the means ± SE for all subjects that completed the study. An ANOVA with repeated measures was used to test for statistical differences between the two conditions, with key independent variable for the ANOVA being the terrain condition (2 levels: Hard and Sand). F-ratios were considered significant for $P < 0.05$. If a statistically significant difference was found, paired t-tests were used to make pairwise comparisons between levels of independent variables.

3.3 Results

3.3.1 Whole Body Energetics

Of the ten subjects enrolled, 8 subjects completed the protocol by maintaining an RER value <1 Values for metabolic rate ($\overline{P}_{met}$) of the subjects increased on sand for the height matched hopping by 23% ($p<0.001$) (Figure 14). Across frequencies, it was found that values of $\overline{P}_{met}$ on sand for the preferred height and matched frequency conditions consistently offset the hard ground $\overline{P}_{met}$ values by 19.2%, with the same U-shaped profile found in our hard ground experiment and in the literature [56]. Similarly, consistent with previous work, we found a local frequency minimum for the self-selected height trials in sand (2.8Hz) and a trend that mimics that on hard ground, with a metabolic offset of ~20%.

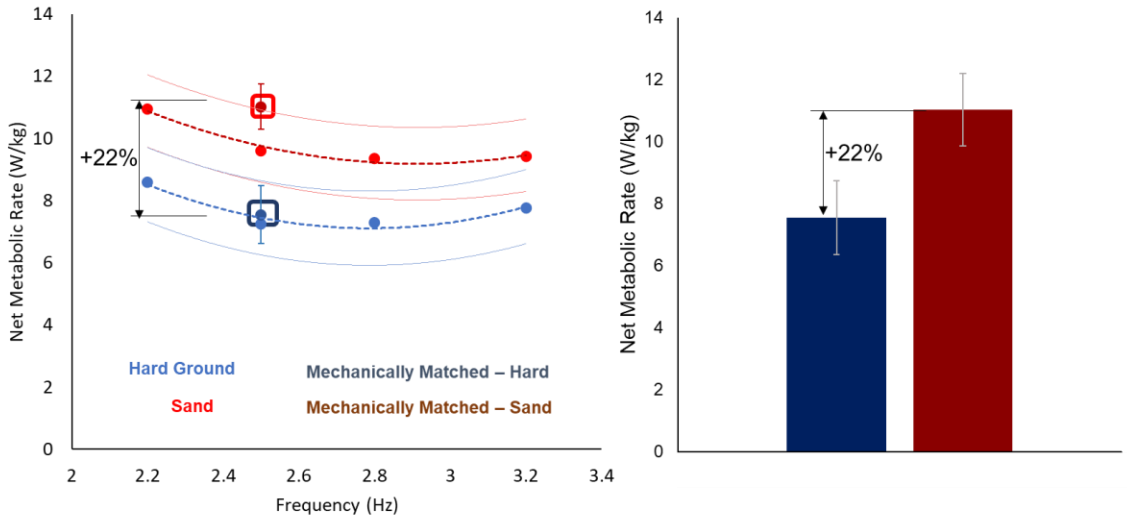

Figure 14 - Net metabolic rate over across frequencies. Subjects were asked to hop at their preferred height across frequencies, as well as asked to hop to a matched height at a frequency of 2.5Hz (circled). These matched conditions are of importance such that we can investigate muscle-level effects during mechanically comparable tasks.

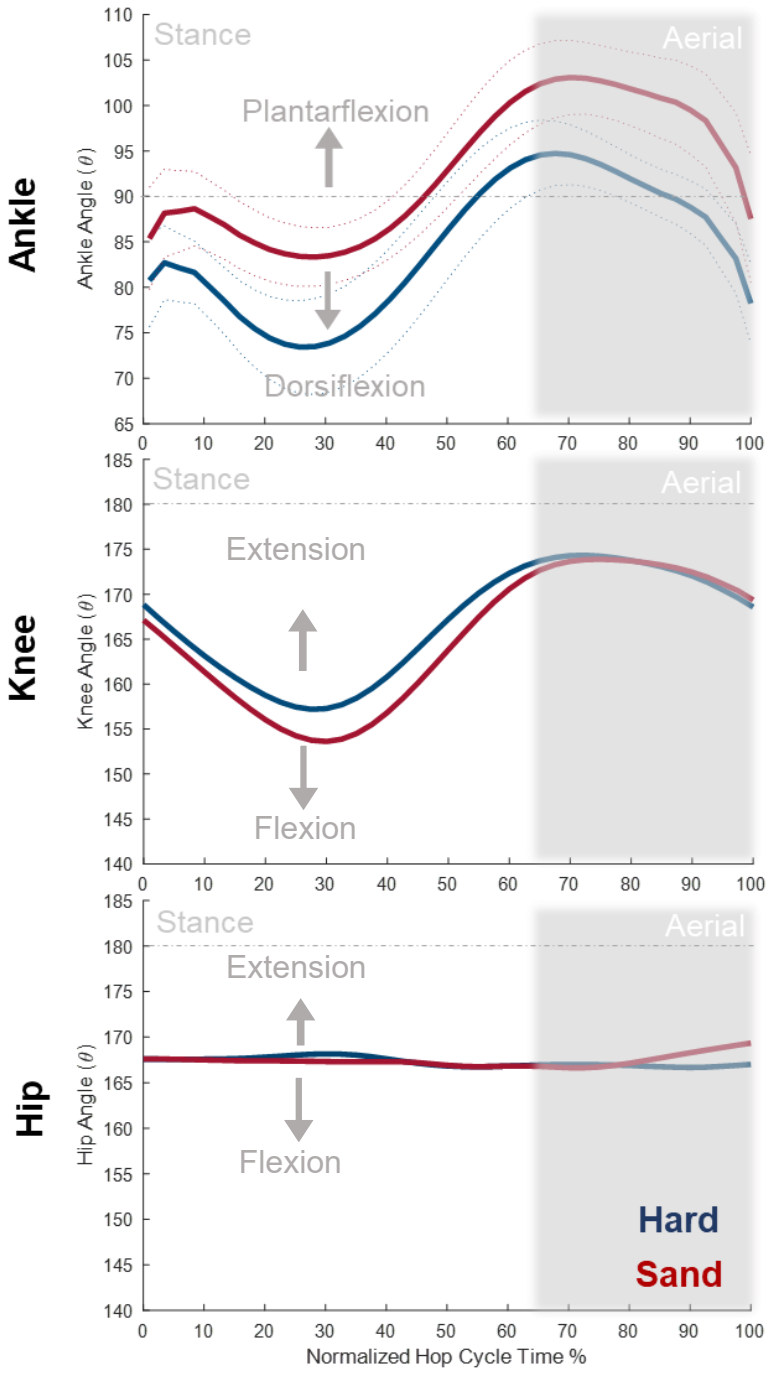

Figure 15 - Mechanics of leg joints highlighting (top) the ankle angle, which was found to be consistently more plantarflexed on sand (p=0.042), (middle) knee angle which showed more flexion during stance and (bottom) hip angle which showed negligible joint angle changes

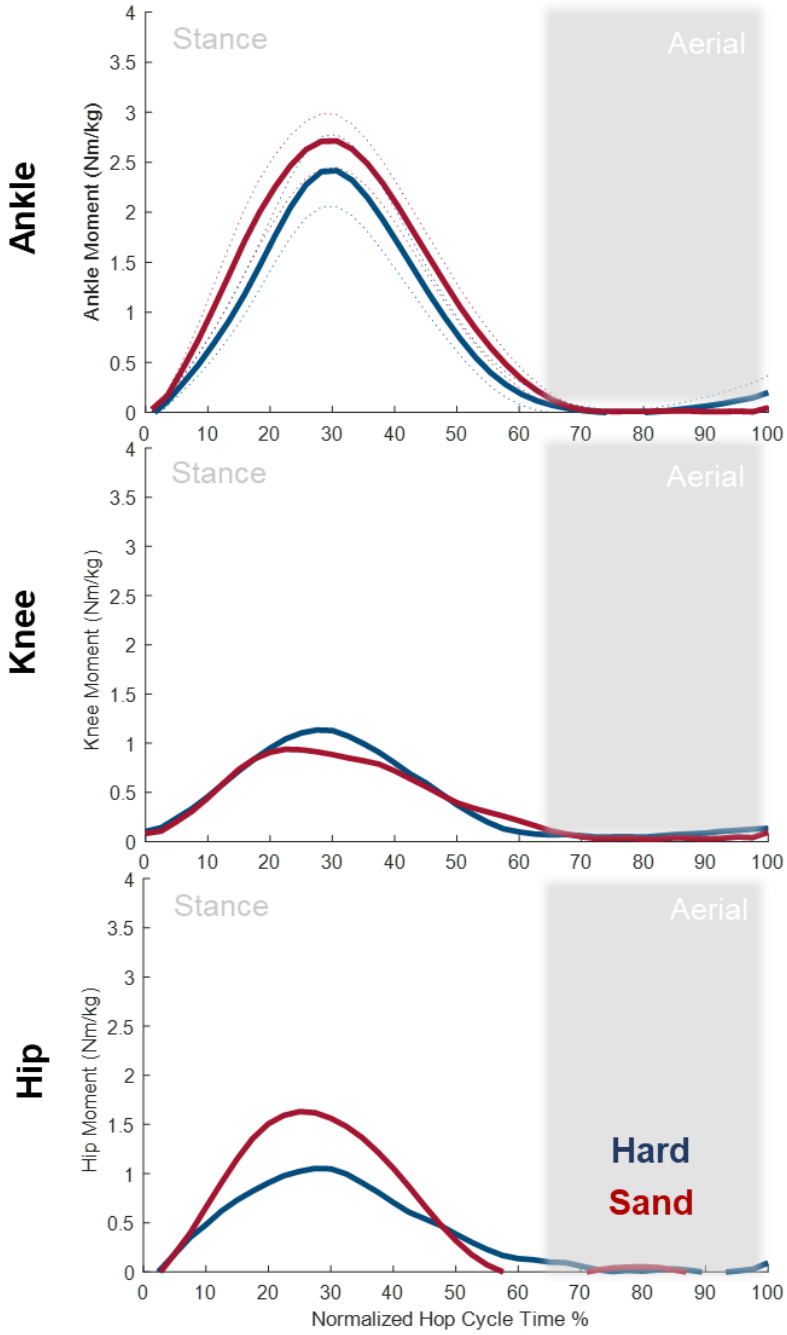

Figure 16 -Mechanics of leg joints highlighting (top) the ankle moment, which was found to have an increase $\bar{M}_{ankle}$ of 25% (p=0.12) over the cycle, (middle) knee moment which showed relatively little change, with a decrease in $\bar{M}_{knee}$ of 7% over the cycle and (bottom) hip moment which showed relatively little change, with an increase in $\bar{M}_{hip}$ of 6% over the cycle

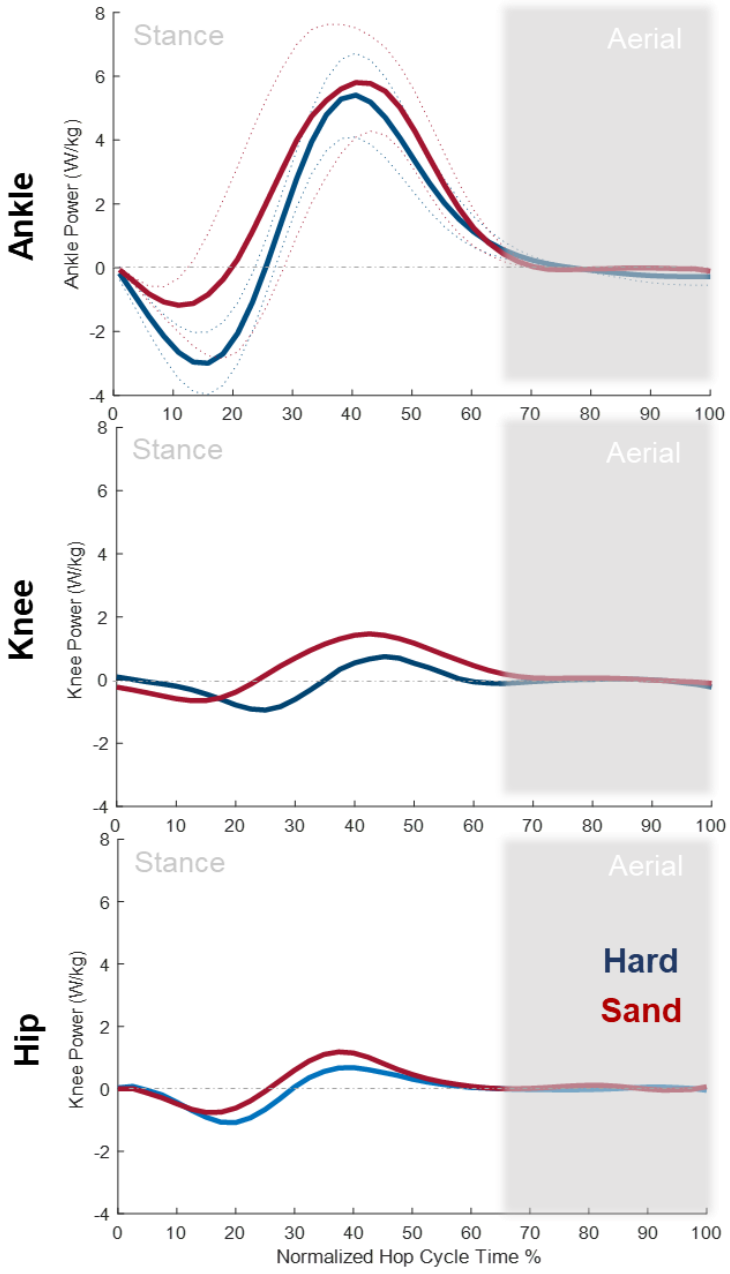

Figure 17 - Mechanics of leg joints highlighting (top) the ankle power, which was found to have an increase in $\overline{P}_{mech\ ankle}^{+}$ of 24% (p=0.04) over the cycle, (middle) knee powers which showed a net increase of $\overline{P}_{mech\ knee}$ = 154%, but at comparatively smaller magnitude and significance resulting smaller overall change (p=0.72), (bottom) hip powers, which showed similar behavior with an increase of net $\overline{P}_{mech\ hip}^{+} \approx$ 112%, but at significantly smaller magnitude and significance when compared to the ankle, resulting in a smaller overall effect (p=0.66)

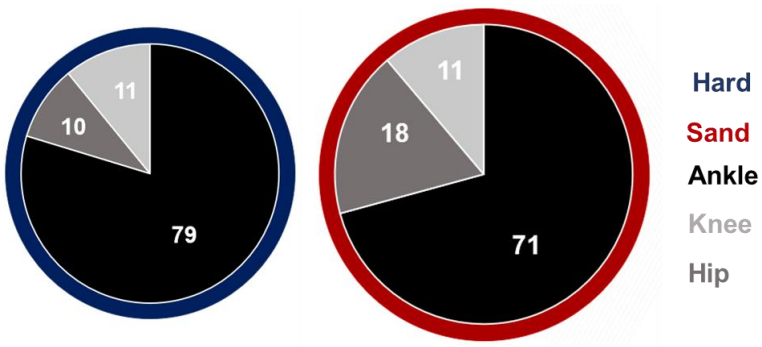

Figure 18 - Joint power sharing with the ankle decreasing from 88% to 78%, the knee increasing from 7% to 15%, and the hip remaining comparable with an increase of 5% to 7% respectively from hard ground to sand.

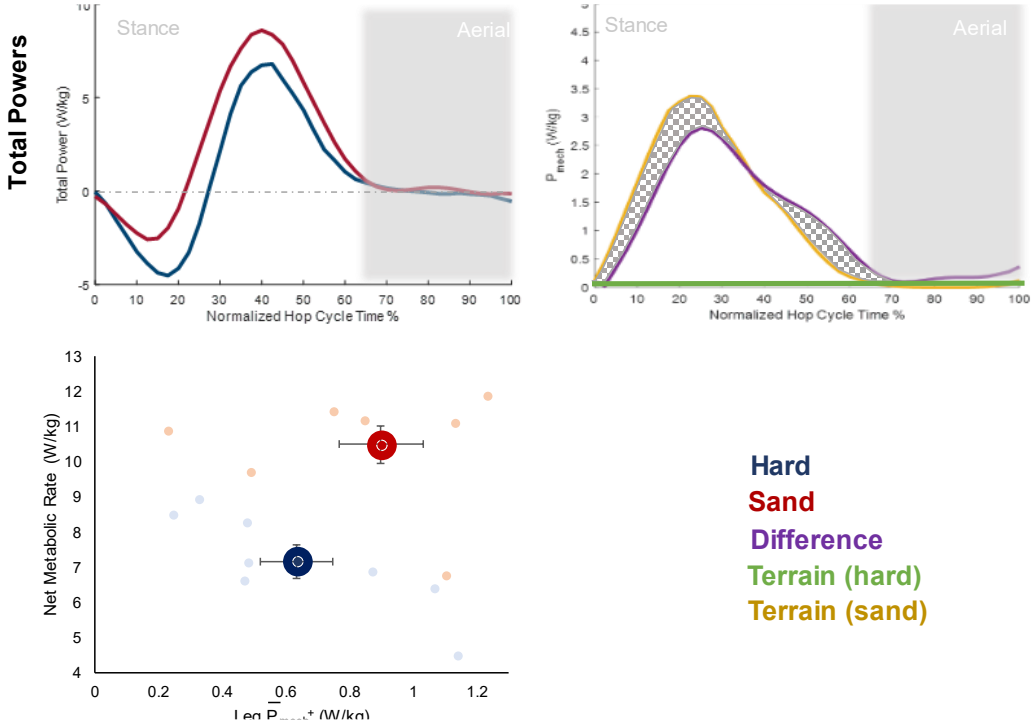

Figure 19 – (Top Left) Positive leg work over the cycle for hard ground was found to be $\bar{P}_{mech\ leg\ hard}^{+}$ = 0.6399 W/kg increasing to $\bar{P}_{mech\ leg\ sand}^{+}$ = 0.8932 W/kg, (Top Right) The power lost to the sandy terrain was given as $\bar{P}_{mech\ sand}^{+}$ = 0.432 W/kg. with increased mechanical work input of $\Delta\bar{P}_{mech\ leg}^{+}$ = 0.2533 W/kg, an increase of 40% from hard ground to sand This also shows a discrepancy of $\bar{P}_{mech\ sand} - \Delta\bar{P}_{mech\ leg} \approx 0.05$ W/kg. Efficiency was found to be $\mu \approx 0.08$ when considering the power output of the combined ankle, knee and hip.

3.3.2 Joint Angles

After whole body energetics were examined, joint level mechanics were investigated. We found that Ankle angles showed more plantarflexion on sand, with an average offset of approximately 5° over the gait cycle (Figure 15). At the knee, we found an offset of ~4° at max flexion, and comparable joint angles at maximum extension. At the hip, we found a consistent hip flexion angle of 167° across both hard and soft ground, with little variation over the gait cycle.

3.3.3 Joint Moments

For Moments at the individual joints, We found that Ankle moment increased on sand by 25%, with an increase in joint moment over each cycle from $\bar{M}_{ank\ hard}$ = 0.3 Nm/kg to $\bar{M}_{ank\ sand}{}^{+}$= 0.38 Nm/kg (Figure 16) (p= 0.12). At the knee, and hip, we found smaller contributions with less statistical significance, with the knee showing an decrease from $\bar{M}_{knee\ hard}{}^{+}$ = 0.16 Nm/kg to $\bar{M}_{knee\ sand}{}^{+}$ = 0.15 Nm/kg (p = 0.72) and the hip showing an increase from $\bar{M}_{hip\ hard}{}^{+}$ = 0.15 Nm/kg to $\bar{M}_{hip\ sand}{}^{+}$ = 0.16 Nm/kg (p=0.66) indicating relatively little change in the moments at these joints.

3.3.4 Joint Powers and Power Sharing

We found that Ankle powers increased on sand, with an increase in power dissipation over each cycle from net $\bar{P}_{mech\ ank}{}^{+}$ = 0. 51 W/kg to $\bar{P}_{mech\ ank}{}^{+}$ = 0.63 W/kg, (Figure 17)

an increase of 24% (p=0.036). At the knee, we found a relatively smaller and less statistically significant relationship between hard ground and sand, with an increase of $\bar{P}_{mech\ knee}{}^{+}$ = 0. 064 W/kg to $\bar{P}_{mech\ knee}{}^{+}$ = 0.16 W/kg, (P>0.05). Similarly, at the hip, we found an increase, though non-statistically significant, from $\bar{P}_{mech\ hip}{}^{+}$ = 0.065 W/kg to $\bar{P}_{mech\ hip}{}^{+}$ = 0.01 W/kg (P>0.05). While the ankle showed the greatest increase in work, we found that the individual average joint contributions varied from hard ground to sand, (Figure 18) with contribution from hard ground to sand at the ankle decreasing from 88% to 78%, the knee increasing from 7% to 15%, and the hip remaining comparable with an increase of 5% to 7% respectively.

3.3.5 Efficiencies, Combined Leg Powers and Sand Power

Additionally, when considering the efficiency, η^{+}, which is given as the ratio of $\Delta\bar{P}_{mech}{}^{+}$ to $\Delta\bar{P}_{met}{}^{+}$ (Figure 19) we found that $\mu \approx 0.04$ when considering the ankle joint in isolation, and $\mu \approx 0.08$ when considering the power output of the combined ankle, knee and hip. Thus, increased metabolic cost exceeds the expected penalty based on efficiency of positive mechanical work of 0.25. (i.e., more than a x4 penalty) [36]. We found the total leg power developed over hard ground to be $\bar{P}_{mech\ leg\ hard}{}^{+}$ = 0.6399, increasing to W/kg $\bar{P}_{mech\ leg\ sand}{}^{+}$ = 0.8932 W/kg over sand and leading to an increased mechanical work input of $\Delta\bar{P}_{leg}{}^{+}$ = 0.253 W/kg and $\Delta\bar{P}_{leg}$ = 0.04 W/kg from hard ground to sand. Comparatively, the power lost to the sandy terrain was given as $\bar{P}_{sand}{}^{+}$ = 0.432 W/kg over the cycle, with sand power being calculated as:

$$P_{sand} = \frac{F_{grf} V_{sand}}{m}$$

With V_{sand} calculated directy from the realtive velocity of a plantar surface level marker relative to a fixed point on the terrain setup, and *m* being the subject mass used in the energetic and joint level moment and power normalizations above. Additional information can be found in Appendices B and C, and a summary of powers can be found in Table 1 below:

Table 1 – Summary of averaged joint and ground powers over a hop cycle for hard ground and sand conditions.

	Hard Ground			**Sand**			**Δ Net**	**Δ +ve**
	$\bar{P}_{mech}^{+}$	$\bar{P}_{mech}^{-}$	**net** $\bar{P}_{mech}$	$\bar{P}_{mech}^{+}$	$\bar{P}_{mech}^{-}$	**net** $\bar{P}_{mech}$	**net** $\Delta \bar{P}_{mech}$	$\Delta \bar{P}_{mech}^{+}$
Ankle $\left(\frac{W}{kg}\right)$	**+0.51**	**-0.264**	**+0.247**	**+0.63**	**-0.07**	**+0.57**	**+0.32**	**+0.12**
Knee $\left(\frac{W}{kg}\right)$	**+0.06**	**-0.012**	**+0.053**	**+0.16**	**-0.055**	**+0.10**	**+0.05**	**+0.1**
Hip $\left(\frac{W}{kg}\right)$	**+0.07**	**-0.049**	**+0.019**	**+0.10**	**-0.051**	**+0.05**	**+0.01**	**+0.03**
Total $\left(\frac{W}{kg}\right)$	**+0.64**	**-0.325**	**+0.32**	**+0.89**	**-0.176**	**+0.72**	**+0.40**	**+0.25**
Sand $\left(\frac{W}{kg}\right)$	**-**	**-**	**-**	**+0.43**	**-**	**+0.43**	**+0.43**	**+0.43**

Discussion

The purpose of this study was to comparatively investigate the joint level mechanics as they relate to the whole-body energetics of human hopping to a fixed height from rest, with conditions of hard ground and sandy terrain. This was done with the primary goal of produce a greater understanding of the locomotion biomechanics of human hopping over metabolically taxing terrain such as sand, snow or mud, and, in turn characterize them at the whole body, joint and muscle level. This was performed as part of a series of studies that takes an approach of a comprehensive modelling, simulation, and real-world series of experiments, with the intention better understanding human locomotion at the muscle-level on dissipative terrain

3.3.6 Whole body Energetics

Based on the literature and our previous work, we hypothesized a significant increase in metabolic cost when running and walking over dissipative terrain for a series of similar tasks. To that end, we hypothesized that a mechanically matched task (hopping to a fixed height at a fixed frequency) would elicit a similar increase. This hypothesis was confirmed by a resulting increase in $\overline{P}_{met}$ of approximately 22% when comparing the mechanically matched hard ground and sand conditions. This agrees well with previous initial findings from work done in modelling and simulation studies (23%) [5, 58], however, this underestimates findings of Lejeune et al, who reported approximate energy expenditure increases of 60% for running (bouncing gait) on a sand track [2]. Unlike that study, however, participants were asked to keep their arms at their sides to avoid added

mechanical or metabolic effects and can help explain a portion of this discrepancy. Additionally, participants were held to a fixed height and hop frequency, while in Lejeune's study, participants were kept to a fixed speed; this may introduce differences in gait effects. Additionally, when considering that the U-shaped profile presented itself on hard ground and soft ground in a similar manner, albeit offset by +19%, we hypothesize that the accept hard ground ideal hopping frequency (2.5-2.8 Hz) may be terrain agnostic, and determined solely by the MTU properties.

3.3.7 Joint Angles

In line with our hypothesis, we found that Ankle angles showed more plantarflexion on sand, with an average offset of approximately 5° over the gait cycle At the hip and knees however, we found comparatively little variation over the gait cycle. As such, this frames our thinking, in terms of the isolated ankle movers being the key muscle group to investigate further. By having a more plantarflexed posture at the ankle, but with limited effect at the knee, we expect a shorter average operating length of the contractile elements in the Triceps-surae-Achilles muscle-tendon unit, with a focus on the soleus plantarflexors.

3.3.8 Joint Moment Effects

For Moments at the individual joints, We found that Ankle moment increased on sand by 25%, with an increase in joint moment over each cycle from $\bar{M}_{ank\ hard}{}^{+}$ = 0.3 Nm/kg to $\bar{M}_{ank\ sand}{}^{+}$ = 0.38 Nm/kg (p= 0.12) for comparable ground reaction forces. In

conjunction with the joint angles above indication comparable lever arms, this therefore means that at the ankle, more muscle force is required to elicit comparable ground reaction forces. Conversely, at the knee, and hip, we found smaller contributions with less statistical significance, with the knee showing an decrease from $\bar{M}_{knee\ hard}^{+}$ = 0.16 Nm/kg to $\bar{M}_{knee\ sand}^{+}$ = 0.15 Nm/kg (p = 0.72) and the hip showing an increase from $\bar{M}_{hip\ hard}^{+}$ = 0.15 Nm/kg to $\bar{M}_{hip\ sand}^{+}$ = 0.16 Nm/kg (p=0.66) indicating relatively little change in the moments at these joints, and further supporting the theory that the ankle is the primary contributor to changes in joint and muscle level behaviors on dissipative substrates.

3.3.9 Joint and Sand Powers

Furthermore, we hypothesized increases in powers across all three joints, with the ankle being the largest contributor. As seen above, we found that Ankle powers increased on sand, with an increase in power dissipation over each cycle from $\bar{P}_{mech\ ank\ hard}^{+}$ = 0.51 W/kg to $\bar{P}_{mech\ ank\ sand}^{+}$ = 0.63 W/kg (Fig. 17), an increase of 24% (p=0.036) with the knee and hip having relatively minor contributions. (an increase of $\bar{P}_{mech\ knee\ hard}^{+}$ = 0.064 W/kg to $\bar{P}_{mech\ knee\ sand}^{+}$ = 0.16 W/kg, (P>0.05) at the knee and an increase of $\bar{P}_{mech\ hip\ hard}^{+}$ = 0.07 W/kg to $\bar{P}_{mech\ hip\ sand}^{+}$ = 0.1 W/kg (P>0.05) at the hip) This ankle dominant effect confirms our hypothesis, shows good agreement with Moritz et al [7, 8], and highlights that the ankle behaves increasingly as an actuator as the surface becomes more damped. We hypothesize that this is due to the ankle still being the most cost-effective mover at steady state hopping at 2.5Hz when compared to the muscles at

the knee and hip. When the entire leg is considered, some interesting trends emerge. As seen above, we found the total leg power developed over hard ground to be $\bar{P}_{mech\ leg\ hard}{}^{+}$ = 0.6399 increasing on sand to W/kg $\bar{P}_{mech\ leg\ sand}{}^{+}$ = 0.89 W/kg, leading to an increased mechanical work input of $\Delta\bar{P}_{mech\ leg}{}^{+}$ = 0.253 W/kg. Comparatively, the power lost to the sandy terrain was given as $\bar{P}_{mech\ sand}{}^{+}$ = 0.432 W/kg over the cycle. This leaves a discrepancy of $\bar{P}_{mech\ sand}{}^{+} - \Delta\bar{P}_{mech\ leg}{}^{+}$ = 0.18 W/kg, or over the entire cycle, a $\bar{P}_{mech\ sand}{}^{+} - \Delta\bar{P}_{mech\ leg}$ = 0.04 when considering both positive and negative work. We hypothesize that these discrepancies were due to work done at joints not covered by our marker set. For example, Birch et al showed that the midfoot, a section of the limb that was not considered in this study, contributed up to an average of 0.13 J/kg for damped surface hopping; factoring this would theoretically account for the majority of this discrepancy, reducing the difference to within a similar order of magnitude. Similarly, although participants were asked to limit arm and torso swing, this indeed could also account for a portion of this discrepancy of, in addition to added work that would not present at the leg limb level. As such, an additional comparative investigation at the full body level set is needed to further determine the magnitude contribution of the upper body.

3.3.10 Efficiencies and Muscle Level Implications

Finally, we hypothesized the metabolic rate would exceed the expected mechanical work, based on an efficiency value of 0.25. In line with this hypothesis. We found that the efficiency, $\eta \approx 0.04$ when considering the ankle joint in isolation, and $\eta \approx 0.08$ when considering the power output of the combined ankle, knee and hip. As hypothesized above

as we examined joint angles, moments, and powers, this highlights the inefficiencies of the ankle movers in particular, and prompt further investigation into the muscle level effects in terms of soleus Activation, Force-Length and Force Velocity. This will be discussed at length in the following chapter.

3.3.11 Limitations and Assumptions

While this study presents the first direct measurement of inverse dynamics on sand, it poses certain limitations that in turn can inform our future work. To date, it has been difficult to obtain reliable ground reaction force vectors on dissipative terrain that can in turn be used to feed into an inverse dynamic pipeline., Lejeune et. al suggests that buried force plates may provide sufficient data for ground reaction force but acknowledges that this is a key assumption that may not hold true [2]. Due to the fact that our subjects locomotion in the z-direction, and gait cycles are averaged, this allows us to simplify our measurements to that of the z-direction forces at the foot-ground boundary- this is an assumption that may not hold for other forms of bouncing gait, such as walking and running. To measure these forces, we partnered with novel Inc (Munich, Germany) and have benchmark their force sensing insole system against our calibrated force plates to collect these plantar boundary forces. These benchmarking studies provide close agreement for inverse dynamic calculations at the hip, knee and ankle for 1 degree of freedom locomotion, and can be found in Appendix C. Another limitation of this study was the use of a lower body marker set that prioritized the ankle, knee and hip. Through the use of an expanded marker set, we believe that much of the discrepancy in the powers over the cycle

lost to the terrain can be explained, by leveraging the inclusion of mechanical powers at the midfoot, torso and arms.

3.4 Conclusions and Future Directions

Human locomotion has been examined at length in the context of hard ground, and indeed, many aspects of dissipative terrain locomotion have been explored in terms of whole-body energetics and joint level neuromuscular changes. We have presented a novel joint level energetic analysis that links the whole-body metabolic energy cost of hopping in sand, to the work done by the primary movers of the leg, and the work done on the surface itself. Continuation of this series of studies will now seek to dive deeper into the muscle level effects around the ankle, in order to develop a more complete understanding of human neuromechanical adaptations to changing substrates that pushes us outside of the realm of traditional laboratory techniques. As we continue this study series, we will then look to wearable devices that can combat these changes, in order to allow humans to effortlessly traverse unstructured terrain without the risk of fatigue.

3.5 Associated Publication

This work will be submitted to the Journal of Experimental Biology following final editing and revision

CHAPTER 4. WHY IS THE METABOLIC COST OF LOCOMOTION HIGHER ON SAND? INSIGHTS AT THE MUSCLE LEVEL.

Locomotion on sand elicits a higher metabolic cost than on hard ground. Previous work attributes this to two main factors: sinkage into the sand itself, and the structural properties of the human leg. Losses due to sinkage into the sand are conventionally estimated as a function of kinematic properties such as depth, contact area, intrusion force, and ground material properties such as density or grain size. However, at the human muscle level, increased metabolic cost exceeds the expected penalty of this extra work required based on efficiency of positive mechanical work of 0.25. Our previous work in-silico and at the joint level suggests that this discrepancy is due to increased MTU length changes and higher CE shortening velocities during locomotion over dissipative substrates, thereby requiring higher muscle activation to meet the force demands of the task. In agreement with this, for a mechanically matched hopping task *in-vivo*, we found that locomotion in sand elicited a higher whole body metabolic cost, stemming from shorter fascicle operating lengths ($p \leq 0.001$), higher operating velocities ($p \leq 0.001$), and higher soleus active muscle volumes and activations ($p \leq 0.001$). This study presents the first muscle-level analysis of human locomotion on dissipative terrain and sets the stage for a new paradigm of terrain-capable wearable device design based on the human physiology-environment relationship.

4.1 Introduction

Human movement is widely adaptable over a variety of terrains [1-4, 26-31, 40, 49]. This adaptability, however, has been found to have tradeoffs, particularly, when locomotion on deformable terrain is compared to that of hard ground [2, 3, 26-31, 40]. Unlike other legged movers, humans are able to maintain stability when walking through terrain such as sand, snow and mud, at the cost of increased metabolic cost [2, 5, 40]. Indeed, while locomotion on deformable media has been studied and quantified for decades, and this increase in metabolic cost is well documented [1-4, 7, 8, 26-31, 38, 40, 49] , little has been done to understand the underlying causes associated with this increased cost of transport.

Lejeune, Willems and Heglund assessed the locomotion mechanics and overall metabolic effects of movement on sand and found mechanical work and energy expenditure requirements of up to 1.15 and 1.6 times higher respectively for walking and bounding gaits on sand when compared to hard ground trials. They highlight that energy expenditure is not linearly scalable to actual mechanical work, especially over dissipative terrain and suggested that the discrepancy between this was due to inefficiencies in the muscles and joints, however, these inefficiencies have yet to be explored [2]

More recently, Moritz and Farley began to explore the joint level effects of locomotion on damped terrain. Through the use of a custom built platform, they explored the effect at the joint level of bouncing gait locomotion through hopping on a damped surface [7, 8]. Through this analysis, they concluded that as the surface became more damped, the leg increasingly became more like an actuator, and less of a spring, as modeled by the

conventional spring-loaded pendulum model of bipedal bouncing gait. Additionally, they found that the ankle was the primary joint that accounted for the additional work needed to overcome dissipation. Birch et al [6] had similar findings, where they concluded that the extra injection of work was most important at the foot surface in order to overcome the effects of damping on a similar apparatus. Kowalsky et al [40] further suggested that some of the additional cost of transport of locomoting in these dissipative terrains stemmed from differences in gait parameters, such as stride length and clearance. Taking these findings into consideration, we chose to focus on a mechanically matched task with the ankle joint as the primary focus for this study. Additionally, when considering that human locomotion is typically in the form of a 'bouncing gait', the rationale for choosing hopping as a locomotor task to analyze damped surface locomotion in this study can be seen [32, 37].

Outside of damped media studies, there have been many studies that explain increased metabolic cost over hard ground as factors stemming from neuromuscular effects. For example, Minetti and Alexander [19] relate added metabolic cost during walking to a combination of muscle activation, as well as some function of muscle force-velocity, and, more recently, Beck et al [55] showed the correlation of active muscle volume variation (which is a function of CE force-length and force-velocity operating points) for the Soleus as a function of activations and metabolic cost. These studies provide unique insight into the neuromuscular causes of changes in cost of transport for isolated muscle groups and hard ground locomotion, and add to the story framed by the studies in the above paragraphs [19, 33, 55] provide insight into the whole-body energetics of damped terrain locomotion. However, the opportunity to investigate the intersection of these two has yet to be explored and is a key objective of our study.

To date, there has been no human study that allows for direct inverse kinematics from dissipative, granular terrain locomotion. Lejeune et. al used buried force plates and relied on the whole-body mechanical vs metabolic cost comparison, and Moritz and Farley were able to approximate damping effects on their damped platform, however neither of these measured at the foot-terrain boundary [2, 7, 8, 50]. While these types of inverse dynamics analyses are well documented for hard ground studies [32, 35-37], there has not been a reliable way to obtain the center of pressure and ground reaction force vector. Using an insole and floating motion capture cameras on the subject to provide center of pressure, and insole ground reaction force readings, we can reliably interpolate the full ground reaction force vector on dissipative substrates. This unique sensor fusion approach lays the foundation for sensing on non-uniform terrain and allows us to now test the implementation of our devices without being confined to the laboratory setting.

While there have been many studies linking metabolic cost and center of mass, limb-joint and muscle-level Neuromechanics on hard ground [2, 6, 7, 32, 40], as well as whole body energetic and joint level analyses of walking in dissipative terrain, little has been done at the neuromuscular level to understand why it is more metabolically expensive, particularly when compared to the increased mechanical work required for locomotion in dissipative environments. Our study begins to bridge this gap, using a customized in-lab apparatus to perform the first comprehensive analysis of the human neuromuscular response to the complex non-linear behavior of propulsion on sand. The goal of this study was to understand why, at the muscle level, it is more metabolically costly to move on sand, when compared to a comparable locomotor task on hard ground. To this end, based on previous findings from modelling and human walking studies, we hypothesized that

participants would (1) show an increase in metabolic cost when performing a mechanically matched task on sand versus hard ground, (2) produce increased muscle activation and less optimal contractile element length and velocity characteristics (higher fascicle velocities and shorter fascicle lengths) versus hard ground when hopping on a dissipative surface, and (3) show increasing active muscle volumes with the expected increase in muscle activations and metabolic costs. These results serve to further the scope of knowledge of bipedal locomotion and will in turn help inform design of wearable devices that can mitigate energetic penalties associated with 'real-world' locomotion over dissipative terrain for applications in healthcare, agriculture, and beyond.

4.2 Methods

To test our hypothesis, we performed hopping trials over a series of frequencies and heights, with a focus on mechanically matched conditions across subjects. eight of the ten volunteers who enrolled in our study completed the protocol in its entirety (average ± standard deviation; age: 23.63 ± 2.67 years; height: 1.78 ± 0.05 m; mass: 81.5 ± 10.1 kg; resting metabolic rate 1.48 ± 0.14 W/kg). The two volunteers were excluded from the analysis were removed due to the inability to maintain a Respiratory Exchange Ratio (RER) < 1 for more than 50% of the trials. All participants reported themselves to be free of cardiovascular and metabolic disorders. Prior to starting study, informed consent was obtained in accordance with the Georgia Tech Institutional Review Board.

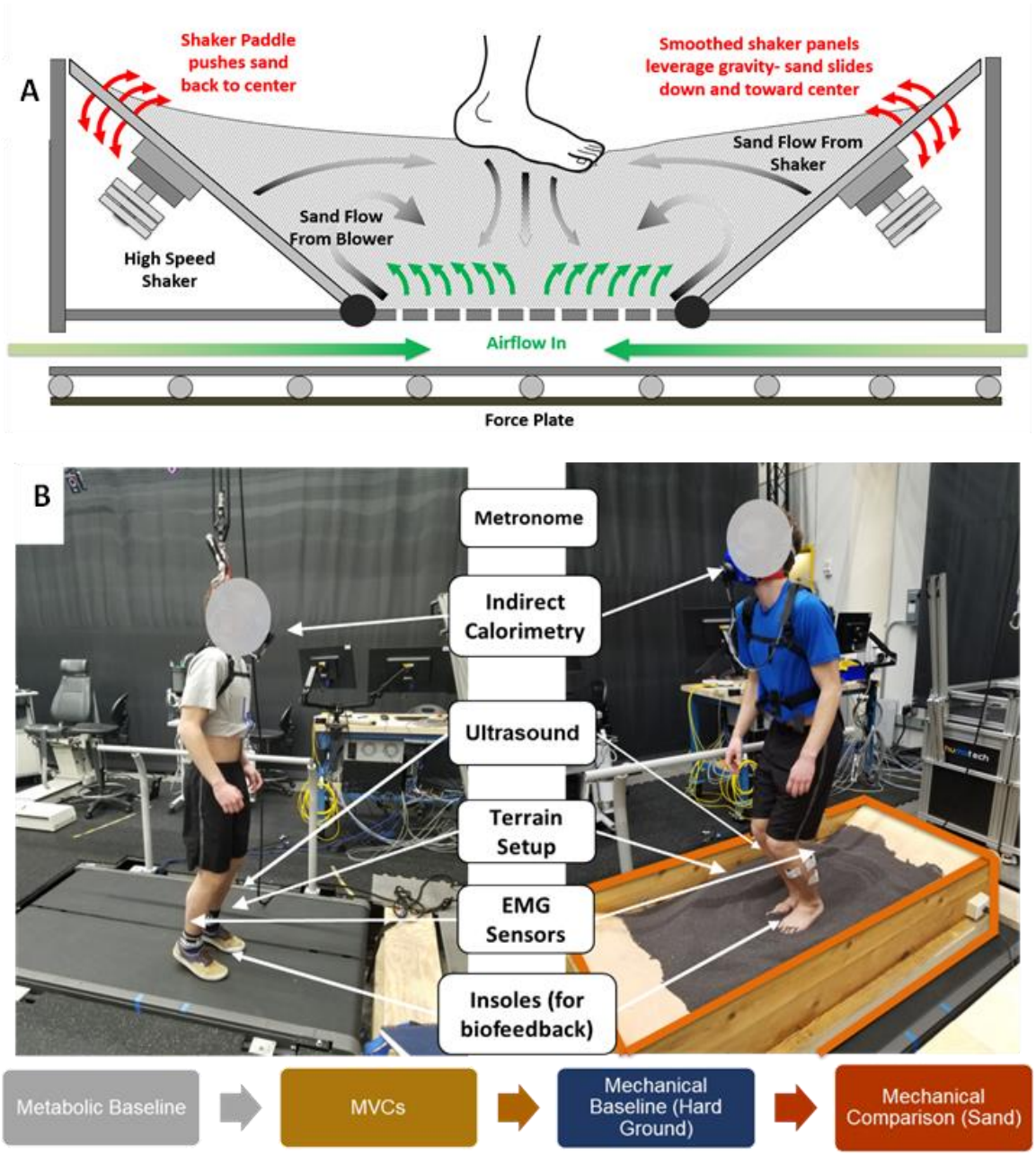

Figure 20 - The experimental setup for the hard ground and sand hopping trials. A custom sandpit setup was built (A) that allowed for sand leveling and prevented "bottoming out" during data collection (B)

4.2.1 Metabolic Trials

For metabolic measurement sessions, participants were asked to fast overnight, and upon arriving in the morning, they were asked to stand still and upright with their hands at their sides. In this standing position, participants performed a 10-minute resting trial while breathing in-and-out of a mask that connected to an indirect calorimetry system (COSMED K5, COSMED Srl, Italy).

For sessions 1 and 2, participants were asked to don a pair of force sensing insoles (novel, Germany), and reflective makers were placed at the left and right posterior superior iliac spine to provide height biofeedback to serve as a secondary biofeedback measure and validation through motion capture (Vicon, Oxford, UK). Subjects were then asked to 6 x 5-minute hopping trials each on hard ground and soft ground for a total of 12 trials over two sessions. Trials were performed at 2.5Hz with to specified height, at 2.2Hz, 2.5Hz, 2.8Hz and 3.2Hz to the subject's preferred height, and finally at the subject's preferred frequency and to a set height. Frequency and terrain conditions were randomized, and height and frequency control were performed using real-time biofeedback and a metronome respectively. Hard ground hopping and Sand hopping were performed on different days in random order to mitigate the effects of subject fatigue, with a corresponding resting trial for each day. During each hopping trial, metabolic expenditure was measured through the same means as the resting trial, but all other measures (motion capture, ultrasound and EMG) were measured during a third, muscle mechanics focused session.

4.2.2 Muscle Mechanics Trials

During the third session, participants were once again asked to don a pair of force sensing insoles (novel, Germany). And then the skin superficial to the muscle bellies of the tibialis anterior, lateral gastrocnemius and the soleus were shaved and then lightly appraised using electrode preparation gel (NuPrep, Weaver and Co., Aurora, CO). A bipolar electrode was then placed on the prepared skin in the same orientation as the underlying muscle fascicles, and then the real-time electromyography signal (EMG) of each electrode signal was visually verified. A B-mode ultrasound probe (Telemed, USA) was then placed on the skin superficial to each participant's right soleus, and reflective makers were placed at the left and right posterior superior iliac spine.

After this, participants were then asked to perform activation baseline trials in the form of maximum voluntary contractions. These were performed in random order of muscle group, with 3 MVC trials taken for each of the recorded muscle groups (lateral gastrocnemius, tibialis anterior, soleus). During the resting and activation trials, we tracked soleus fascicle length (100 Hz) during stance, and recorded soleus, tibialis anterior, and lateral gastrocnemius muscle activity (1000 Hz), as well as a full lower body Vicon plug-in gait marker set.

Subjects were then asked to complete 6 x 2-minute hopping trials each on hard ground and soft ground for a total of 12 trials. Trials were once again performed at 2.5Hz with to specified height, at 2.2Hz, 2.5Hz, 2.8Hz and 3.2Hz to the subject's preferred height, and finally at the subject's preferred frequency and to a set height. Frequency and terrain conditions were randomized, and height and frequency control were performed using real-

time biofeedback and a metronome respectively. During these trials, raw activations (EMG) and muscle fascicle ultrasound data was captured.

4.2.3 Outcome Measures and Data Analysis

For the 5-minute metabolic trials, we recorded the rates of oxygen uptake and carbon dioxide production ($V0_2$ and $VC0_2$) over the last minute of each trial, from which we were able to calculate the normalized metabolic power (W/kg). To obtain the metabolic cost of each trial, we subtracted the normalized resting condition (W/kg). We removed two of one hundred and eight metabolic data points from our analyses because the corresponding respiratory exchange ratio reflected a respiratory quotient value that fell outside of the range that indicated nominal and/or carbohydrate oxidation (0.7-1.0)

Using B mode ultrasound, we recoded images of the medial soleus during the last 30 seconds of the session 3 trials. We used semi-automated tracking software to post process the images in order to determine fascicle length and pennation angles over 5 hop cycles. Each frame was visually inspected to ensure accuracy of the software, and manual adjustments were made for those frames that did not accurately reflect the length and position of the respective fascicle. We then filtered soleus fascicle angle and lengths using a fourth-order low-pass Butterworth filter (6 Hz) and took the derivative of fascicle length with respect to time to determine fascicle velocity (MathWorks Inc., Natick, MA, USA).

Using a custom MATLAB script (MathWorks Inc., Natick, MA, USA to sync force data from the force plates and insoles data with fascicle and activations. Ankle torques and

powers were then computed using a Vicon plug-in gait pipeline. We averaged ankle torque from 5 consecutive hopping cycles that aligned with those used in the ultrasound muscle fascicle data. Additionally, we estimated the soleus muscle-tendon moment arm lengths and assumed that the[59] Achilles tendon moment arm lengths and ground reaction center of pressures were constant over the course of the trials. We then divided ankle-joint moment (M_{ank}) by the Achilles tendon moment arm (r_{AT}) then again divided that by the cosine of the soleus fascicle pennation angle (θ_p) to determine soleus force (F_{sol}). [55]

$$F_{sol} = \left(F_{grf} \times EMA\right) \Big/ cos\theta_p = \frac{\frac{M_{ank}}{r_{AT}}}{cos\theta_p}$$

We assumed that maximal soleus velocity was $4.4 l_o$/s.

Each of the soleus, tibialis anterior and gastrocnemius EMG signals was band pass filtered between 20 and 450 Hz from 5 hop cycles We then full-wave rectified the filtered EMG signals and low-ass filtered the signal with at 6Hz.

Values and results presented in this chapter are the means ± SE for all subjects that completed the study. An ANOVA with repeated measures was used to test for statistical differences between the two conditions, with key independent variable for the ANOVA being the terrain condition (2 levels: Hard and Sand). F-ratios were considered significant for $P < 0.05$. If a statistically significant difference was found, paired t-tests were used to make pairwise comparisons between levels of independent variables.

4.3 Results

4.3.1 Whole Body Energetics and Ankle Mechanics

Of the ten subjects enrolled, 8 subjects completed the protocol. To reiterate initial findings in Chapter 3, our values for metabolic rate (P_{met}) of the subjects increased on sand for the mechanically matched condition by 23% ($p<0.001$) (Figure 21). As seen in Chapter 3, Across frequencies, it was found that values of P_{met} on sand for the preferred height and matched frequency conditions consistently offset the hard ground P_{met} values by 19.2%, with the same U-shaped profile found in our experiment and in the literature [56]. Similarly, consistent with previous work, we found a local frequency minimum for the self-selected height trials in sand (2.8Hz) and a trend that mimics that on hard ground, with a constant metabolic offset of ~20%. We found that Ankle powers increased on sand, with an increase in power dissipation over each cycle from $\bar{P}_{mech}{}^{+}$ = 0.51 W/kg to$\bar{P}_{mech}{}^{+}$ = 0.63 W/kg (Figure 22) and an increase of 24% ($p=0.036$). Additionally, when considering the efficiency, η which is given as the ratio of $\Delta\bar{P}_{mech}{}^{+}$ to $\Delta\bar{P}_{met}$. We found that $\eta \approx 0.04$. Thus, increased metabolic cost exceeds the expected penalty based on efficiency of positive mechanical work of 0.25. (i.e., more than a x4 penalty) [36].

4.3.2 Muscle Dynamics

After whole body energetics and joint level mechanics were examined, muscle level effects were investigated. Activations for the loose sand conditions showed a 14% increase for the mechanically matched case when moving from hard ground to sand, ($p = 0.03$), with an

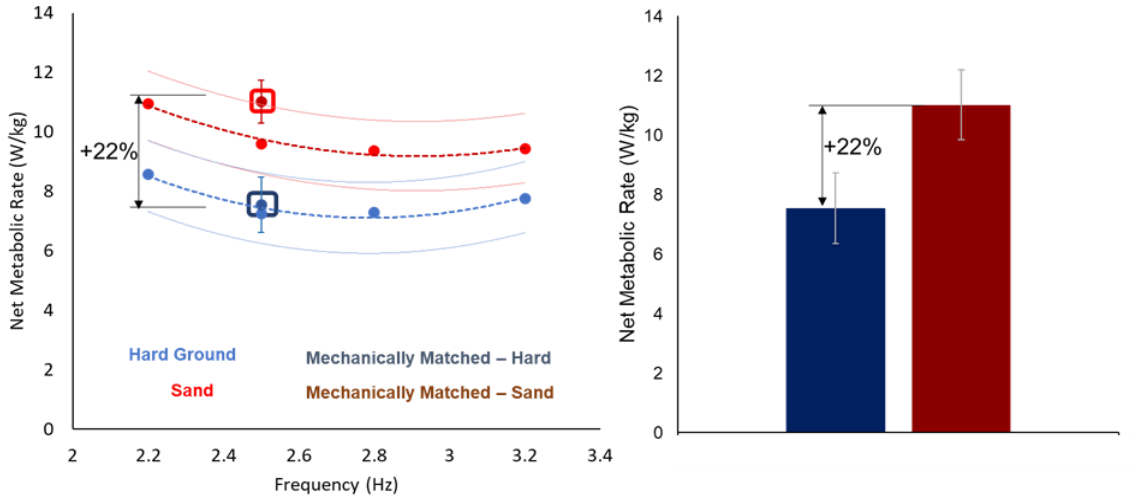

Figure 21 - Net metabolic rate over across frequencies. Subjects were asked to hop at their preferred height across frequencies, as well as asked to hop to a matched height at a frequency of 2.5Hz (circled). These matched conditions are of importance such that we can investigate muscle-level effects during mechanically comparable tasks.

overall trend across conditions displaying a similar U-shaped profile to the metabolic rate result (Figure 23). Peak F_{grf} also saw a 4% decrease on sand (p=0.49), indicating no statistically significant differences and comparable hop heights.

In addition to an increase in activations, there were decreases in fascicle length operating lengths of 13% when compared to mechanically comparable hopping in sand (p=0.014) (Figure 24), with the force-length (F-L) relationship shown as a function of l_{CE}/l_0. This shorter operating point shifts the theoretical force-length relationship to a lower expected force output at a given activation. Similarly, there was an increase in shortening velocities. we found a 25% decrease in fascicle shortening velocity when compared to mechanically comparable hopping in sand (p=0.034). Similar to the force- length relationship, this shifts the theoretical force-velocity relationship (represented by v_{CE}/v_{max}) to a region that allows for less force production at a given activation, eliciting higher soleus activation for a similar task.

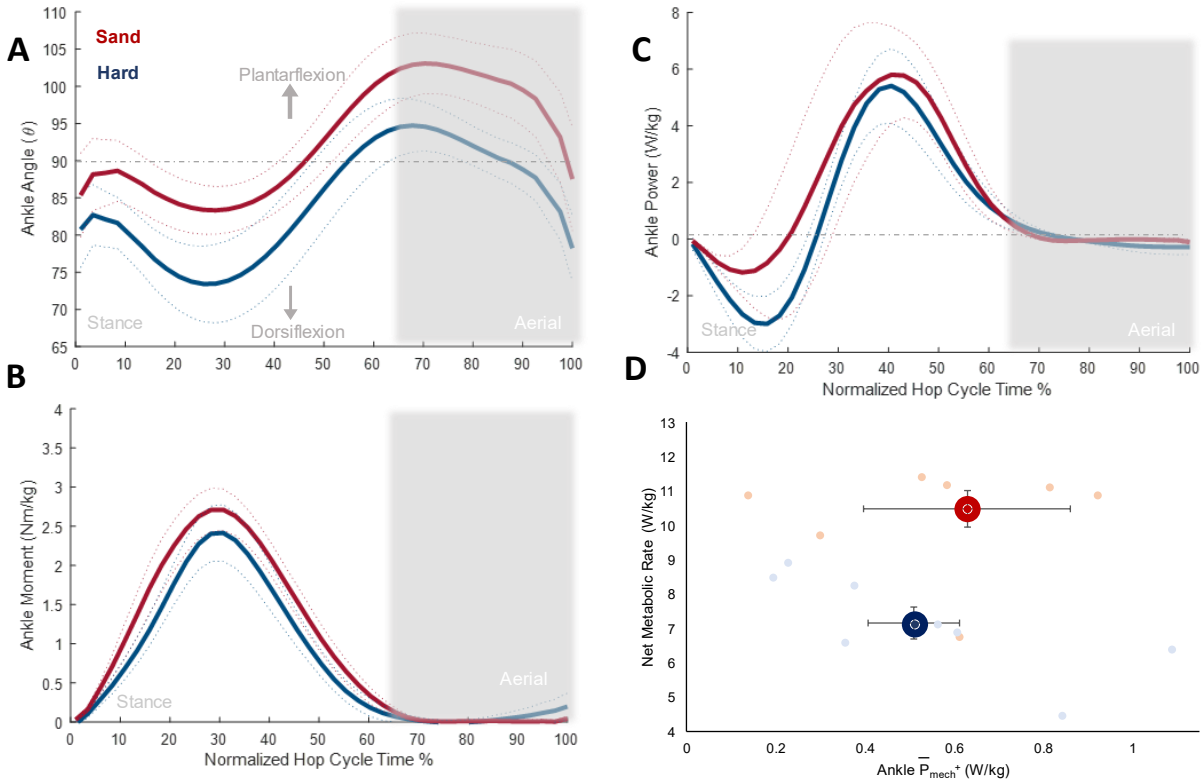

Figure 22 - Mechanics around the ankle joint highlighting (A) the ankle angle, which was found to be consistently more plantarflexed on sand (p=0.042), (B) joint moment which showed a slight increase in peak values of 10%, (C) power over the hop cycle, which showed significantly lower power loading than hard ground, as well as higher peak powers and (D) $\Delta\bar{P}_{mech}^{+}$ compared to $\Delta\bar{P}_{met}$, as a measure of the efficiency of positive work, η

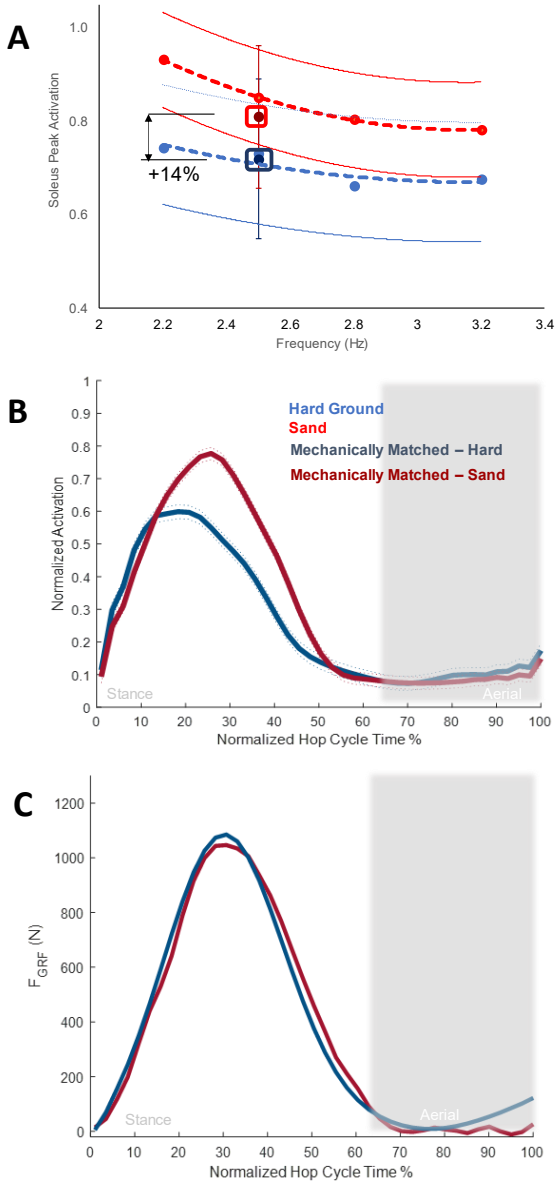

Figure 23 - (A) Average peak activation over across frequencies. As in the case of the metabolic sweep, subjects were asked to hop at their preferred height across frequencies, as well as asked to hop to a matched height at a frequency of 2.5Hz (circled). These matched conditions are of importance such that we can investigate muscle-level effects during mechanically comparable tasks. The averaged activation over the hop cycle can be seen in (B). It should be noted that similar ground reaction forces were produced (p= 0.49), suggesting little change in hop height from hard ground to sand.

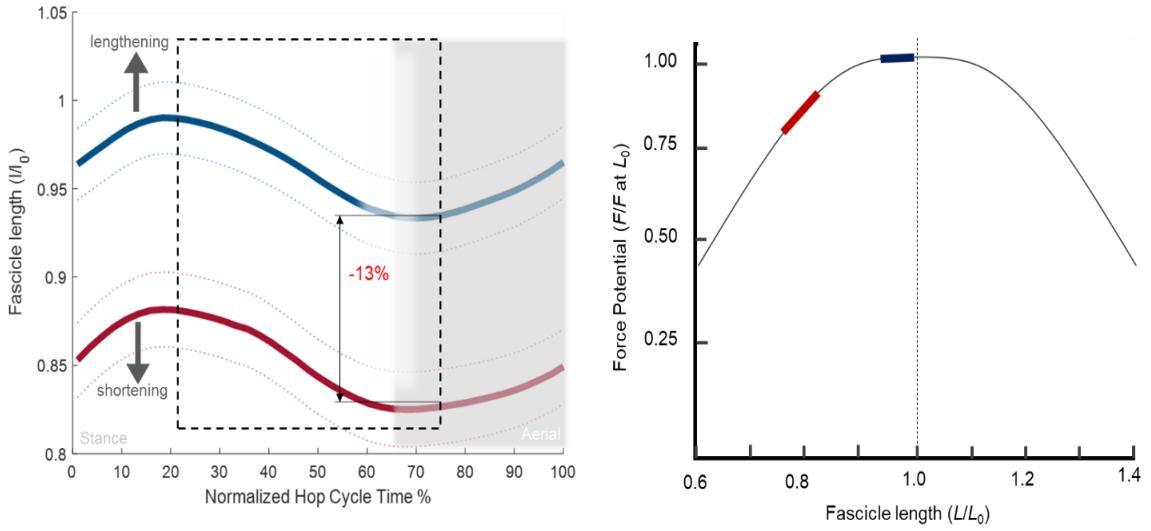

Figure 24 - Time series data for fascicle length at a matched height at a frequency of 2.5Hz. we found a 13% decrease in fascicle operating length when compared to mechanically comparable hopping in sand (p=0.014). This shifts the theoretical force-length relationship to a less efficient region.

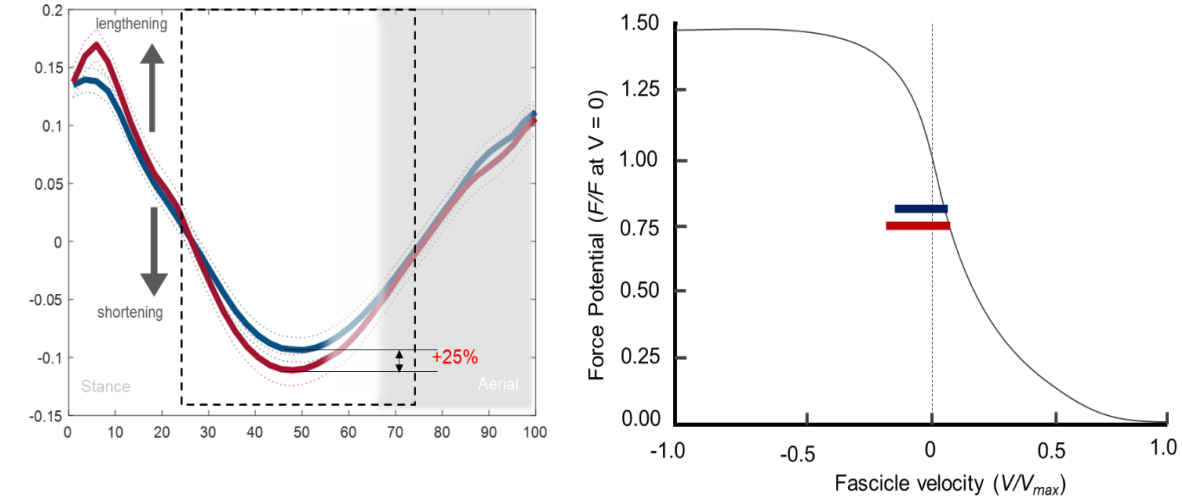

Figure 25 - Time series data for fascicle velocity at a matched height at a frequency of 2.5Hz. we found a 25% decrease in fascicle shortening velocity when compared to mechanically comparable hopping in sand (p=0.034). Similar to the force-length relationship, this shifts the theoretical force-velocity relationship to a less efficient region.

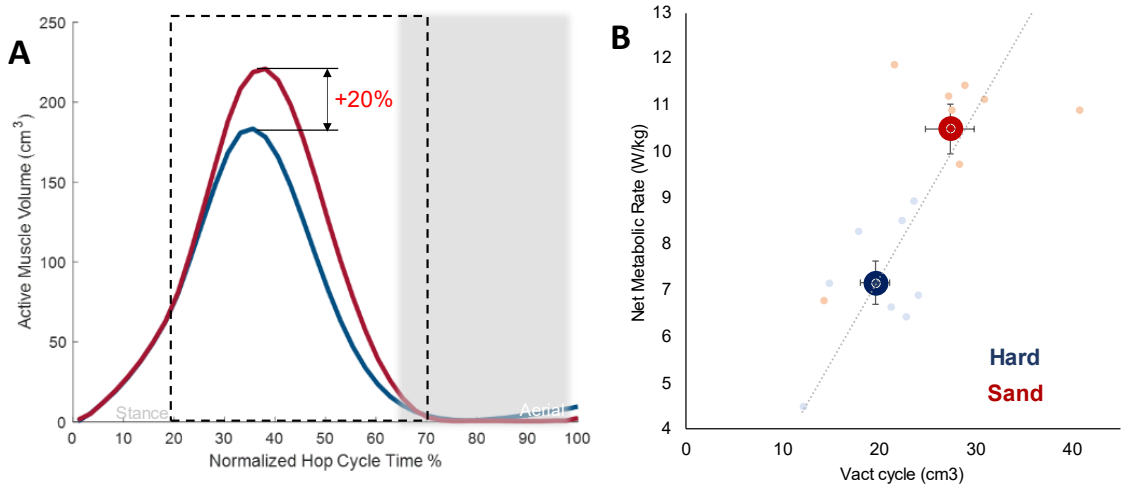

Figure 26 - (A) Active muscle volume increased from the hard ground to the sand condition. Both peak and average AMV increased by approximately 20% (p = 0.0181). (B) this continues to highlight the relationship between active muscle volume and metabolic cost

4.3.3 Active Muscle Volumes

For the soleus muscle, the active muscle volume at any point in time of the gait cycle was found to be:

$$V_{act} = \frac{F_{sol} CSA_{sol} l_0}{FL.FV}$$

Where CSA_{sol} was estimated to be 230.04cm^2 [60], and l_o was found to be 3.6cm. For comparable force values, V_{act} became an inverse function of the CE F-L and F-V relationships as shown above. As such, we found that both peak and average AMV increased by approximately 20% (p = 0.0181) for a mechanically matched condition, and, in line with previous work [55], we found a positive relationship (r = 0.96) between active muscle volume and metabolic cost, regardless of terrain.

4.4 Discussion

The purpose of this study was to comparatively investigate the ankle mechanics and energetics of human hopping to a fixed height from rest, with conditions of hard ground and sandy terrain- to this end, our primary goal was to produce a greater understanding of energetic profiles of human locomotion over metabolically taxing terrain such as sand, snow or mud, and, in turn characterize them at the whole body, the joint, and the muscle level. This was performed as the second *in-vivo* step in a comprehensive modelling, simulation, and real-world series of experiments, with the intention better understanding human locomotion at the muscle-level on dissipative terrain.

4.4.1 Comparative Energetics

Both modeling and experimental studies in literature showed a significant increase in metabolic cost when running and walking over dissipative terrain for a series of similar tasks. To that end, we hypothesized that for a mechanically matched task (hopping to a fixed height at a fixed frequency) would elicit a similar increase. This first hypothesis was confirmed by a resulting increase in P_{met} of approximately 22% when comparing the mechanically matched hard ground and sand conditions. This agrees well with previous initial findings from work done in modelling and simulation studies (23%) [5, 58], however, this underestimates findings of Lejeune et al, who reported approximate energy expenditure increases of 60% for running (bouncing gait) on a sand track [2]. Unlike this study, however, participants were asked to keep their arms at their sides to avoid added mechanical or metabolic effects and can help explain a portion of this discrepancy.

Additionally, participants were held to a fixed height and hop frequency, while in Lejeune's study, participants were kept to a fixed speed; this may introduce differences in gait effects.

4.4.2 Muscle Dynamics

Secondly, we hypothesized that our results would show increased muscle activation and less optimal contractile element length and velocity characteristics (higher fascicle velocities and shorter fascicle lengths) versus hard ground when hopping on a dissipative surface. These activation and velocity changes have been shown to directly relate to an increase in P_{met}, in literature [55]. Additionally in the case of prior modelling work, we used the metabolic cost estimation presented by Minetti et al, which presented a case for unfavorable shortening velocities and higher activations during 1 DOF Hill-Type hopping for comparable mechanical tasks [19]. We found that our model's activation, length and velocity behaviors agreed with this hypothesis. As seen in Figure 23, peak activations for the loose sand conditions showed a 14% increase for the mechanically matched case when moving from hard ground to sand, while averaged activations over the cycle increased by 29% ($p = 0.03$). To begin to address the increase in this activation, we examined the operating of the length of the Soleus CE. We found that the CE average operating lengths across conditions decreased up to 13% per cycle ($p=0.014$) from hard ground to dissipative terrain. This value is associated with more costly force production as it lowers the force-producing capability of the CE, thereby necessitating more activation. This is further highlighted by the ankle angle (Figure 22) being more plantarflexed, indicating a shorter Achilles-Tricep-Surae MTU length. This is consistent with previous experimental

literature [61], as well as previous studies that analyze muscle level dynamics for increasing P_{met}, however this is a result is contrary to previous work *in-silico.* We predict that for the in-vivo experimental realization of this study, we were not limited by the assumption of flat-footed hopping that caused CE length to be relatively unchanged in our modelling framework.

Maximum push off velocity (Figure 25) was found to increase by 25% ($p=0.034$), again providing a less energetically favorable condition for force production as highlighted on the FV curve, and also explains, in part, the necessitated increase in soleus activation. This value is similarly associated with slightly more costly force production leading us to conclude that the combination of length and velocity effects necessitate higher activations, which in turn lead to higher metabolic rates over comparable tasks. This will be examined further in our third hypothesis.

4.4.3 Active Muscle Volumes

Finally, we predicted that the Soleus CE would show increasing active muscle volumes with our expected increase in muscle activations and metabolic costs from our first two hypotheses. Confirming this hypothesis, we found that both peak and average AMV increased by approximately 20% ($p = 0.0181$) for a mechanically matched condition, and, in line with previous work [55], we found a strong correlation ($r = 0.96$) between active muscle volume and metabolic cost, regardless of terrain (Figure 26). This adds to the body of literature that suggests that for steady state locomotion, V_{act} can be a reliable predictor of P_{met}, agnostic to the locomotor task [55].

4.4.4 Limitations and Assumptions

It should be noted that our study was not without its' challenges. To date, it has been difficult to truly assess joint-level kinematics for dissipative terrain, due to the difficulty of obtaining reliable force data over dissipative terrain. Lejeune et. al suggests that buried force plates may provide sufficient data for ground reaction force but acknowledges that this is a key assumption that may not hold true [2]. As such, to measure ground reaction forces accurately, and in turn get sufficient data to perform our joint level assessment, it is of the utmost importance that forces are measured directly at the foot-ground boundary. This series of experiments analyzed human hopping, and as such, it was necessary to measure, at the least, the vertical component of the ground reaction force vector. To measure this, we partnered with novel Inc (Munich, Germany) and have benchmark their force sensing insole system against our calibrated force plates to collect these plantar boundary forces, using only the z-direction component for our inverse dynamics calculations. These benchmarking studies provide close agreement for inverse dynamic calculations at the hip, knee and ankle for 1 degree of freedom locomotion, and can be found in the Appendix C.

4.5 Conclusions and Future Directions

4.5.1 Conclusions and Future Work

Bipedal bouncing gait has examined for decades, but little work has been done to yield a general formula for locomotion over dissipative terrain. We have presented a

muscle level energetic analysis to examine the metabolic energy cost of hopping in sand, from the whole-body metabolic level, down to the muscle level of the prime ankle movers. Continuation of this series of studies will move beyond the unassisted locomotion, to being to combat the muscle level effects found in this chapter. Informed by the results of this study, we are developing an exoskeletal device with the intention of lowering the energy cost on dissipative terrains by tacking the neuromuscular effects and inefficiencies highlighted in this study. This requires development from the ground up, so that the device considers the complex, non-linear physics of the interaction between the user and the environment [10, 22, 43]. We plan to adopt a bio-inspired approach that builds on well-established schemes for hard ground locomotion cost reduction, modelling and simulation results, and cues from nature's most efficient locomotors over sandy terrain. Thus, a key long-term goal of this study is to discover the fundamental principles that govern the energetics and mechanics of locomotion on dissipative terrain, and, once these are understood, work to augment and optimize these with respect to physical and metabolic function. This allows us to open up a new class of wearables that allow us to go further and farther than ever before.

4.6 Associated Publication

This work will be submitted to the Royal Society Interface following final editing and revision

APPENDIX A. DEVELOPMENT OF A FOOT-ANKLE EXOSKELETON TO NAVIGATE DISSIPATIVE TERRAINS

Much of this Appendix has been adapted from reports by various design teams that have worked on the Exoskeleton Project, headed up by me, Jonathan Gosyne, with key contributions from Qingyi Lou, Claudia Vitale, Nil Patel, Michael Bick, Maharshi Mrittika Khan, Peter Oliveira Soens and Max Anderton. The material presented in this chapter has been and will continue to be presented at Various conferences over the years, such as Dynamic Walking 2021 and ASB 2022/ASB2023.

Sand, gravel, and other surfaces consisting of granular media have more complex interactions to a human's walking gait than static surfaces (like a paved road). These surfaces often show non-linear and dissipative behavior, resulting in them being sensitive to applied forces, dynamically changing over time, and energy intensive to traverse. Currently, lower-limb exoskeletons are not designed or optimized for these surfaces. This gap in functionality is the focus of this project; the goal being to design an exoskeleton meant specifically to handle the challenges posed by sandy terrain, while reducing the energetic cost of movement. The technical challenges involved are non-trivial, as the complex and multifaceted nature of the problem tends to complicate the adaption of currently existing products into this new space.

The device developed by the Basilisk Boot Team combined a novel, outsole with a conventional passive exoskeleton. The soles leveraged biomimicry using mechanisms such as spring-loaded expansion to distribute force as the user applies pressure to the ground,

thereby reducing the energy dissipated to a granular media, similar in operation to rattlesnakes, or through cupped soles, similar to the plantar surfaces of camels. The parallel passive spring at the ankle of the exoskeleton enables a user to operate with a stiffer ankle joint and even recycle more energy from each stride, with the aim of reducing the overall cost of dissipative terrain locomotion.

Various prototypes of the device were manufactured using rapid prototyping techniques; with preliminary testing using various proof-of-concept designs showing a metabolic cost reduction of 28% of walking at a brisk pace in sand, and 13% reduction in metabolic cost when subjects were asked to perform a mechanically matched task across hard ground and sand, (with and without the exoskeleton).

A.1 Analysis of *in-silico* Results

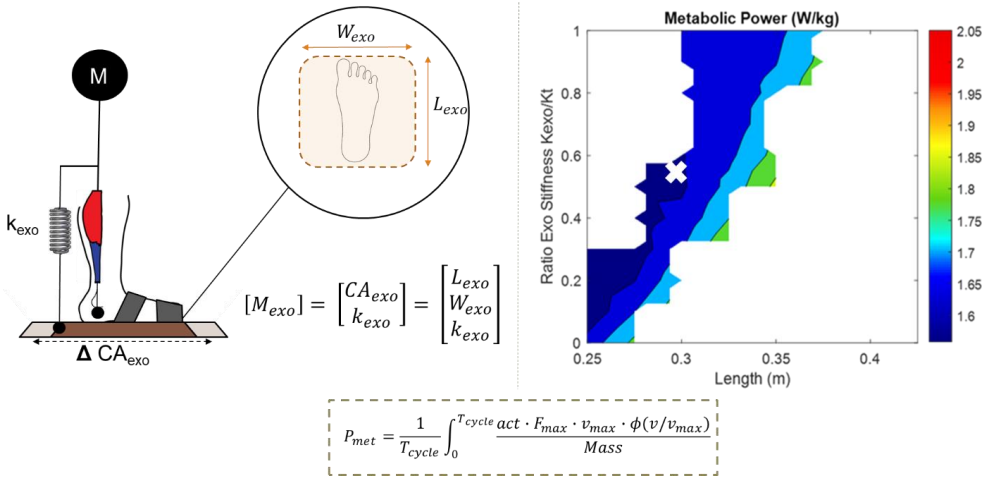

Figure 27 - Average metabolic rate for the various combinations of the exoskeleton used for augmentation of the loose sand condition. with X highlighting the chosen parameters. And - - showing a constant Pmet (W was held at 0.25m).

As seen in Chapters 2 and 3, we have developed a computer model and verified in human experiments that the metabolic cost of hopping increases by over 20% during hopping in sand vs. on solid ground across a range of frequencies. Our modelling work indicates that a foot-ankle exoskeleton with optimized geometry and stiffness can eliminate the metabolic penalty associated with energy dissipation during locomotion on dissipative substrates. Now, we seek to translate these ideas into a physical prototype that can be used to investigate human hopping in sand, with and without the assistive device. We hypothesize that for an *in-vivo* study, a wearable device combining a larger than human foot contact profile with a stiffer than human elastic element in-parallel to the ankle plantarflexors will minimize dissipation of lower-limb muscle mechanical power to the environment during locomotion in sand, thereby reducing whole-body metabolic rate. This study will better characterize human-terrain interactions and will allow us to create more informed devices and solutions for novel wearable robotics paradigms in recreation, agriculture, defense, and beyond.

A.2 Exoskeleton Design Study

A.2.1 Design Considerations

The design team aimed to develop a novel passive ankle exoskeleton. that aims to reduce the metabolic cost of the end user. While initially, the device will be used in a research setting, the intention of this device is to provide a platform for the development of a new class over wearable devices that make it easier to traverse various terrains.

As seen in our modelling and simulation work, a key device function is to distribute a user's body weight over a larger surface area, thereby reducing the pressure and distributing ground reaction forces acting on the ground. This will reduce the sinkage into the unstable, granular terrain thus reducing the energy lost to the environment. The device should also augment the power output by the muscle-tendon unit to the ground by incorporating moderately increased ankle stiffness, allowing for more combined soleus muscle-exoskeleton power output over the gait cycle at a given metabolic cost. Details about relevant user needs can be found in the User Needs table below:

Table 2: Design Considerations for the Proposed Exoskeleton Design Study

User Need	Design Considerations	Functions	Constraints
Portable	• Weight • Size • Modularity	• Wearer specific fit • Easily Removed • Easily Transported	• Light enough to be carried by a single user
Energy saving	• Mode of passive energy reduction • Efficiency • Amount of energy saved • Energy storage and regeneration	• Reduces metabolic cost of moving through sand • Stores energy • Applies energy • Adjusts to changing Conditions	
Load bearing	• Static force production • Foot-to-ground pressure	• Holds a static load • Applies force at various speeds • Reduces foot-to-ground pressure	

Comfort	• Relative range-of-motion • Effect on natural human gait	• Interfaces between exo and joints • Supportive of plantar surface	
Safety	• Risk • Possible injury or damage • Redundancy • Reliability	• Warns user before injury or damage • Warns user of component failure	• Safe to wear; noninvasive • Not clinical; minimal amount of external regulation needed
Affordability	• Design cost • Engineering cost • Manufacturing cost • Operating costs		

A.2.2 Current Work

An exoskeleton is defined as a device that is composed of "an external, powered, motorized orthosis that is placed over a person's paralyzed or weakened limbs for medical purposes" (FDA regulation number 890.5500). The purpose of such an exoskeleton is to improve the mobility of the user. Rewalk, Parker Indigo, and Ekso Bionics are the only three companies with active FDA-approval on exoskeleton products as of December 2022.

All three companies adopt similar design concepts, which includes full lower-limb suit, gait cycle monitoring through integrated sensors, and power supply at hip joint and knee joint. Their products aim to enable patients with lower limbs control issues or patients with injured spinal cords to move around on their own. While only three companies hold FDA-approved exoskeleton products, there are more than 550 patented lower limb

exoskeleton designs. Among them three designs stood out as relevant to this project. US8894592B2, currently assigned to Ekso Bionics, incorporated a stance sensor component, a force sensor component, and a pressure sensor component in its design. The stance sensor is integrated with the purpose to indicate whether the leg is in the stance phrase and the pressure sensor is to monitor the power system. DE102018106846B3, approved and published in July, 2019, has one hydraulic unit with two pumps located at the medial and lateral of a knee to inject power to the joint. Also, US10124484B1, assigned to Lockheed Martin, highlights power units coordinated by onsite captured EMG data.

A foot-ankle orthosis is characterized to be "plastic, rigid anterior tibial section (floor reaction), [and] custom fabricated" (FDA regulation number 890.3475 and HCPCS number L1945). The purpose of the current ankle-knee orthosis product is to improve mobility among patients with diseased lower limb joints. While orthoses of different brands are available on the market, no current product addresses the energetics of locomotion. This is in part due to orthoses being a medical device whose acute purpose is to correct imbalance gait or to reduce foot pain in a clinically relevant setting

More studies, as well as prototypes, have been proposed on prosthetics rather than exoskeletons, partly due to the clinical necessity. However, inspirations can be drawn from prosthetic design; both prosthetics and exoskeletons share structural and functional similarities as lower limb wearable devices. A pneumatic ankle prosthetic proposed by Mrazsko, et. al., is an example of such. It features a device with variable stiffness and a large range of motion. The former feature is achieved by the implementation of a gas pump and the latter is through the mechanical design of the system.

While all of the designs discussed above balance the ergometry with the mechanical function of the exoskeleton, the majority of these products are meant for rehabilitative populations in clinical use. Therefore, they address terrains such as solid flat ground, inclined slope walking, and some stair-up functionality, commonly found in an urban setting.

A.2.3 Design Requirements

Design Considerations for concept ideation were formed using the concept matrix shown in the table below. Using these sources of information, several concepts were generated, showcasing several alternative means of satisfying the specified needs

Table 3 Design Considerations for the exoskeleton prototypes during the ideation phase of development

User Need	Design Considerations
Portable	• Lightweight components • Long operating life • Embedded sensing and data collection
Anthropometric and Ergonomic considerations	• Safe weight distribution • One size fits most (external attachment)

Ease of use	• Intuitive sole design • Simple spring design • Easily removable
Low Energy	• Semi-active or fully passive design based on springs

A.2.4 Device Ideation

The initial idea based on the design considerations and requirements above was to create a shoe that make it easier to navigate sandy terrains. Thus, a primary focus was to mitigate sinkage; informed by the modelling study, this was achieved by increasing the contact area of the shoe sole with the terrain. Elastic materials like nylon were considered for shoe sole design to account for shock absorption and walking energy transfer to the spring system. Initially, based on the hypothesis in Chapter 3 that the midfoot also dissipates power over the gait cycle, we first explored midfoot level springs, such as the ENKO shoe. The dual spring system was expected to conserve a portion of the user's walking energy from each step and relay that back to the user for the next step, acting as an energy recycler. The key shortcoming of this was the absence of a hard surface for spring loading, and as such, other designs were explored

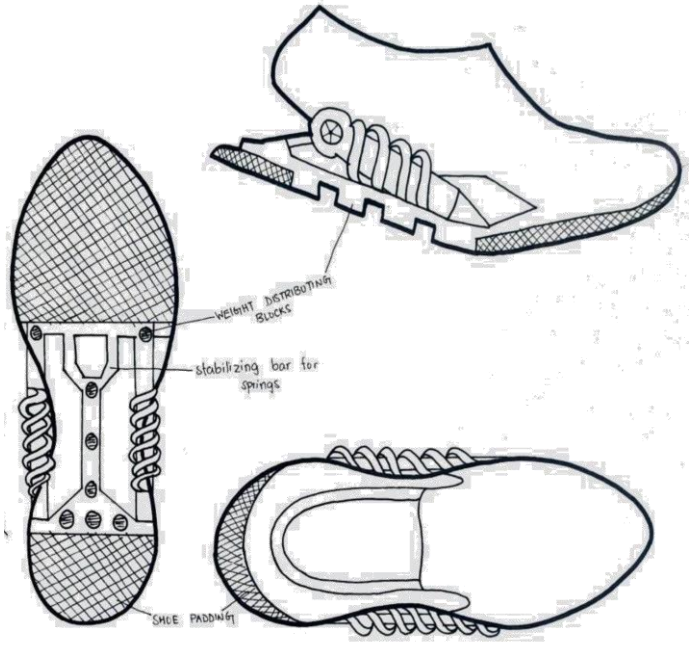

Figure 29 - Initial exoskeleton concept using midfoot springs and increased surface area. This concept necessitated a compacted surface for spring loading, which is not present in sand.

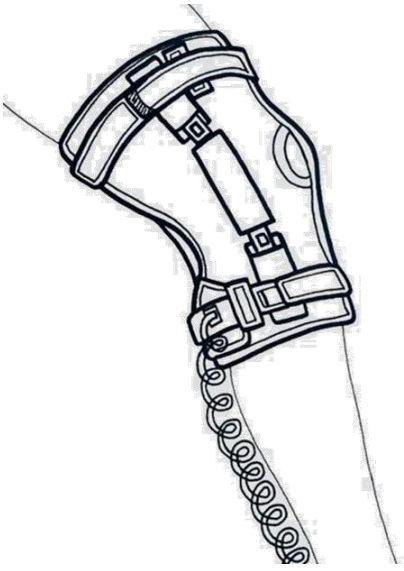

Figure 28- The upper attachment of the exoskeleton design. This was inspired by previous work by Sawicki et al.

We then looked to previous work that showed success on hard ground. We opted for a passive elastic soft exo design; this was designed piecewise. Firstly, at the knee, we proposed an attachment that contains integrated hooks for spring attachments to vary the spring constant of the exoskeleton for passive elastic assistance, and can be configured for data collection of forces and torques. Linked by a spring, this portion gave way to the "shoe" portion of the design.

For the foot, inspired by paper-folding origami techniques, we proposed a foldable V-shape "flap sole" to be placed between the bottom of a conventional sneaker and the dissipative ground. The motivation of our design came from the primary agenda of the project which was to enable more efficient locomotion over soft substrates. The most practical strategy to achieve this goal of is to avoid sinkage is to increase ground contact area, since sinkage is largely pressure dependent. However, a major inconvenience brought up by a larger sole is an interference with the normal walking gait of the user. For an oversized sole, gait patterns change, as the user needs to maintain a larger distance between the two feet to avoid medial interference between the legs, as well as. needing to account for the lengthened sole especially at heel strike and toe off. Additionally, extra neuromuscular adaptations are required for the user to habituate to walking in an enlarged sole. As such, we proposed a mechanism that only achieved full size while on the ground. By incorporating a folding mechanism, our design allowed for expansion of the ground contacting area only during the time between heel strike and toe off where pressure is exerted to the ground to support body weight. This used a fully passive, spring-loaded foot model as seen below, and integrated seamlessly with the top end of the exoskeleton.

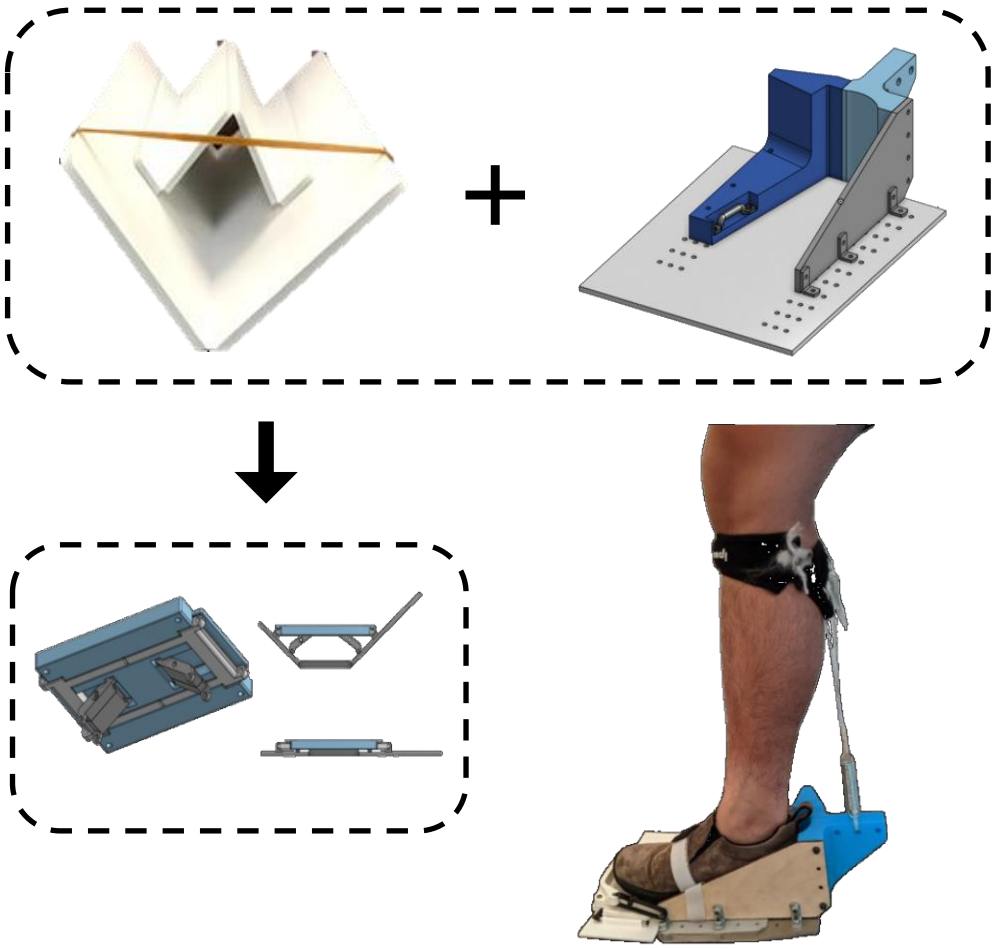

Figure 30- The combination of a folding concept with the need for larger surface are allows for the development of an expanding that is equivalent to added surface area with minimal interference. This integrates seamlessly with the added parallel spring.

A.2.5 Initial Prototype Selection - Biomimetic Concepts- from Lizards to Camels

While the above designs provided an effective first prototype, during user testing, we found two key issues- The theoretical required surface area required to mitigate the dissipative effects not captured by the spring was too large and smooth, thereby still causing stability effects through acting like a “ski” on dry sand. Additionally, the device

still presented issues with medial interference between legs, and sand was collecting on the dorsal region of the proposed foot.

As such, we turned to nature to examine how other organisms locomote on sand. While rattlesnakes and fringe toed lizards can move quickly enough to use the "ski effect" to their advantage, we found that these are low mass creatures that operate for short bursts; our attention turned to long distance, high mass movers on sand- camels. We found that camels have a variety of adaptations, including fat pads, and webbed toes, that serve to expand contact area and increase traction at a given footprint. The modifications to the initial foot design can be seen below:

Table 4 – Modifications to the initial exoskeleton that address issues from user feedback.

Required Modification	Design Elements
Need to redistribute surface area for weight distribution while reducing interference	• Wider in the front than in the back; chosen to reduce interference and emulate more of a camel hoof shape. • Not more than 1.5 times wider than the actual front of the 10-11 men's shoe size range to remain aware of balance issues for people walking
Need to reduce amount of sand that can sit on top of foot	• Guide splines for loft were specifically made to make it easier for sand to slide off and not accumulate on the top of the 'hoof'; fillets were also added along the top for this reason • Chose a sole thickness of 30 mm to provide added height to put the actual foot of the person higher above the sand, while still trying to keep the overall weight of the 'hoof' down

Need a way to increase friction between step and sand surface	• Cut-out designed around center of mass of the "human hoof" to increase surface area while also maintaining the general shape/footprint of the foot for a more even weight distribution and traction

User feedback from this iteration proved to be more positive, and early and final prototypes of this iteration were used in a series of following studies. The final device can be seen below:

Figure 31 Initial CAD Design of the modified foot portion of the device. The expansion mechanism was no longer included on this version of the foot.

Figure 32 – Final Prototype of the 'shoe' portion of the exoskeleton device (left) and the entire system (right). Pinch closures were used for easy slip on and removal.

A.3 Exoskeleton Prototype Real-World and User Testing

A.3.1 Study Introduction

As previously mentioned, the field of wearable robotics is advancing quickly, however, most devices still struggle in environments with complex terrain such as sand, snow, mud or dirt. Perhaps, this poor field performance of wearable devices stems from mechatronic design that does not consider the non-linear physics of interaction between the human-machine system and the environment. Indeed, for wearable systems to effectively stand up to harsh environments as users wander off the beaten path, current devices need to be redesigned from the ground up. Even so, many control and design schemes implemented on wearable systems today still have the same primary underpinnings of more traditional devices developed in decades past. As such, although many modern devices are significantly more functional and technologically complex than their earlier counterparts, their effective context of use (locomotion on flat, even terrain) has thus remained largely the same. In this study, we sought to combine the knowledge from past studies of locomotion on granular substrates and insights from wearable devices designed to interact with the physiological properties of underlying musculoskeletal structures. By combining all these individual components, we open the possibility for a new class of wearable devices that can mitigate the metabolic penalty of moving in complex, dissipative terrain.

A.3.2 Methods and Materials

One male participant (age = 23yrs, height = 1.72 m, mass = 86.50 kg) was asked to complete walking trials for four different conditions (standing, hard ground, sand, sand + exoskeleton), at 1.23 ± .045 m/s. For non-exoskeleton trials, equivalent mass was added to the dorsal region of the participant's foot. Gross metabolic power was measured using indirect calorimetry. Each trial lasted 7.5 minutes, with the participant taking 10 minutes rest between trials to minimize fatigue effects due to the physically demanding nature of the protocol. Metabolic data were averaged over the last two minutes of each trial. The order of conditions was randomized. Hard ground walking was performed over an outdoor running track, and sand walking was performed in a standard sized sand volleyball court. The exoskeleton consisted of an in-parallel spring (k = 1444.44N/m) that increases stiffness of the ankle joint, and a hinged aluminium sandal (length = 0.3125m, width = 0.25m) that increased contact area.

A.3.1 Results, Discussion and Conclusions

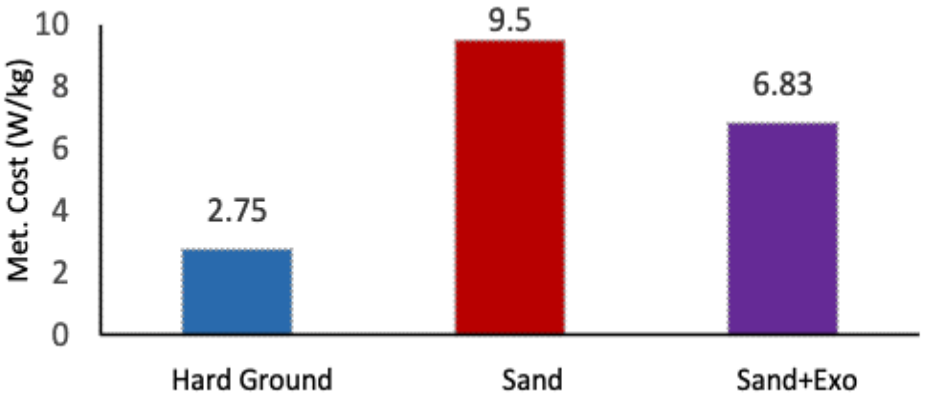

Figure 33 - Graph showing metabolic cost (W/kg) and terrain relationship for walking on hard ground, sand and with exoskeleton assistance at 1.23 ± .045 m/s.

As seen in Figure 33, we found a hyperbolic metabolic pattern for the metabolic costs of the hard, sand and sand + exoskeleton trials respectively, with increase in metabolic power of 245% from hard ground to sand, and a decrease of 28% when using exoskeleton assistance on sand. The hard and sand conditions agreed with experimental literature [2, 4, 28, 31], and the exoskeleton metabolic cost reduction aligned with proposed models [58]. Anecdotally, the subject found that the exoskeleton was difficult to walk in due to interference near the ankle joint. We thus conclude that even with the effects of non-ideal gait parameters, the combination added contact area between foot and ground with modified stiffness around the ankle joint allows for significant reduction of the penalty associated with energy dissipation during locomotion on granular substrates and informs the final design of our device for in-lab testing.

A.4 Final Exoskeleton Comparative Mechanical Task Testing

A.4.1 Experiment Introduction

The goal of this section of the study was to investigate the ability of a passive exoskeleton with specific morphology and added stiffness around the ankle joint could mitigate the muscle level causes of the increase in metabolic cost on dissipative terrain as detailed in chapter 4. To this end, based on previous findings from modelling and human walking studies, we hypothesized that participants would (1) show a decrease in metabolic cost when performing a mechanically matched task with the exoskeleton on sand versus without, (2) more optimal contractile element length and velocity characteristics (lower fascicle velocities and longer fascicle lengths) versus unassisted hopping when hopping

with our device on a dissipative surface, and (3) show decreasing active muscle volumes with the expected decrease in metabolic costs. These results serve to further the scope of knowledge of bipedal locomotion and are a first step in the design of wearable devices that can mitigate energetic penalties associated with 'real-world' locomotion over dissipative terrain for applications in healthcare, agriculture, and beyond.

A.4.2 Methods

After minor modifications to address interference, for a final test of our device, we performed hopping trials over a series of frequencies and heights, with a focus on mechanically matched conditions across conditions. Biodata was taken from a volunteer that enrolled in this study (age: 22 years; height: 1.784m; mass: 88.8kg; resting metabolic rate 1.53 W/kg). The participant reported themselves to be free of cardiovascular and metabolic disorders. Prior to starting the study, informed consent was obtained in accordance with the Georgia Tech Institutional Review Board.

A.4.2.1 Metabolic Trials

For metabolic measurement sessions, the participant was asked to fast overnight, and upon arriving in the morning, they were asked to stand still and upright with their hands at their sides. In this standing position, participants performed a 10-minute resting trial while breathing in-and-out of a mask that connected to an indirect calorimetry system (COSMED K5, COSMED Srl, Italy).

For session 1, the participant was asked to don a pair of force sensing insoles (novel, Germany), and reflective makers were placed at the left and right posterior superior iliac spine to provide height biofeedback and to serve as a secondary biofeedback measure and validation through motion capture (Vicon, Oxford, UK). The subject was then asked to perform 4 x 5-minute hopping trials. Trials were performed at 2.5Hz to matched height on hard ground, on sand, with only the foot on sand, and with the entire exoskeleton on sand. Terrain conditions were randomized. During each hopping trial, metabolic expenditure was measured through the same means as the resting trial, but all other measures (ultrasound and joint mechanics) were measured during a second, muscle mechanics focused session.

A.4.2.1 Muscle Mechanics Trials

During the second session, the participant was once again asked to don a pair of force sensing insoles (novel, Germany). A B-mode ultrasound probe (Telemed, USA) was then placed on the skin superficial to each participant's right soleus, and reflective makers were placed on the participant representing a lower body Vicon Plugin gait marker set.

Subjects were then asked to complete 4 x 2-minute hopping trials each on hard ground and soft ground for a total of 12 trials. Trials were once again performed at 2.5Hz to specified height on hard ground, on sand, with only the foot on sand, and with the entire exoskeleton on sand. terrain conditions were randomized. During these trials, forces, motion data, and raw muscle fascicle ultrasound data were captured.

A.4.2.3 Outcome Measures and Data Analysis

Outcome measures and analysis techniques can be found in Chapter 4 above.

A.4.3 Results and Discussion.

A.4.3.1 Whole Body Energetics

Our values for metabolic rate (P_{met}) of the subject increased on sand for the mechanically matched condition by 44%, while only increasing for the foot only and the exoskeleton conditions by 28% and 26% respectively, representing potential metabolic savings of 13% over nominal sand locomotion for this subject. This confirms our first hypothesis

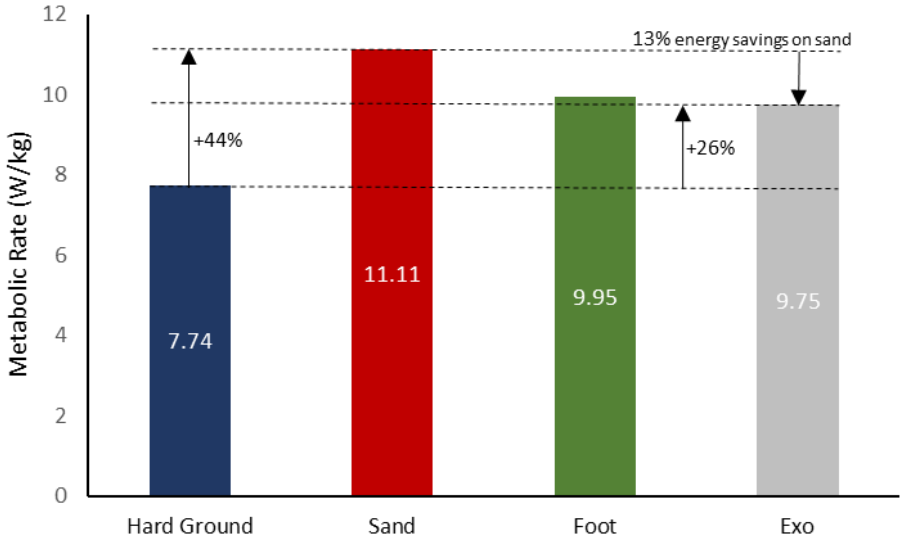

Figure 34 – Normalized metabolic rate for hard ground, sand, and augmented hopping for our test subject.

A.4.3.2 Muscle Dynamics

After whole body energetics was examined, muscle level effects were investigated. We found decreases in fascicle operating lengths on sand of when compared to mechanically comparable hopping on hard ground, with the force-length (F-L) relationship shown as a function of l_{CE}/l_0. We found that the addition of the foot and the exoskeleton returned the operating length of the muscle to a similar region as that of hard ground. Unlike the force- length relationship, we found no appreciable changes in the force-velocity relationship (represented by v_{CE}/v_{max}). We expect to see a reduced shortening velocity dure to the reduction in metabolic cost, and thus will continue to investigate this as the number of enrolled subjects increase.

A.4.3.3 Joint Mechanics

Around the ankle joint, even with one subject, we begin to see trends emerging that agree with our findings in Chapter 3. We found that for the Foot and Exoskeleton conditions particularly, there was a more dorsiflexed posture, indicating longer MTU lengths. We found comparable behaviors in terms of moments and powers around the ankle joint, when compared to hard ground, and as such, we hypothesize that much of the added metabolic cost between the hard ground and assisted conditions exists further up the leg at the knee and hip joints respectively.

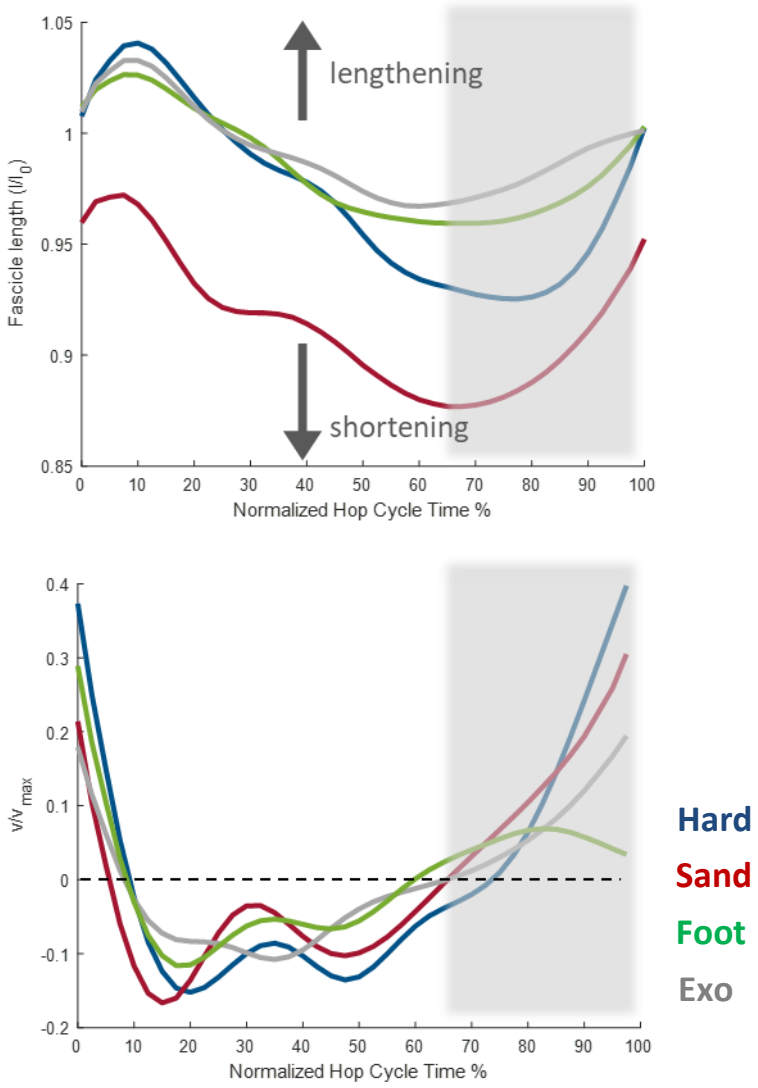

Figure 35 – Figures showing the muscle operating lengths (l/lo) and velocities (v/vmax). In agreement with our result in Chapter 4, we found that the fascicle operated at a shorter length in sand, and, in line with our hypothesis, we found a shift to a longer operating point after augmentation. Results of the shortening velocities are inconclusive, needing more subjects to confirm any trend.

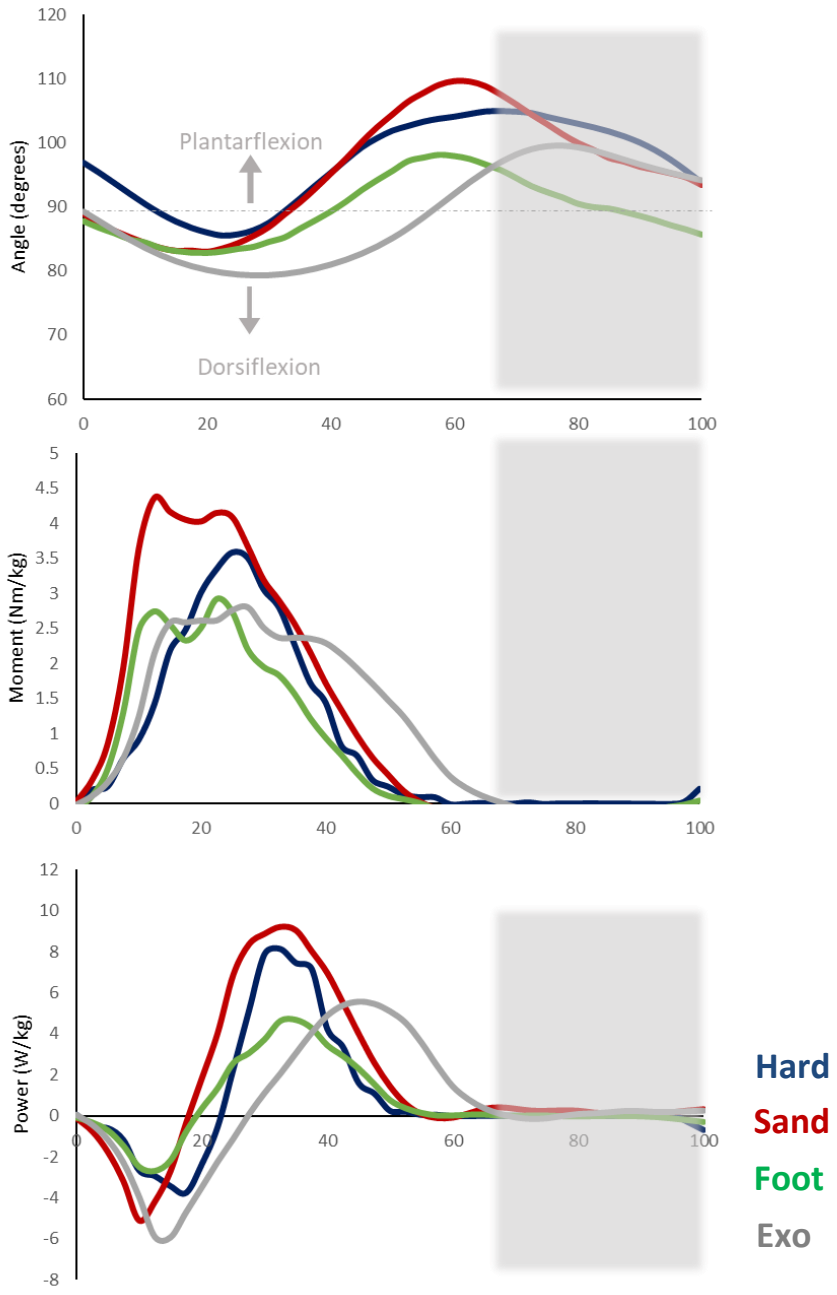

Figure 36 - An analysis of ankle joint angle (top), moment (middle) and power (bottom) for the hard ground, sand, and the two augmented conditions. We find agreement with the results in chapters 2 and 3 for the hard and sand conditions and find little difference between the hard ground and assisted conditions, prompting the investigation of the knee and hip.

A.4.3.4 Active Muscle Volumes

For the soleus muscle examined, we used the active muscle volume relationship highlighted in Chapter 4. CSA_{sol} was estimated to be 230.04cm^2 [60], and l_o was found to be 2.3cm. We found agreement with the results in chapters 2 and 4 for the hard and sand conditions (Higher AMV on sand) and find little difference between the hard ground and assisted conditions, prompting the investigation of the knee and hip.

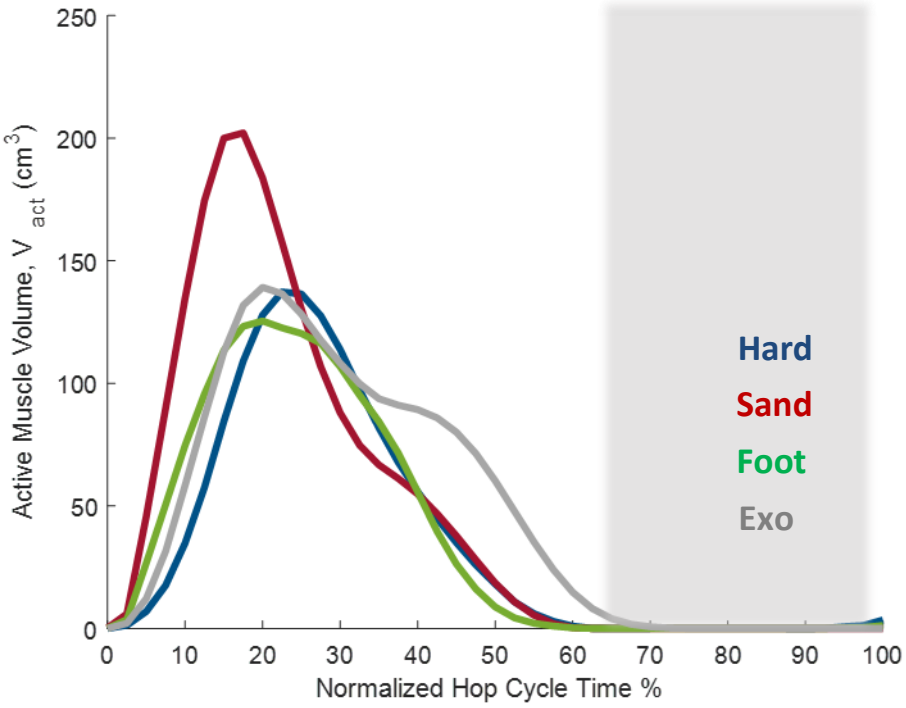

Figure 37 - Active muscle volume relationships for the tested participant. Much like our joint level result, We find agreement with the results in chapters 2 and 3 for the hard and sand conditions, and find little difference between the hard ground and assisted conditions, prompting the investigation of the knee and hip.

A.4.4 Conclusions

The goal of this section of the study was to investigate the ability of a passive exoskeleton with specific morphology and added stiffness around the ankle joint could mitigate the muscle level causes of the increase in metabolic cost on dissipative terrain as detailed in chapter 4. In agreement with our previous modelling and pilot results, we found a decrease in metabolic cost when performing a mechanically matched task with the exoskeleton on sand versus without. When examining the muscle level, we found more optimal contractile element length characteristics, and inconclusive results with respect to the fascicle velocities, likely due to our sample size. Finally, we showed decreasing active muscle volumes with the expected decrease metabolic costs, with comparable active muscle volumes for the hard and augmented conditions. As such, we believe that the knee and hips are responsible for much of the remaining discrepancy in metabolic cost in the augmented condition, perhaps due to the rigidity of the device. This, however serves as an informative first step as we seek to design wearable devices that can mitigate energetic penalties associated with ‘real-world’ locomotion over dissipative terrain for applications in healthcare, agriculture, and beyond.

APPENDIX B. MODELLING AND SIMULATION SYSTEM PARAMETERS

Parameters listed below can also be found in Roberson et al [36], as well as our previous modelling and simulation work [5, 58].

B.1 Modelling Parameters

Table 5 – Fixed Parameters used in the modelling and simulation framework

Muscle Parameters (CE)	**Value**
F_{max}	6000 N
v_{max}	-0.45 m/s
l_o	0.055 m
K_m	90,000 N/m
Tendon Parameters (SEE)	**Value**
l_{slack}	.237 m
k_t	180,000 N/m
Activation Parameters	**Value**

τ_{act}	0.033 s
τ_{deact}	0.091 s

Environment Dynamics	Value
g	9.8 m/s^2
m	35 kg*

*per leg

B.2 Modelled Equations and Relationships

Table 6 – Equations used for the modelling and Simulation Framework

Muscle Force Length	Equation	Values
FL_{active}	$e^{\lvert((l_m-l_o)^b-1)/s\rvert^a}$	b=0.8698, s=0.3914, a=3.1108
$FL_{passive}$	$A \times e^{\left(b\times\left(\left(\frac{l_m}{l_o}\right)-1\right)\right)}$	A= 2.38 x10$^{-2,}$ b=5.31

Muscle Force Velocity	Equation	Values

FV when $v_m>0$	$\frac{1-\left(\frac{v_{CE}}{v_{max}}\right)}{1+\left(\frac{v_{CE}}{k\times v_{max}}\right)}$	k = 0.17
FV when $v_m>0$	$1.8-0.8\left(\frac{1+\left(\frac{v_{CE}}{v_{max}}\right)}{1-7.56\left(\frac{v_{CE}}{k\times v_{max}}\right)}\right)$	k = 0.17

Tendon Stiffness	**Equation**	**Values**
k_{see}	$k_t \times (1+(0.9/-e^{\left(\frac{Q\times F_{CE}}{F_{max}}\right)})$	Q = 20

Metabolic Rate	**Equation**	**Values**
$p(v_{ce})$ for $v_{ce}>0$	$0.01-0.11\left(\frac{v_{CE}}{v_{max}}\right)+0.06e^{\left(-\frac{8v_{CE}}{v_{max}}\right)}$	-
$p(v_{ce})$ for $v_{ce}<0$	$0.23-0.16e^{\left(-\frac{8v_{CE}}{v_{max}}\right)}$	-

Activation Dynamics	**Equation**	**Values**
α(t)	$\int\left[\left(\frac{u(t)}{\tau_{act}}\right)-\left(\frac{1}{\tau_{act}}\right)\times(\beta+(1-\beta)\times u(t))\right]dt$	$\beta=\frac{\tau_{act}}{\tau_{deact}}$

EMA	**Equation**	**Values**
EMA	$0.33\ \frac{\left(L_{nominal}-\left(L_{nominal}/4\right)\right)}{\left(L_{exo}-\left(L_{nominal}/4\right)\right)}$	$L_{nominal}$ = 250

Environment	Equation	Values
x_{sink}	$x_{sink} = \frac{F_{grf}}{\kappa A_{exo}}\left(1 - e^{-(\kappa/\beta)t}\right)$	-

APPENDIX C. VERIFICATION AND BENCHMARKING OF BIOFEEDBACK AND INVERSE DYNAMICS ON DISSIPATIVE TERRAIN USING PORTABLE, FORCE SENSITIVE INSOLES.

As stated at the beginning of this document, to date, there has been no human study that allows for direct inverse kinematics from human locomotion studies. Lejeune et. al used buried force plates and relied on the whole-body mechanical vs metabolic cost comparison [2]. While these analyses are well documented for hard ground studies, there has not been a reliable way to obtain the center of pressure and ground reaction force vector [18, 23-25]. Through the use of an insole (loadsol, novel GmBH) on the subject to provide center of pressure, and insole force readings, we can reliably interpolate the full ground reaction force vector on dissipative substrates. This unique sensor fusion approach lays the foundation for sensing on non-uniform terrain and allows us to now test the implementation of our devices without being confined to the laboratory setting. To this end, in this appendix we seek to (i) leverage the loadsol's unique portability to pioneer a research effort that empirically characterizes the complex interaction, dynamics, and biomechanics of human locomotion over granular material through ground reaction force sensing and (ii) use our findings as a foundation for development of a bio-inspired wearable robotic device that enables its user to effortlessly traverse complex terrain. Our novel scheme will serve to provide a far more robust, adaptive platform for real-world locomotion on changing terrain than currently available wearable devices. Verification of these insoles, as well as the design process used, is shown in this appendix.

C.1 Loadsol Benchmarking Methods Results

This experiment was conducted in order to test the validity of the force readings obtained from the novel insole system when compared to Bertec's in-ground force plates. In order to do this, we tested loadsols against a force plate on hard ground to verify the agreement of forces We collected fixed frequency and fixed height on hard ground (real time biofeedback using force plate F_{GRF} to enforce a height after about 30s of settling. After this, enforced the same F_{GRF} target on Sand using the Loadsols in order to determine if ground reaction force is a reliable measure of hop height on sand by post processing the hop height from sacral markers for both trials. We found excellent agreement between the Bertec force plate forces and the loadsol forces (Figure 39, R^2= 0.96), with and as such continued with the verification process.

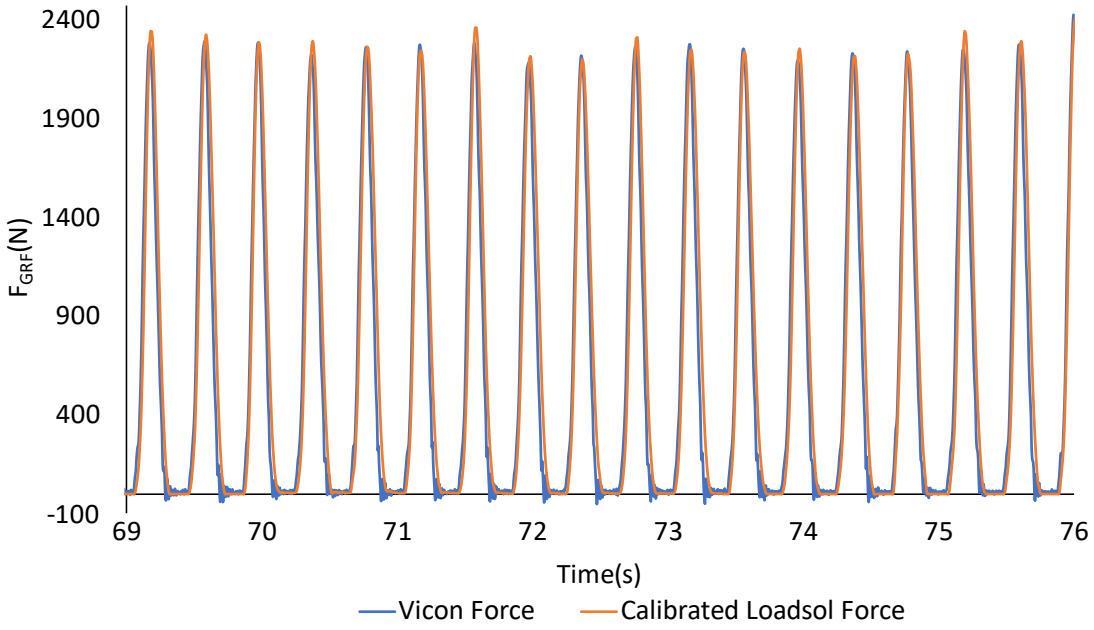

Figure 38 - Comparative testing of z-direction force plate and Loadsol force readings

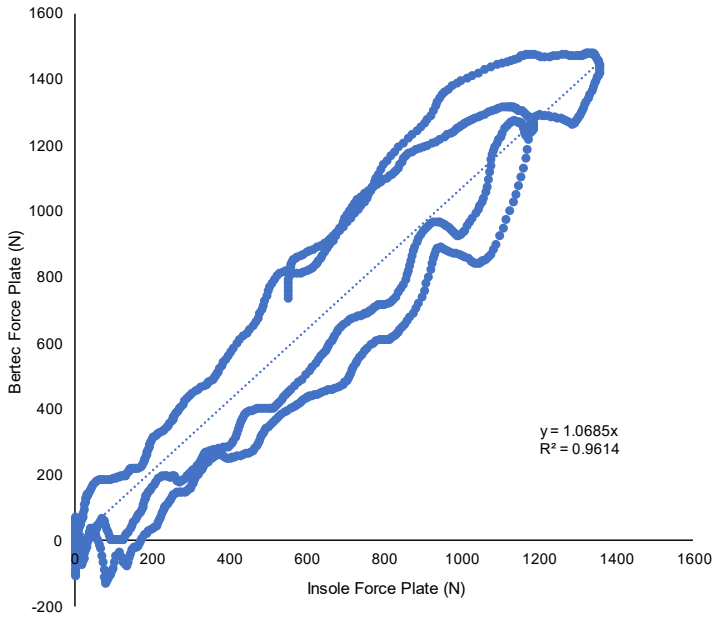

Figure 39 - Verification fits of the forces obtained during benchmarking. R^2 values were used to quantify correlation, and gains were used to determine the magnitude of the average discrepancy.

C.2 Biofeedback Verification

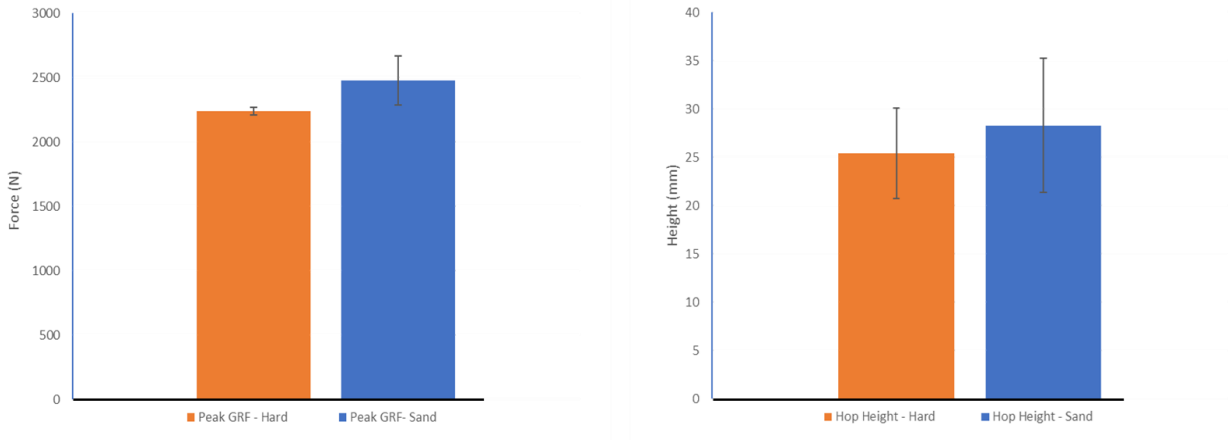

Figure 40 - Comparison of ground reaction forces and enforced heights from the loadsols over 10 cycles

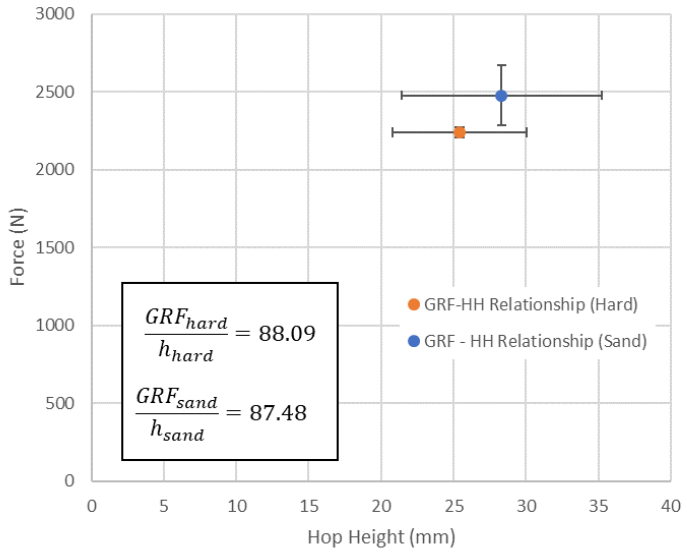

Figure 41 - the ratio of ground reaction force magnitudes to hop heights. These are almost the same for hard ground and sand, suggesting that just like in hard ground studies, F_{grf} can be used as a metric to enforce hop height if measured at the plantar surface.

C.3 Inverse Dynamics Process Flow and Verification

Upon Verification of the accuracy of the insoles for force measurement and biofeedback, we sought to test them in the context of their use for inverse dynamics calculations. This flow process can be seen in Figure 42.

Upon development of this cycle, we then ran a comparative study for a subject hopping to an enforced height at a set frequency on hard ground, with sensor data being collected from both the Bertec Force plates and the insoles. We found agreement between the Moments and Powers obtained from the Bertec Force plates and the loadsol insoles, with comparatively small fluctuations. We hypothesize this is due to small changes in the direction of the ground reaction force directions, and sampling rate matching. To combat

this, we therefore will use the loadsols for both hard and soft ground analyses, with the Bertec force plate dynamics being used as verification.

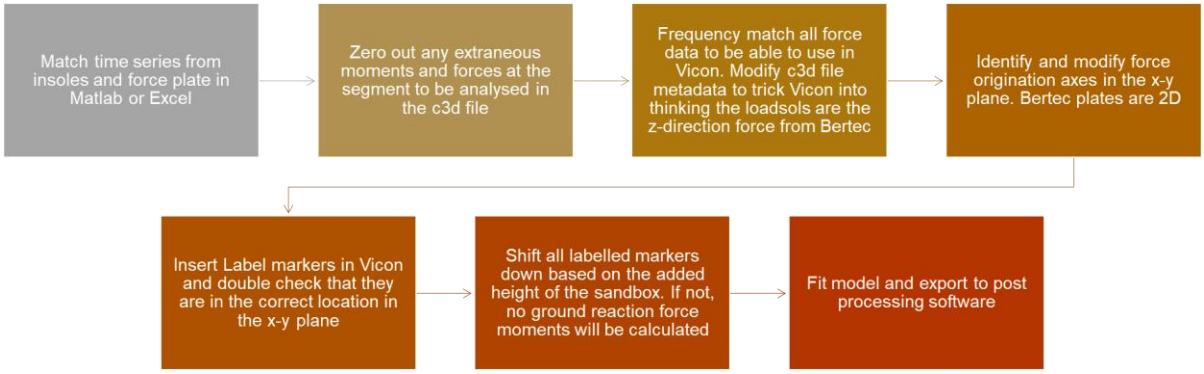

Figure 42 – Workflow for developing a pipeline for inverse dynamics calculations from insole forces.

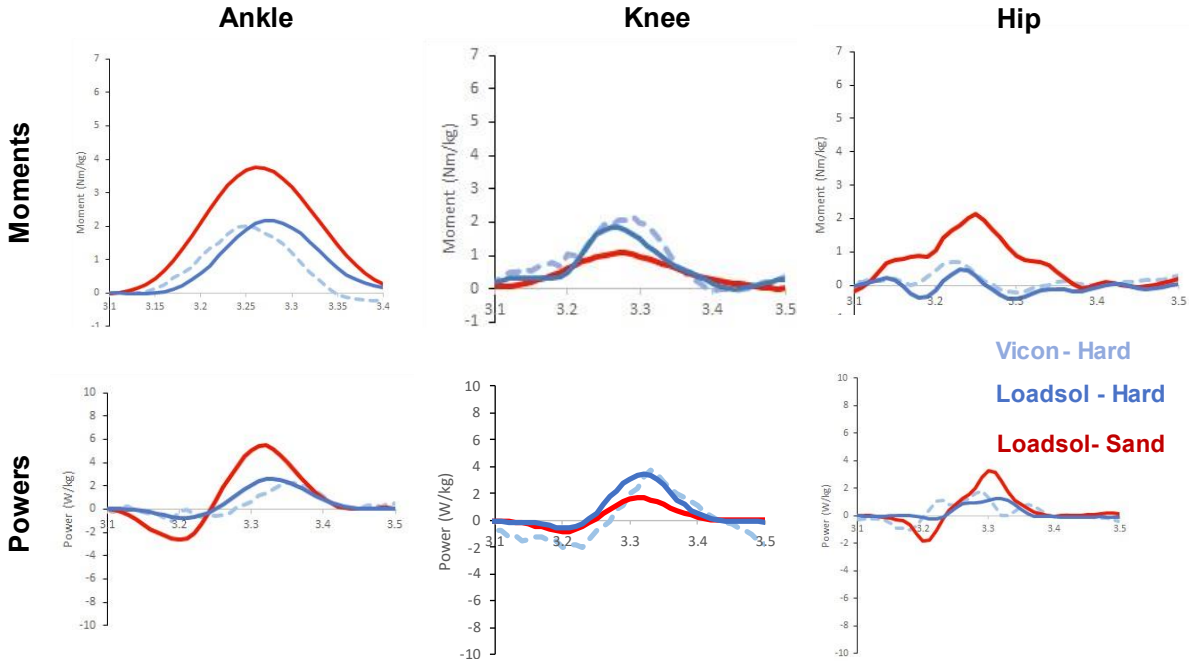

Figure 43 – Inverse dynamics comparisons for the loadsols and Vicon force plate data for a series of 10 cycles.

To further quantify these discrepancies, we verified the agreement of these hard ground inverse dynamics relationships, we used an r-squared based verification on force plate- insole calibrations curves at each point in the gait cycle, ensuring that the fit passed through the origin (Figure 44). For the ankle moments and powers, and the knee moments and powers, we found a strong positive correlation, with R^2 greater that 0.8 at each instance. At the hip, we found the moment value to have an R^2 value of ~0.7, and the power correlation to have an R^2 value of ~0.79, indicating a positive correlation. We also found the gains of our moment and power fits to be between, ~0.8 and 1.12 at the ankle, knee and hip indicating a very close agreement between force plate and insole average magnitudes over the cycle.

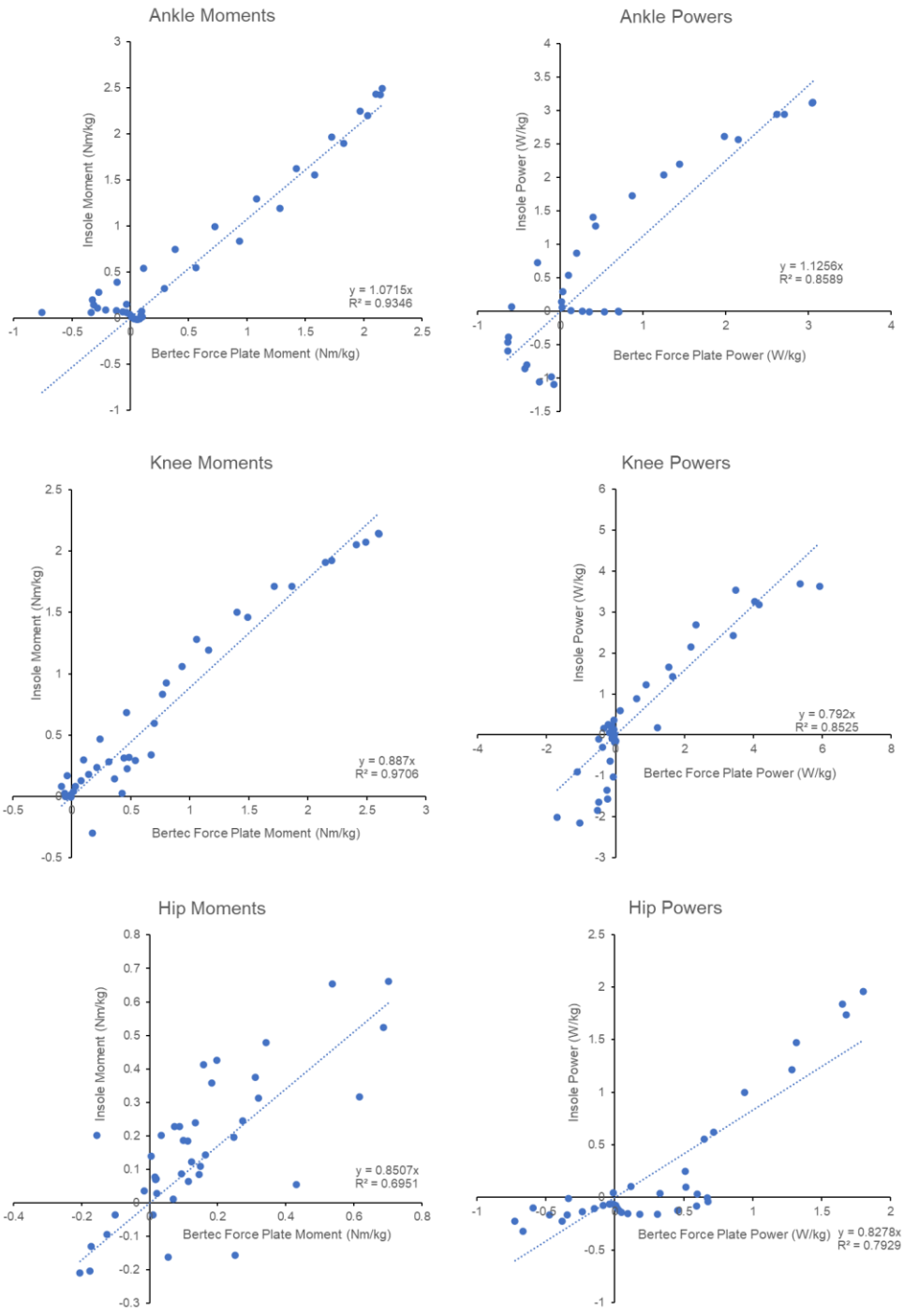

Figure 44- Verification fits of the moments and powers calculated using the insole inverse dynamics pipeline at the ankle, knee and hip. R^2 values were used to quantify correlation, and gains were used to determine the magnitude of the average discrepancy.

C.4 Conclusions

Based on the above experiments, we conclude that we can use biofeedback and inverse dynamic calculations from loadsol force data to enforce hop height and examine joint-level mechanics of subjects during hopping on dissipative terrain.

REFERENCES

[1] P. E. Alcaraz, J. M. Palao, J. L. L. Elvira, and N. P. Linthorne, "Effects of a sand running surface on the kinematics of sprinting at maximum velocity," *Institute of Sport,* 2011.

[2] T. M. Lejeune, P. A. Willems, and N. C. Heglund, "Mechanics and energetics of human locomotion on sand.," *Journal of Experimental Biology,* vol. 201, pp. 2071–2080, 1998.

[3] S. Muramatsu, A. Fukudome, M. Miyama, M. Arimoto, and A. Kijima, "Energy expenditure in maximal jumps on sand," *Journal of physiological anthropology,* vol. 25, pp. 59–61, 2006.

[4] H. Pinnington and B. Dawson, "Running economy of elite surf iron men and male runners, on soft dry beach sand and grass," *European journal of applied physiology,* vol. 86, pp. 62–70, 2001.

[5] J. R. Gosyne, Q. Lou, and G. S. Sawicki, "The Effect of Frequency on the Energetics of Hopping in Dissipative Terrain," in *The American Society Of Biomechanics*, Atlanta, 2020.

[6] J. V. Birch, D. J. Farris, R. Riddick, A. G. Cresswell, S. J. Dixon, and L. A. Kelly, "Neuromechanical adaptations of foot function when hopping on a damped surface," *Journal of Applied Physiology,* 2022.

[7] C. T. Moritz and C. T. Farley, "Human hopping on damped surfaces: strategies for adjusting leg mechanics," *Proceedings of the Royal Society of London B: Biological Sciences,* vol. 270, pp. 1741–1746, 2003.

[8] C. T. Moritz, S. M. Greene, and C. T. Farley, "Neuromuscular changes for hopping on a range of damped surfaces," *Journal of Applied Physiology,* vol. 96, pp. 1996–2004, 2004.

[9] J. Gosyne, "Bipedal Robotic Walking on Granular Material: An Inertial and Kinematic Control Approach," Master's thesis 2018.

[10] J. Gosyne, C. Hubkici, X. Xiong, A. Ames, and D. Goldman, "Bipedal Locomtion Up Sandy Slopes: Systematic Experiments Using Zero Moment Point Methods," *Humanoid Robots (Humanoids), 2018 18th IEEE-RAS International Conference on,* 2018.

[11] J. Aguilar *et al.*, "A review on locomotion robophysics: the study of movement at the intersection of robotics, soft matter and dynamical systems," *Reports on Progress in Physics,* vol. 79, p. 110001, 2016.

[12] C. E. Collins and C. P. McGowan, "Turning mechanics of the bipedal hopping Desert kangaroo rat (Dipodomys deserti)." *bioRxiv*, p. 509398, 2019.

[13] K. Hashimoto *et al.*, "Realization of biped walking on soft ground with stabilization control based on gait analysis," in *Intelligent Robots and Systems (IROS), 2012 IEEE/RSJ International Conference on*, 2012, pp. 2064–2069.

[14] M. A. Kingsbury, "A robophysics approach to bipedal walking in granular media," Ph.D. dissertation 2016.

[15] S. Komizunai, A. Konno, S. Abiko, X. Jiang, and M. Uchiyama, "Dynamic simulation of biped walking on loose soil," *International Journal of Humanoid Robotics*, vol. 9, p. 1250032, 2012.

[16] S. Komizunai, A. Konno, S. Abiko, and M. Uchiyama, "Development of a static sinkage model for a biped robot on loose soil," in *System Integration (SII), 2010 IEEE/SICE International Symposium on*, 2010, pp. 61–66.

[17] S. Komizunai, S. Konno, A. Abiko, and M. Uchiyama, "Slip characteristics identification for biped walking of a humanoid robot on sand," in *Proceedings of Eighth International Conference on Flow Dynamics*, 2011, pp. 9–11.

[18] H. Minakata, "A study of flexible shoe system for biped robot," in *Advanced Motion Control, 2004. AMC'04. The 8th IEEE International Workshop on*, 2004, pp. 387–392.

[19] A. E. Minetti and R. M. Alexander, "A theory of metabolic costs for bipedal gaits," *Journal of Theoretical Biology*, vol. 186, pp. 467–476, 1997.

[20] T. Takuma, K. Hosoda, and M. Asada, "Walking stabilization of biped with pneumatic actuators against terrain changes," in *Intelligent Robots and Systems, 2005.(IROS 2005). 2005 IEEE/RSJ International Conference on*, 2005, pp. 4095–4100.

[21] J.-c. Wu and Z. Popović, "Terrain-adaptive bipedal locomotion control," *ACM Transactions on Graphics (TOG)*, vol. 29, p. 72, 2010.

[22] X. Xiong, A. D. Ames, and D. I. Goldman, "A stability region criterion for flat-footed bipedal walking on deformable granular terrain," in *Intelligent Robots and Systems (IROS), 2017 IEEE/RSJ International Conference on*, 2017, pp. 4552–4559.

[23] N. Crevier-Denoix *et al.*, "Ground reaction force and kinematic analysis of limb loading on two different beach sand tracks in harness trotters," *Equine veterinary journal*, vol. 42, pp. 544–551, 2010.

[24] D. A. Jacobs and D. P. Ferris, "Evaluation of a low-cost pneumatic plantar pressure insole for predicting ground contact kinetics," *Journal of applied biomechanics,* vol. 32, pp. 215–220, 2016.

[25] J. Lacirignola *et al.*, "Instrumented footwear inserts: A new tool for measuring forces and biomechanical state changes during dynamic movements," in *Wearable and Implantable Body Sensor Networks (BSN), 2017 IEEE 14th International Conference on*, 2017, pp. 119–124.

[26] D. A. Connolly, "The energy expenditure of snowshoeing in packed vs. unpacked snow at low-level walking speeds," *The Journal of Strength & Conditioning Research,* vol. 16, pp. 606–610, 2002.

[27] A. O. HEINONEX, M. J. KARVONES, and R. Ruosteenoja, "The energy expenditure of walking on snow at various depths," *Ergonomics,* vol. 2, pp. 389–394, 1959.

[28] H. C. Pinnington and B. Dawson, "The energy cost of running on grass compared to soft dry beach sand," *Journal of Science and Medicine in Sport,* vol. 4, pp. 416–430, 2001.

[29] S. S. Ramaswamy *et al.*, "Effect of looseness of snow on energy expenditure in marching on snow-covered ground," *Journal of applied physiology,* vol. 21, pp. 1747–1749, 1966.

[30] P. W. Richmond, A. W. Potter, D. P. Looney, and W. R. Santee, "Terrain coefficients for predicting energy costs of walking over snow," *Applied ergonomics,* vol. 74, pp. 48–54, 2019.

[31] P. Zamparo, R. Perini, C. Orizio, M. Sacher, and G. Ferretti, "The energy cost of walking or running on sand," *European journal of applied physiology and occupational physiology,* vol. 65, pp. 183–187, 1992.

[32] D. J. Farris and G. S. Sawicki, "The mechanics and energetics of human walking and running: a joint level perspective," *Journal of The Royal Society Interface,* p. rsif20110182, 2011.

[33] R. Kram and C. R. Taylor, "Energetics of running: a new perspective," *Nature,* vol. 346, p. 265, 1990.

[34] Y. O. Aydin, J. M. Rieser, C. M. Hubicki, W. Savoie, and D. I. Goldman, "Physics approaches to natural locomotion: Every robot is an experiment," in *Robotic Systems and Autonomous Platforms*: Elsevier, 2019, pp. 109–127.

[35] D. J. Farris, B. D. Robertson, and G. S. Sawicki, "Elastic ankle exoskeletons reduce soleus muscle force but not work in human hopping," *Journal of Applied Physiology,* vol. 115, pp. 579–585, 2013.

[36] B. D. Robertson, D. J. Farris, and G. S. Sawicki, "More is not always better: modeling the effects of elastic exoskeleton compliance on underlying ankle muscle–tendon dynamics," *Bioinspiration & biomimetics*, vol. 9, p. 046018, 2014.

[37] G. S. Sawicki, C. L. Lewis, and D. P. Ferris, "It pays to have a spring in your step," *Exercise and sport sciences reviews*, vol. 37, p. 130, 2009.

[38] D. P. Ferris, M. Louie, and C. T. Farley, "Running in the real world: adjusting leg stiffness for different surfaces," *Proceedings of the Royal Society of London B: Biological Sciences*, vol. 265, pp. 989–994, 1998.

[39] V. Weerdesteyn, K. L. Hollands, and M. A. Hollands, "Gait adaptability," in *Handbook of clinical neurology*, vol. 159: Elsevier, 2018, pp. 135–146.

[40] D. B. Kowalsky, Rebula, J. R., Ojeda, L. V., Adamczyk, P. G., & Kuo, A. D. , "Kowalsky, D.B., Rebula, J.R., Ojeda, L.V., Adamczyk, P.G. and Kuo, A.D., 2021. Human walking in the real world: Interactions between terrain type, gait parameters, and energy expenditure," *PLoS one*, vol. 16(1), p.e0228682., 2021.

[41] A. K. Ashmawy, R. Salgado, S. Guha, and V. P. Drnevich, "Soil damping and its use in dynamic analyses," 1995.

[42] C. T. Chang, M. D. Zoback, and others, "Viscous rheology and state of stress in unconsolidated sands," in *SPE/ISRM Rock Mechanics in Petroleum Engineering*, 1998.

[43] C. Li, T. Zhang, and D. I. Goldman, "A terradynamics of legged locomotion on granular media," *Science*, vol. 339, pp. 1408–1412, 2013.

[44] C. Chang, D. Moos, and M. D. Zoback, "Anelasticity and dispersion in dry unconsolidated sands," *International Journal of Rock Mechanics and Mining Sciences*, vol. 34, pp. 48–e1, 1997.

[45] D. J. Farris, A. Hampton, M. D. Lewek, and G. S. Sawicki, "Revisiting the mechanics and energetics of walking in individuals with chronic hemiparesis following stroke: from individual limbs to lower limb joints," *Journal of neuroengineering and rehabilitation*, vol. 12, p. 24, 2015.

[46] Y. F. Zheng *et al.*, "Humanoid robots walking on grass, sands and rocks," in *Technologies for Practical Robot Applications (TePRA), 2013 IEEE International Conference on*, 2013, pp. 1–6.

[47] S. F. Roberts and D. E. Koditschek, "Mitigating energy loss in a robot hopping on a physically emulated dissipative substrate," *University of Pennsylvania ScholarlyCommons*, 2019.

[48] A. H. Chang, C. M. Hubicki, J. J. Aguilar, D. I. Goldman, A. D. Ames, and P. A. Vela, "Learning to jump in granular media: Unifying optimal control synthesis with

Gaussian process-based regression," in *Robotics and Automation (ICRA), 2017 IEEE International Conference on*, 2017, pp. 2154–2160.

[49] H. C. Pinnington, D. G. Lloyd, T. F. Besier, and B. Dawson, "Kinematic and electromyography analysis of submaximal differences running on a firm surface compared with soft, dry sand.," *European journal of applied physiology,* vol. 94, pp. 242–253, 2005.

[50] D. P. Ferris, K. Liang, and C. T. Farley, "Runners adjust leg stiffness for their first step on a new running surface," *Journal of biomechanics,* vol. 32, pp. 787–794, 1999.

[51] K. Yamane and L. Trutoiu, "Effect of foot shape on locomotion of active biped robots," in *Humanoid Robots, 2009. Humanoids 2009. 9th IEEE-RAS International Conference on*, 2009, pp. 230–236.

[52] N. Scott, T. Yoneyama, H. Kagawa, and K. Osada, "Measurement of ski snow-pressure profiles," *Sports Engineering,* vol. 10, pp. 145–156, 2007.

[53] M. G. Moseley, "Sand walking sandal," in *Sand walking sandal*, ed: Google Patents, 2007.

[54] R. Riddick and A. Kuo, "Mechanical work accounts for most of the energetic cost in human running," *Scientific reports,* vol. 12, no. 1, pp. 1-11, 2022.

[55] O. N. Beck, J. Gosyne, J. R. Franz, and G. S. Sawicki, "Cyclically producing the same average muscle-tendon force with a smaller duty increases metabolic rate," *Proceedings of the Royal Society B,* vol. 287, no. 1933, p. 20200431, 2020.

[56] D. J. Farris and G. S. Sawicki, "Linking the mechanics and energetics of hopping with elastic ankle exoskeletons," *Journal of applied physiology,* vol. 113, no. 12, pp. 1862-1872, 2012.

[57] T. M. Griffin, T. J. Roberts, and R. Kram, "Metabolic cost of generating muscular force in human walking: insights from load-carrying and speed experiments," *Journal of applied physiology*, vol. 95, no. 1, pp. 172-183, 2003.

[58] J. Gosyne and G. Sawicki, "Optimizing Contact Area and Joint Stiffness of a Passive Foot-Ankle Exoskeleton for Locomotion on Deformable Terrain," in *APS March Meeting Abstracts*, 2021, vol. 2021, p. F14. 006.

[59] M. F. Bobbert, P. A. Huijing, and G. J. van Ingen Schenau, "A model of the human triceps surae muscle-tendon complex applied to jumping," (in eng), *Journal of biomechanics,* vol. 19, no. 11, pp. 887-98, 1986.

[60] T. Fukunaga *et al.*, "Physiological cross-sectional area of human leg muscles based on magnetic resonance imaging," *Journal of orthopaedic research,* vol. 10, no. 6, pp. 926-934, 1992.

[61] J. R. Gosyne and G. S. Sawicki, "Why is the Metabolic Cost of Locomotion Higher on Sand?," in *The North American Congress on Biomechanics*, Ottawa, 2022.